DISSERTATION ZUR ERLANGUNG DES DOKTORGRADES
DER NATURWISSENSCHAFTEN (DR. RER. NAT.)
DER NATURWISSENSCHAFTLICHEN FAKULTÄT III –
BIOLOGIE UND VORKLINISCHE MEDIZIN DER
UNIVERSITÄT REGENSBURG

Control of epithelial Na^+ channels
by
CFTR, receptors and kinases

vorgelegt von
Tanja Bachhuber
aus Anleng
Juli/2007

Promotionsgesuch eingereicht am: 10. Juli 2007
Promotionsprüfung erfolgreich abgelegt am: 29. November 2007

Die Arbeit wurde angeleitet von: Prof. Dr. K. Kunzelmann

Prüfungsausschuss:
Vorsitzender: Prof. Dr. A. Kurtz
1. Prüfer: Prof. Dr. K. Kunzelmann
2. Prüfer: Prof. Dr. S. Schneuwly
3. Prüfer: Prof. Dr. W. Minuth
Ersatzprüfer: Prof. Dr. R. Wirth

Die Dissertation wurde von Prof. Dr. K. Kunzelmann angeleitet.

Contents

List of abbreviations

%	per cent
µ	micro
Ω	ohm
°	degree
16HBE	bronchial epithelial cells
^{2}	square
A	amp, amiloride, ATP
aa	amino acid(s)
AB, Ab	antibody
ABC	ATP binding cassette
AC	adenylate cyclase
ADP	adenosine diphosphate
Aldo	aldosterone
Amil, amil	amiloride
ATP	adenosine triphosphate
BHK	baby hamster kidney
bp	base pair
BSA	bovine serum albumin
But., but.	sodium butyrate
C terminus	carboxyl terminus
C	centigrade
cf	compare
cAMP	cyclic adenosine 3',5'-monophosphate
cDNA	complementary deoxyribonucleic acid
CF	cystic fibrosis
CFTR	cystic fibrosis transmembrane conductance regulator
CK2	casein kinase 2
$[Cl^-]_i$	intracellular chloride concentration
cm	centimetre
CO_2	carbon dioxide
cRNA	complementary ribonucleic acid
Da	Dalton
DAPI	4',6'-diamidino-2-phenylindole
DEG	degenerin
DMAT	2-dimethylamino-4,5,6,7-tetrabromo-1H-benzimidazole

dNTP	deoxyribonucleotide triphosphate
DTT	dithiothreitol
e.g.	exempli gratia
Edelf	edelfosine
EGF	epidermal growth factor
EGFR	epidermal growth factor receptor
ENaC	epithelial sodium channel
endo H	endoglycosidase H
ER	endoplasmic reticulum
ERK	extracellular-regulated kinase
EST	expressed sequence tags
etc.	et cetera
FBS	fetal bovine serum
Fig.	figure
FITC	fluorescein isothiocyanate
Fors, Fsk	forskolin
G	conductance
g	gram
GDP	guanosine diphosphate
GFP	green fluorescent protein
Glib	glibenclamide
Grb2	growth factor receptor bound protein 2
Grk2	G protein-coupled receptor kinase 2
G_{te}	transepithelial conductance
GTP	guanosine triphosphate
h	hour
HDAC	histone deacetylase
HEPES	4-(2-Hydroxyethyl)piperazine-1-ethanesulfonic acid
HRP	horseradish peroxidase
I	current
i.e.	id est
I/F	IBMX/Forskolin
IBMX	3-isobutyl-1-methylxanthine
I_m	whole cell current
inhib.	inhibition
Ins	insulin
IRS1	insulin receptor substrate 1

I_{sc}	short-circuit current
k	kilo
K	lysine
l	litre
M	mega, mol
m	milli, metre
M1, M2	transmembrane domains of ENaC
m-3M3FBS	2,4,6-Trimethyl-N-(m-3-trifluoromethylphenyl)benzenesulfonamide
mAb	monoclonal antibody
MAPK1/2	mitogen-activated protein kinase 1/2
MDCK	Madin-Darby canine kidney
MEK	mitogen-activated kinase kinase
min	minute(s)
MR	mineralocorticoid receptor
mRNA	messenger ribonucleic acid
mut	mutant
N terminus	amino terminus
n	nano
N	non-polar
n	number
NBD1	nucleotide binding domain 1
Nedd4-2	neural precursor cell expressed, developmentally downregulated protein 4-2
Neo	neomycin
NHE	Na^+/H^+ exchanger
NHERF	Na^+/H^+ exchange regulatory factor
NMDG	N-methyl-D-glucamine
p	pico
P	proline
pAb	polyclonal antibody
PAR, Par	parental
PBS	phosphate buffered saline
PC-2	polycystin-2
PCR	polymerase chain reaction
PDK	phosphatidylinositol-dependent protein kinase
PH	pleckstrin homology
Phe, F	phenylalanine

P_i	inorganic phosphate
PI(4)5K	phosphatidylinositol 4-phosphate 5-kinase
PI3K	phosphatidylinositol 3-kinase
PI_4 kinase	phosphatidylinositol 4-kinase
PIP_2	phosphatidylinositol 4,5-bisphosphate
PIP_3, IP_3	phosphatidylinositol 3,4,5-trisphosphate
PKA	protein kinase A
PKC	protein kinase C
PLC	phospholipase C
PNGase F	peptide N-glycosidase F
P_o	open probability
PO	phenylarsine oxide
PP2A	protein phosphatase 2A
PY motif	PPPXYXXL sequence
R	arginine
R59022	6-[2-[4-[(4-Fluorophenyl)phenylmethylene]-1-piperidinyl]ethyl]-7-methyl-5H-thiazolo-[3,2-a]-pyrimidin-5-one
Ref., ref.	reference
rENaC	rat ENaC
RT	reverse transcriptase, room temperature
R_{te}	transepithelial resistance
S	siemens
SDS-PAGE	sodium dodecyl sulphate polyacrylamide gel electrophoresis
sec, s	second(s)
Ser, ser, S	serine
SGK1	serum- and glucocorticoid-dependent kinase isoform 1
siRNA	small interfering RNA
SK channel	small conductance Ca^{2+}-activated K^+ channel
SNARE	N-ethyl-maleimide-sensitive factor attachment protein receptor
SOS	son of sevenless protein
TBB	4,5,6,7-tetrabromobenzotriazole
TBS	Tris buffered saline
Thr, thr, T	threonine
TRITC	Tetramethylrhodamine isothiocyanate
TRPL channel	transient receptor potential like channel
TRPP channel	transient receptor potential P(PKD)-type channel
U	unit(s)

u. a.	unter anderem
U73122	1-[6-(17β-3-methoxyestra-1,3,5(10)-trien-17-amino)hexyl]-1H-pyrrole-2,5-dione
Ub	ubiquitin
UTP	uridine triphosphate
V	valine, volt, voltage,
Vaso	vasopressin
V_c	membrane voltage
V_{te}	transepithelial voltage
WB	Western blot
WT, wt	wild-type
×	-fold
Y	tyrosine

Chapter 1

General introduction

Structure, distribution and function of the epithelial Na^+ channel (ENaC)

ENaC is a heteromeric ion channel, composed of three homologous subunits: α-, β- and γENaC. Each subunit consists of short (~ 50–100 amino acids) intracellular amino- and carboxyl termini and two hydrophobic transmembrane domains (M1 and M2) connected by a large (~ 500 amino acids) hydrophilic extracellular loop (Fig. 1; (37;38;71;148)). The C terminus contains a highly conserved PPPXYXXL sequence (PY motif), which is important for endocytosis and degradation of ENaC (50).

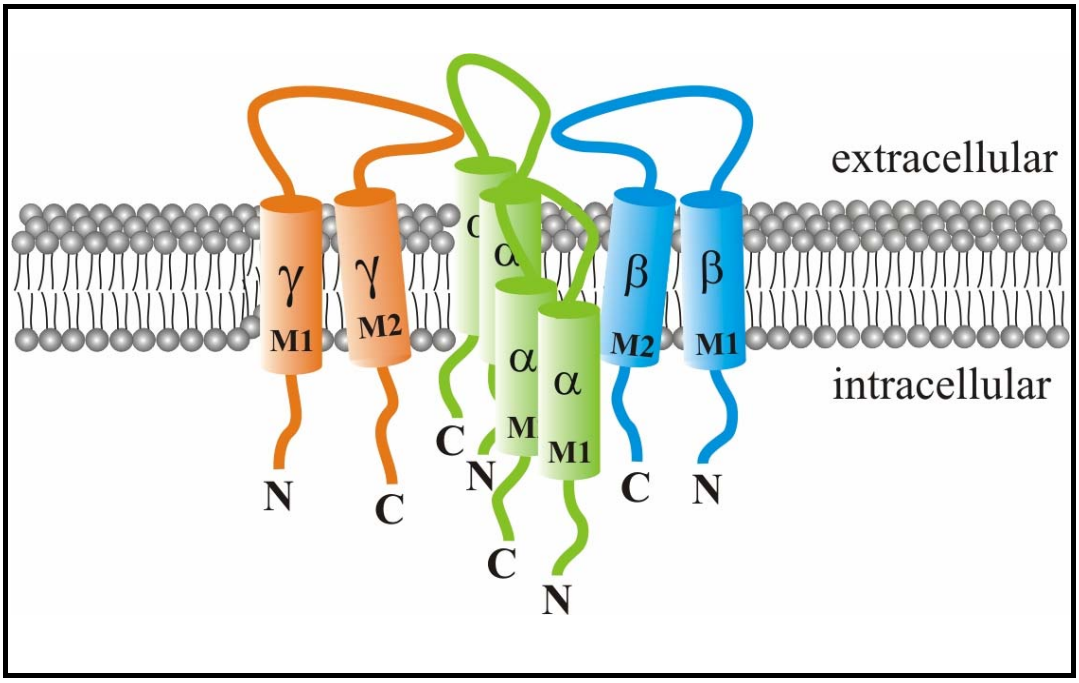

Fig. 1: Structure of ENaC. Three homologous subunits form the ion channel: 2 α-, 1 β- and 1 γENaC (66), but other combinations may exist, too (202).

Expression and assembly of probably 2 α-, 1 β- and 1 γENaC are necessary to get a full functional channel with a few remarkable features (74;81):

i) non-voltage gated and non-inactivating channel with a high selectivity for Na^+

ii) low single channel conductance (~ 5 pS)
iii) long closing and opening times
iv) blocked by the diuretic amiloride at submicromolar concentrations

As a member of the ENaC/DEG superfamily (3;17;103), ENaC plays a key role in Na^+ transport. Localized in the apical membranes of absorbing epithelia, including kidney, airways, distal colon, sweat and salivary ducts (38;66;74), ENaC is responsible for electrogenic uptake of Na^+ into the cells. At the basolateral membranes, the Na^+/K^+ ATPase is pumping Na^+ out of the cells (73).

The regulation of Na^+ transport by ENaC is crucial to a variety of physiological functions (172):
i) normal blood pressure
ii) control of urinary Na^+ reabsorption
iii) maintenance of extracellular fluid volume homeostasis
iv) regulation of volume and composition of airway surface liquids
v) mucociliary clearance in airway epithelia
Changes in expression or activity of ENaC lead to defects in the regulation of Na^+ transport and cause several human diseases, including Liddle's syndrom (an inherited form of salt-sensitive hypertension), pseudohypoaldosteronism type I (an inherited form of severe salt-wasting and hypotension) and cystic fibrosis (28;187).

Regulation of ENaC

Before ENaC subunits were cloned from rat distal colon 1993 (37;130), the knowledge about the regulation of ENaC was limited, so that a non-regulated ENaC was taken into account. Today, we know a wide variety of hormonal and non-hormonal mechanisms to regulate ENaC and to fine-tune Na^+ absorption.

Hormonal regulation of ENaC

Several hormones, including aldosterone, insulin and vasopressin, are involved in Na^+ transport via ENaC. The hormones influence surface expression and/or activity of the Na^+ channel by stimulating different signalling cascades.

Activation of ENaC via aldosterone-regulated SGK1

Aldosterone (Aldo) is the most important hormonal regulator of renal Na^+ absorption. Its binding to the mineralocorticoid receptor (6) stimulates transcription of the serum- and

glucocorticoid-dependent kinase isoform 1 (SGK1) and other genes (6;29;58;208;222;223). After activation of SGK1 by a phosphatidylinositol 3-kinase (PI3K)-dependent pathway (see below), SGK1 phosphorylates the ubiquitin ligase Nedd4-2 (50;204). Usually, non-phosphorylated Nedd4-2 binds to ENaC and tags it with ubiquitin, targeting it for internalization and degradation (50;156). But when it is phosphorylated, Nedd4-2 shows reduced affinity for ENaC because phosphorylation induces the binding of an inhibitory 14-3-3 dimer to Nedd4-2 (Fig. 2; (19;93)). As a result, ENaC surface expression increases. In its phosphorylated form, Nedd4-2 ubiquitinates SGK1, leading to degradation of the kinase (241). This negative feedback mechanism restricts the influence of the SGK1 pathway to ENaC.

Insulin-dependent regulation of ENaC

It is well known that insulin (Ins) increases renal Na^+ reabsorption, and two models exist, which describe the corresponding intracellular signalling.
Both pathways have a common starting point:
The binding of insulin to its receptor on the basolateral membrane stimulates phosphorylation of the insulin receptor substrate 1 (IRS1), which results in activation of PI3K (173). In the first model the activation of PI3K is associated with its translocation to the plasma membrane. Here PI3K catalyzes formation of phosphatidylinositol 3,4,5-trisphosphate (PIP_3) from phosphatidylinositol 4,5-bisphosphate (PIP_2) in the inner leaflet of the plasma membrane (24). Then, PIP_3 diffuses along the lateral membrane, crossing the thight junction and entering the apical membrane. This leads to a changed lipid composition, supporting the insertion of ENaC into the apical membrane (25). It is assumed that PI3K and ENaC are co-localized along the lateral membrane from where it moves to the apical side (24). In the second pathway model PI3K forms PIP_3, leading to activation of phosphatidylinositol-dependent protein kinases (PDK; (39)). PDK1 phosphorylates SGK1, which enables SGK1 to phosphorylate the ubiquitin ligase Nedd4-2 (Fig. 2; (50;204)). Phosphorylation of Nedd4-2 prevents binding to ENaC and subsequent endocytosis.

Regulation of ENaC by vasopressin

In case of hypovolemia or hypotension, vasopressin (Vaso) is secreted by the hypothalamus to enhance Na^+ transport in renal collecting duct cells (59). The hormon binds to V2 receptors at the basolateral membrane and activates the adenylate cyclase (AC), leading to an increase in intracellular cAMP. High cAMP levels stimulate protein kinase A (PKA). Through phosphorylation of the ubiquitin ligase Nedd4-2, PKA inhibits endocytosis and degradation of ENaC (Fig. 2; (203)). The effect of vasopressin is synergistic with that of aldosterone.

ENaC inhibition by epidermal growth factor

The epidermal growth factor receptor (EGFR)-signalling pathway in renal collecting duct cells is an example for negative regulation of Na^+ absorption by aldosterone (75;115). Aldosterone upregulates EGFR (114;115) and Ras (146;207). Activation of this pathway antagonizes its own positive action on ENaC (77). Binding of the epidermal growth factor (EGF) to EGFR activates via active GTP-complexed Ras, a MAPK1/2 cascade that results in ERK-mediated phosphorylation of ENaC (196). This facilitates the interaction between the Na^+ channel and ubiquitin ligase Nedd4-2 (197), leading to internalization and subsequent degradation of ENaC (Fig. 2; (50;156)).

Small GTPases activate ENaC

K-Ras and RhoA are GTP-dependent, small G proteins, which increase ENaC activity through distinct and independent signalling cascades (175;205). Aldosterone induces expression and activation of K-Ras (82;146;207). The active GTP-bound form of K-Ras activates PI3K, which catalyzes formation of PIP_3 (206). Subsequent interaction between PIP_3 and the C terminus of γENaC results in enhanced channel open probability and activity of ENaC (177). The RhoA signalling pathway is less understood but it is known that GTP-complexed RhoA interacts with Rho kinase to activate phosphatidylinositol 4-phosphate 5-kinase (PI(4)5K; (171;228;233)). Production of PIP_2 augments ENaC membrane surface expression. Because of the importance of RhoA for cytoskeletal rearrangement and vesicle trafficking (185;214) and the role of PIP_2 in the exocytotic process (5;100;227), it is assumed that RhoA enhances surface expression by promoting trafficking of ENaC to the plasma membrane (176).

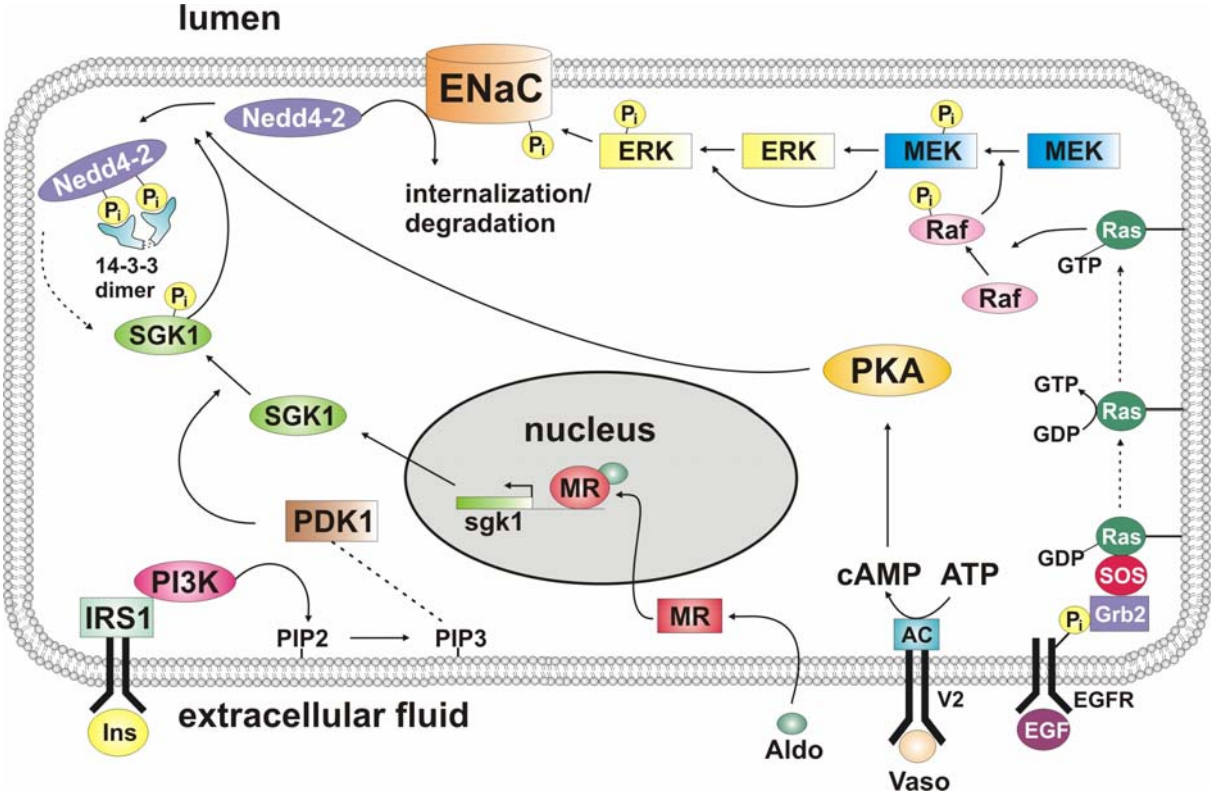

Fig. 2: Hormonal regulation of ENaC. Not all of the described signalling pathways are shown here. Small circled P_i, inorganic phosphate. See text for explanations and abbreviations. Modified from ref. 20.

Non-hormonal regulation of ENaC

Apart from hormonal regulation of the epithelial Na^+ channel as outlined in the previous paragraphs, also non-hormonal mechanisms for Na^+ channel regulation have been described. These include phosphorylation not related to hormonal stimulation, interaction with phospholipids and in addition, regulation by proteases and other ion channels, which interact with ENaC.

Activation of ENaC by proteolysis

Proteases-dependent cleavage of α- and γENaC leads to release of two inhibitory peptides, resulting in enhanced channel open probability (P_o). The serine endoprotease furin cleaves the α subunit at two sites and the γ subunit at a single site within the extracellular loop (92). The dual cleavage of αENaC removes a 26 amino acids (aa) inhibitory peptide (41). For the excision of a second inhibitory peptide (43 aa), a double cleavage in γENaC must occur. The serine protease prostasin cleaves this subunit at a site distal to the furin cleavage site (35).

Regulation of ENaC by PIP_2

The anionic phospholipid phosphatidylinositol 4,5-bisphosphate (PIP_2) is localized in the inner leaflet of the plasma membrane and consists of a lipophilic tail, anchoring PIP_2 in the membrane and a hydrophilic, negatively charged head group, which extends into the cytoplasm and allows interaction with cytosolic proteins. Some of its purposes are the activation of enzymes and the regulation of transporters and ion channels (83). The epithelial Na^+ channel is one of them (137;235) and chapter 2 (119) describes one possible way for ENaC regulation via PIP_2. As mentioned above, PIP_2 is involved in enhancing surface expression of ENaC via distinct signalling cascades. However, these known pathways do not require direct binding of PIP_2 to the channel.

It was demonstrated that there are PIP_2 binding sites in the N termini of β- and γENaC and direct interaction between PIP_2 and ENaC has been detected, influencing the open probability of the channel (137;235). Furthermore, it is known that stimulation of purinergic receptors inhibits epithelial Na^+ channels (47;127;190). For that a phospholipase C (PLC)-dependent mechanism is proposed (124;136). Chapter 2 (119) presents a regulatory pathway taking the following into account: Stimulation of the purinergic $P2Y_2$ receptors by extracellular ATP activates PLC, leading to hydrolysis of PIP_2. A drop in PIP_2 levels causes a decrease in ENaC open probability.

Protein kinase CK2 regulates ENaC

CK2 is a constitutively active Ser/Thr protein kinase that is ubiquitously expressed in eukaryots. The enzyme is composed of two catalytic α- and two regulatory β subunits, forming a heterotetramer that targets more than 300 proteins (131;151). With that, CK2 is involved in numerous cellular processes such as regulation of protein expression, cell proliferation and development (23). Furthermore, it fulfils also a role in regulation of ion channels like CFTR and ENaC. In the C termini of β- and γENaC there are binding- and phosphorylation sites for CK2 (198). The phosphorylation of these sites by CK2 influences both surface expression and open probability of ENaC, although not to the same extent. CK2-dependent regulation of ENaC will be subject of chapter 5 (8).

CFTR-mediated inhibition of ENaC

The cystic fibrosis transmembrane conductance regulator (CFTR) is a member of the ATP binding cassette (ABC) transporter superfamily. CFTR functions as a Cl^- channel in the apical membrane of epithelial tissues, including kidney, airways, intestine and sweat ducts and participates in ion and water transport across the epithelium. The cAMP-dependent

phosphorylation via PKA and the binding and hydrolysis of ATP regulate the activity of this Cl^- channel (70). CFTR, in turn, also controls numerous other proteins, including the epithelial Na^+ channel (210). Chapter 3 (9) will deal with this, too.

Cystic fibrosis (CF) is a lethal, autosomal recessive disease of the Caucasian population and is caused by mutations in the CFTR gene (26). One mutation alone, F508del-CFTR, is found in approximately 90% of CF patients (27). Typical for CF is a deficient Cl^- secretion and an enhanced Na^+ absorption in airways mediated by ENaC, leading ultimately to respiratory failure, the most common cause of death in CF patients (104). The loss of CFTR-dependent inhibition of ENaC in CF and the resulting clinical problems of defective mucociliary clearance illustrate the biological relevance of the interaction between CFTR and ENaC. That is why great efforts are spent on the identification of the underlying mechanism. In chapter 3 (9) it is demonstrated that Cl^- ions as well as the C terminus of βENaC are involved in CFTR-mediated inhibition of ENaC.

Thesis outline

Regulation of epithelial Na^+ channels became very complex. Numerous regulatory pathways are known, but for most of them no detailed knowledge exists. This thesis aims in deciphering several of these regulatory mechanisms in more detail. The different regulatory pathways described here have in common that they are either based on the function of CFTR or on Cl^- ions moving through CFTR Cl^- channels.

The first part (chapter 2 (119)) focuses on the inhibition of epithelial Na^+ channels by stimulation of purinergic receptors (47;124;127;190). The hypothesis is put forward that the negatively charged phospholipid PIP_2 directly interacts with positively charged sequences within the N termini of β- and γENaC, which influences the open probability of the channel. We wonder whether hydrolysis of PIP_2, caused by stimulation of purinergic receptors and a decline in PIP_2 levels, is responsible for the decrease in ENaC activity. We consider also a Cl^--dependence of this receptor-mediated inhibition. That could mean, Cl^- ions compete against PIP_2 for the binding to the ENaC subunits.

The second part (chapter 3 (9)) deals with Cl^--dependent inhibition of ENaC. It is known that activation of CFTR inhibits ENaC (34;95;98;111;129;138;139;142;210). We were interested in the role of Cl^- ions in CFTR-mediated ENaC inhibition. Furthermore, we want to know to what extent the C termini of ENaC subunits are involved in this mechanism.

Considering the importance of CFTR for ENaC regulation, the third part (chapter 4 (155)) describes the creation of two new cell lines, in order to have better cell models for CFTR-related studies. Madin-Darby canine kidney (MDCK) cells were used for that because

- they are polarized epithelial cells (153;161;200). Hitherto most CFTR studies were carried out in non-epithelial/non-polarized cells. However, protein trafficking and membrane expression in non-epithelial cells is different to that observed in epithelial cells. Investigation of protein trafficking is a major issue in CFTR research, since about 80% of all patients with cystic fibrosis demonstrate a trafficking defect of CFTR. Trafficking pathways in MDCK cells are well-documented (161).
- they grow well on permeable supports and form tight junctions. That makes MDCK cells very suitable for Ussing chamber experiments (an electrophysiological method to measure transepithelial voltages; (158)).
- MDCK type II cells have no endogenous CFTR. Two types of MDCK cells exist (184). Type I are derived from the distal collecting duct and express endogenous CFTR (14). Type II are derived from the proximal tubule and have no endogenous CFTR (159).

These and other cellular properties are the reason why MDCK type II cells were taken to generate two new cell lines, stably expressing wt- or F508del-CFTR.

In the fourth part of the thesis (chapter 5 (8)) we investigate the involvement of protein kinase CK2 in the regulation of epithelial Na^+ channels. CFTR functions not only as a regulator of ENaC but also as an anchor for numerous other proteins, e.g. protein kinase CK2. CK2 binds to and phosphorylates CFTR (150;216). However, there are also binding- and phosphorylation sites for CK2 within the C termini of β- and γENaC (198). This raises the question whether proteins, in this case CK2, that bind to CFTR, take also part in the regulation of ENaC.

Chapter 2

Purinergic inhibition of the epithelial Na^+ transport via hydrolysis of PIP_2

Abstract

Stimulation of purinergic receptors inhibits amiloride-sensitive Na^+ transport in epithelial tissues by an unknown mechanism. Because previous studies excluded the role of intracellular Ca^{2+} or protein kinase C, we examined whether purinergic regulation of Na^+ absorption occurs via hydrolysis of phospholipid such as phosphatidylinositol-bisphosphates (PIP_2). Inhibition of amiloride-sensitive short-circuit currents ($I_{sc\text{-}Amil}$) by adenine 5'-triphosphate (ATP) in native tracheal epithelia and M1 collecting duct cells was suppressed by binding of neomycin to PIP_2, and recovery from ATP inhibition was abolished by blocking phosphatidylinositol 4-kinase or diacylglycerol kinase. Stimulation by ATP depleted PIP_2 from apical membranes, and PIP_2 co-immunoprecipitated the β subunit of ENaC. ENaC was inhibited by ATP stimulation of $P2Y_2$ receptors in *Xenopus* oocytes. Mutations in the PIP_2 binding domain of βENaC but not γENaC reduced ENaC currents without affecting surface expression. Collectively, these data supply evidence for a novel and physiologically relevant regulation of ENaC in epithelial tissues. Although surface expression is controlled by its C terminus, N-terminal binding of βENaC to PIP_2 determines channel activity.

Introduction

Na^+ absorption in kidney, airways, colon, and other epithelial tissues is provided by the amiloride-sensitive Na^+ channel ENaC. Stimulation of luminal purinergic receptors co-localized with ENaC in luminal membranes transiently activates Ca^{2+}-dependent Cl^- secretion and induces long-lasting inhibition of Na^+ absorption. This has become an important issue for the pharmacotherapy of cystic fibrosis (CF), where increased Na^+ absorption is found in the airways of CF patients (30;122;181).

We and others reported recently regulation of amiloride-sensitive Na^+ absorption ($I_{sc\text{-}Amil}$) in native trachea and mouse collecting duct (M1) cells by stimulating purinergic receptors with ATP or UTP (47;124;127;190). Inhibition of Na^+ absorption during stimulation of purinergic P2Y receptors with ATP is independent of an increase in intracellular Ca^{2+} or activation of protein kinase C (124;143;143). It was shown, however, that U73122, an inhibitor of phospholipase C (PLC) but not the inactive homologue U73343, suppresses the effects of ATP on Na^+ absorption in mouse trachea. Thus a PLC-dependent process was suggested (124;136). ATP-dependent inhibition via activation of PLC was also shown to mask a stretch activation of ENaC, as membrane stretch causes release of ATP (136). Two recent publications supply evidence for the regulation of ENaC by anionic phospholipids in A6 cells and *Xenopus* oocytes (137;235). Both β- and γ subunits of ENaC but not αENaC contain substantial numbers of positively charged amino acids in their N termini. These putative N-terminal phosphatidylinositol 4,5-bisphosphate (PIP_2) binding domains of ENaC may regulate ENaC activity by binding positively charged amino acids to PIP_2. This is further supported by co-immunoprecipitation data that suggest binding of both ENaC subunits to PIP_2 (235). Moreover, the data available provide evidence for PIP_2 regulation of the channel open probability rather than surface expression or ENaC trafficking (137). Another study, however, showed regulation of ENaC by phosphatidylinositol 3,4,5-trisphosphate (IP_3) and phosphatidylinositol 3,4-bisphosphate rather than phosphatidylinositol 4,5-bisphosphate (215). These data are supported by studies that identified IP_3 as an early mediator of insulin-stimulated transport in A6 cells (145;182). Thus, the importance of the putative PIP_2 binding motifs for maintaining ENaC activity, its relation to cellular PIP_2 metabolism, and the physiological relevance of PIP_2-dependent regulation of ENaC remain obscure. Here we provide convincing evidence for a physiologically relevant PIP_2-dependent regulation of ENaC by demonstrating purinergic inhibition of amiloride-sensitive Na^+ absorption through hydrolysis of PIP_2.

Material and Methods

Ussing chamber experiments

Mouse tracheas were removed after sacrificing animals by cervical dislocation and were opened by a longitudinal cut. Connective tissues were removed. Tissues were put into cold buffer of the following composition (mmol/l): NaCl 145, KCl 3.8, D-glucose 5, $MgCl_2$ 1, HEPES 5, Ca-gluconate 1.3. The tissues were mounted into a modified Ussing chamber with a circular aperture of 0.95 mm^2. M1 cells are derived from mouse cortical collecting duct and have properties of principal cells (kindly provided by C. Korbmacher, Physiologisches Institut, Universität Erlangen, Germany). The cells were grown to confluence on permeable supports, and inserts were mounted into a perfused Ussing chamber. The luminal and basolateral sides of the epithelium were perfused continuously at a rate of 10 ml/min (chamber volume 2 ml). The bath solution had the following composition (mmol/l): NaCl 145, KH_2PO_4 0.4, K_2HPO_4 1.6, D-glucose 5, $MgCl_2$ 1, HEPES 5, Ca-gluconate 1.3. pH was adjusted to 7.4. Bath solutions were heated to 37°C using a water jacket.

Experiments were performed under open-circuit conditions. Values for transepithelial voltages (V_{te}) were referred to the serosal side of the epithelium. Transepithelial resistance (R_{te}) was determined by applying short (1 s) current pulses (ΔI=0.5 μA). Voltage deflections obtained under conditions without the mucosa present in the chamber were subtracted from those obtained in the presence of the tissues. R_{te} was calculated according to Ohm's law ($R_{te} = \Delta V_{te}/\Delta I$). The equivalent short-circuit current (I_{sc}) was calculated ($I_{sc}=V_{te}/R_{te}$), and the amiloride-sensitive I_{sc} ($I_{sc\text{-}Amil}$) is used to express the amount of equivalent short-circuit current that is inhibited by 10 μmol/l amiloride. Tissue preparations were accepted only if the transepithelial resistance exceeded that obtained for an empty chamber at least by a factor of 3. The transepithelial resistance of filter grown M1 cells was 320 ± 38 Ωcm^2 (*n*=36), while that of mouse trachea was 55.6 ± 6.7 Ωcm^2 (*n*=42). Measurements under open-circuit conditions are in general more protective and less exhausting for tissue preparations. They seem more likely to reflect the *in vivo* situation because the epithelium *in vivo* is not short-circuited. As a result, the obtained I_{sc} are in general quite high and the recordings are usually stable for 3–4 h.

cRNAs for ENaC subunits and ENaC PIP_2 binding mutants

cDNAs encoding rat $\alpha\beta\gamma$ENaC (kindly provided by B. Rossier, Pharmacological Institute of Lausanne, Switzerland) and the purinergic $P2Y_2$ receptor were linearized in pBluescript or pTLN (105) with *Not*I or *Mlu*I and were *in vitro* transcribed using T7, T3, or SP6 promotor and polymerase (Promega, Madison, WI). For some experiments, cDNAs of $\alpha\beta\gamma$ENaC subunits

were used, which were FLAG-tagged (kindly provided by B. Rossier, University of Lausanne, Switzerland, (67)). Isolation and microinjection of oocytes have been described in a previous report (141). In brief, after isolation from adult *Xenopus laevis* female frogs (*Xenopus* express, South Africa), oocytes were dispersed and defolliculated by a 45 min-treatment with collagenase (type A, Boehringer, Germany). Subsequently, oocytes were rinsed and kept at 18°C in ND96-buffer (in mmol/l): NaCl 96, KCl 2, $CaCl_2$ 1.8, $MgCl_2$ 1, HEPES 5, sodium pyruvate 2.5 (pH 7.55), supplemented with theophylline (0.5 mmol/l) and gentamycin (5 mg/l). Mutations in the N-terminal PIP_2 binding domains of β- and γENaC were generated by replacing 2 (β2N, γ2N) and 4 (β4N, γ4N) positively charged amino acids by non-polar (N) amino acids as shown in Fig. 5A, using PCR techniques (191).

Double electrode voltage clamp

Oocytes were injected with cRNA (1–10 ng) after dissolving in 47 nl double-distilled water (Nanoliter Injector WPI, Germany). Water-injected oocytes served as controls. Two to four days after injection, oocytes were impaled with two electrodes (Clark instruments), which had a resistance of <1 MΩ when filled with 2.7 mol/l KCl. Using two bath electrodes and a virtual-ground headstage, the voltage drop across R_{serial} was effectively zero. Membrane currents were measured by voltage clamping of the oocytes (Warner oocyte clamp amplifier OC725C) in intervals from –90 to +30 mV, in steps of 10 mV, each 1 s. Conductances were calculated according to Ohm's law, and amiloride-sensitive conductances (G_{Amil}) were used in the present report to express the amount of whole cell conductance that is inhibited by 10 μmol/l amiloride. During the whole experiment, the bath was continuously perfused at a rate of 5–10 ml/min. All experiments were conducted at room temperature (22°C).

Immunoprecipitation and Western blot

Lysates of M1 cells were incubated with a phosphatase inhibitor cocktail 2 (Sigma, St. Louis, MO) and PIP_2 (10 μM, Sigma) for 30 min and were immunoprecipitated using an anti-PIP_2 antibody (mouse monoclonal IgM, Echelon, San Jose, CA) and protein A/G Plus-agarose (Santa Cruz Biotechnology, Santa Cruz, CA). Immunoprecipitates are resolved by 7% SDS-PAGE, transferred to Hybond-P (Amersham Pharmacia Biotech, Uppsala, Sweden) and incubated with rabbit anti-β- or anti-γENaC antibodies (Zymed, South San Francisco, CA). Proteins were visualized using a donkey anti-rabbit IgG conjugated to horseradish peroxidase and ECL Advance Detection Kit (Amersham Pharmacia Biotech). Yolk-free homogenates were prepared three days after injection of cRNA. Pools of 30 oocytes were lysed in 500 μl homogenization buffer (1% Elugent C12E6 (Calbiochem, Darmstadt, Germany)), 100 mM NaCl, 20 mM Tris (pH 7.6). Lysates were centrifuged three times at 200

g for 5 min at 4°C and one time at 20000 g for 30 min at 4°C. Supernatants were mixed with loading buffer, and the protein of 12 oocytes was resolved by 7% SDS-PAGE, transferred to Hybond-P (Amersham Pharmacia Biotech) and incubated with anti-FLAG M2 monoclonal antibody (Sigma). Proteins were visualized using a sheep anti-mouse IgG conjugated to horseradish peroxidase and ECL Advance Detection Kit (Amersham Pharmacia Biotech).

Cell culture and transfections

M1 cells were grown at 37°C with 5% CO_2 as described previously (47). For transient transfections, cells were grown without antibiotics on millicell-CM transwell filters (Millipore). Sub-confluent monolayers were transiently transfected with 1 μg of plasmid DNA ($PH_{PLC\delta}$-GFP, Dynamin-GFP). $PH_{PLC\delta}$-GFP plasmid encoded the PH domain of the phospholipase $C_{\delta 3}$, while the Dynamin-GFP plasmid encoded the relatively non-specific PH domain of dynamin. Transfection was performed with LipofectAMINE 2000 reagent (Invitrogen, Carlsbad, CA), according to the manufacturer's protocol. The cells were processed two days after transfection for use in confocal microscopy analysis. The transfection efficacy was typically between 30–40%. All data were obtained in at least three independent experiments with cells of different passages (between 15 and 35).

Confocal microscopy

Confluent layers of cells grown on transwell filters were fixed for 30 min at room temperature using 4% paraformaldehyde in PBS and followed by quenching using 50 mM NH_4Cl in PBS for 10 min. The cell membranes were permeabilized using 0.1% saponin/0.1% Triton X-100 and incubated with either the actin filament staining phalloidin-rhodamine (0.1 M; Calbiochem), or non-specific antibody binding was blocked by 0.2% BSA/0.2% fish skin gelatin (Sigma) in PBS for 10 min. All transwell filters were washed extensively with PBS before mounting using Mowiol (Calbiochem), and confocal immunofluorescence images were obtained using a Nikon Eclipse E600 upright microscope with a Bio-Rad Radiance 2000 confocal scanning system with a × 100 oil-immersion Nikon objective.

Chemiluminescence measurements

Oocytes were incubated for 60 min at 4°C in ND96 media (in mM: 96 NaCl, 2 KCl, 1.8 $CaCl_2 \cdot 2\ H_2O$, 1 $MgCl_2 \cdot 6\ H_2O$, 5 HEPES, 2.5 sodium pyruvate, adjusted to pH 7.5 with NaOH) with 1% bovine serum albumin (BSA) to block non-specific binding of antibodies. Afterwards, oocytes were incubated for 60 min at 4°C with 1 μg/ml mouse monoclonal anti-FLAG M2 antibody (clone M2, Sigma-Aldrich, Taufkirchen, Germany) in 1% BSA/ND96, washed eight times at 4°C with 1% BSA/ND96, and incubated with sheep anti-mouse IgG peroxidase-

linked whole antibody (Amersham Biosciences, Freiburg, Germany) diluted 1: 20000 in 1% BSA/ND96 for 40 min at 4°C. Then oocytes were washed for 60 min at 4°C in 1% BSA/ND96 and in ND96 (60 min, 4°C) and placed separately in 50 μl ECL Plus Western Blotting Detection Reagents (Amersham Biosciences, Freiburg, Germany). After an incubation period of 5 min at room temperature, chemiluminescence was measured in a BioOrbit 1250 Luminometer (Turku, Finland). The integration period was 1 s, and the results are given in millivolts (mV).

Fluorescence measurements

Oocytes were incubated for 60 min at 4°C in ND96 media (in mM: 96 NaCl, 2 KCl, 1.8 $CaCl_2 \cdot 2\ H_2O$, 1 $MgCl_2 \cdot 6\ H_2O$, 5 HEPES, 2.5 sodium pyruvate, adjusted to pH 7.5 with NaOH) with 1% bovine serum albumin (BSA) to block non-specific binding of antibodies. Afterwards oocytes were incubated for 60 min at 4°C with 1 μg/ml mouse monoclonal anti-FLAG M2 antibody in 1% BSA/ND96, washed eight times at 4°C with 1% BSA/ND96 and incubated with goat anti-mouse IgG_1 fluorescein isothiocyanate (FITC)-conjugated (Santa Cruz Biotechnology, Heidelberg, Germany) in 1% BSA/ND96 for 60 min at room temperature and in the dark. Oocytes were washed for 60 min at room temperature and in the dark in 1% BSA/ND96 and then under the same conditions for 60 min in ND96. Images were obtained using a Zeiss Axiovert 35 inverted microscope with a × 3.2 objective and digitized with a Nikon D100 camera.

Materials and statistical analysis

All used compounds were of highest available grade of purity. Neomycin, wortmannin, phenylarsine oxide, phosphatidylinositol-specific phospholipase C from *Bacillus cereus*, and ATP were from Sigma (Taufkirchen, Germany). Edelfosine, R59022 and m-3M3FBS were from Calbiochem. The anti-PIP_2 antibody was from Echelon. Student's *t*-test *P* values <0.05 were accepted to indicate statistical significance; *n* indicates the number of experiments.

Results

Stimulation of purinergic receptors by ATP inhibits amiloride-sensitive Na^+ absorption

We examined the inhibition of amiloride-sensitive Na^+ absorption ($I_{sc\text{-}Amil}$) during a 20 min stimulation of purinergic receptors by ATP (100 μmol/l) in mouse trachea and mouse collecting duct cells (M1) in Ussing chamber experiments (Fig. 1A–D). After mounting tracheas and M1 monolayers in perfused Ussing chambers, transepithelial voltages (V_{te}) of –8.4 ± 2.4 mV (trachea, *n*=7) and –14.4 ± 1.4 mV (M1, *n*=12) were measured and equivalent short-circuit currents (I_{sc}) were calculated (Fig. 1E and F). V_{te} and I_{sc} were largely reduced by

amiloride (10 μmol/l), an inhibitor of ENaC. Luminal ATP induced transient changes in V_{te} and attenuated Na^+ absorption, as demonstrated by the reduced effects of amiloride on V_{te} and I_{sc}. The transient increase in I_{sc} is due to activation of Cl^- secretion, which contributes to the lumen negative V_{te} and thus explains why amiloride does not completely block V_{te}. Neomycin is known to bind to PIP_2 with high affinity and to inhibit hydrolysis by PLC (72). Because biological membranes are relatively impermeable for neomycin, tracheas and M1 cells were incubated in a buffer with high (5 mmol/l) neomycin concentration for 3 and 24 h, respectively. By use of this approach, regulation of the Na^+/H^+-exchanger NHE1 by PIP_2 could be demonstrated in a previous study (2). Neomycin treatment suppressed amiloride-sensitive Na^+ transport and interfered with inhibitory effects of ATP on Na^+ absorption (Fig. 1E and F). Activation of PLC by binding of ATP to purinergic receptors in airway cells, leads to an increase in intracellular Ca^{2+} and transient activation of Ca^{2+}-dependent Cl^- channels (143). Inhibition of PLC hydrolysis by neomycin reduced ATP-induced Cl^- secretion to 69.9 ± 14.3 μA/cm^2 (*n*=5), which was 224.7 ± 11.4 μA/cm^2 under control conditions (*n*=7). In contrast to mouse trachea, activation of Cl^- conductance and thus negative voltage deflection by ATP was not observed in M1 cells (Fig. 1C). The transepithelial resistances remained largely unaffected by neomycin incubation and were for M1 287.4 ± 31.2 Ωcm^2 (control) and 296.6 ± 37.4 Ωcm^2 (Neo) and for the trachea 58.2 ± 13.1 Ωcm^2 (control) and 56.1 ± 15.9 Ωcm^2 (Neo). Similar to neomycin, inhibition of $I_{sc\text{-}Amil}$ by ATP in mouse trachea was also largely attenuated by the selective inhibitor of PLC, edelfosine (ET-18-OCH3; (178), Fig. 1G). Moreover, inhibition of PIP_2 hydrolysis by edelfosine (3 h, 10 μmol/l) completely blocked the inhibitory effects of ATP on $I_{sc\text{-}Amil}$ in M1 cells (data not shown).

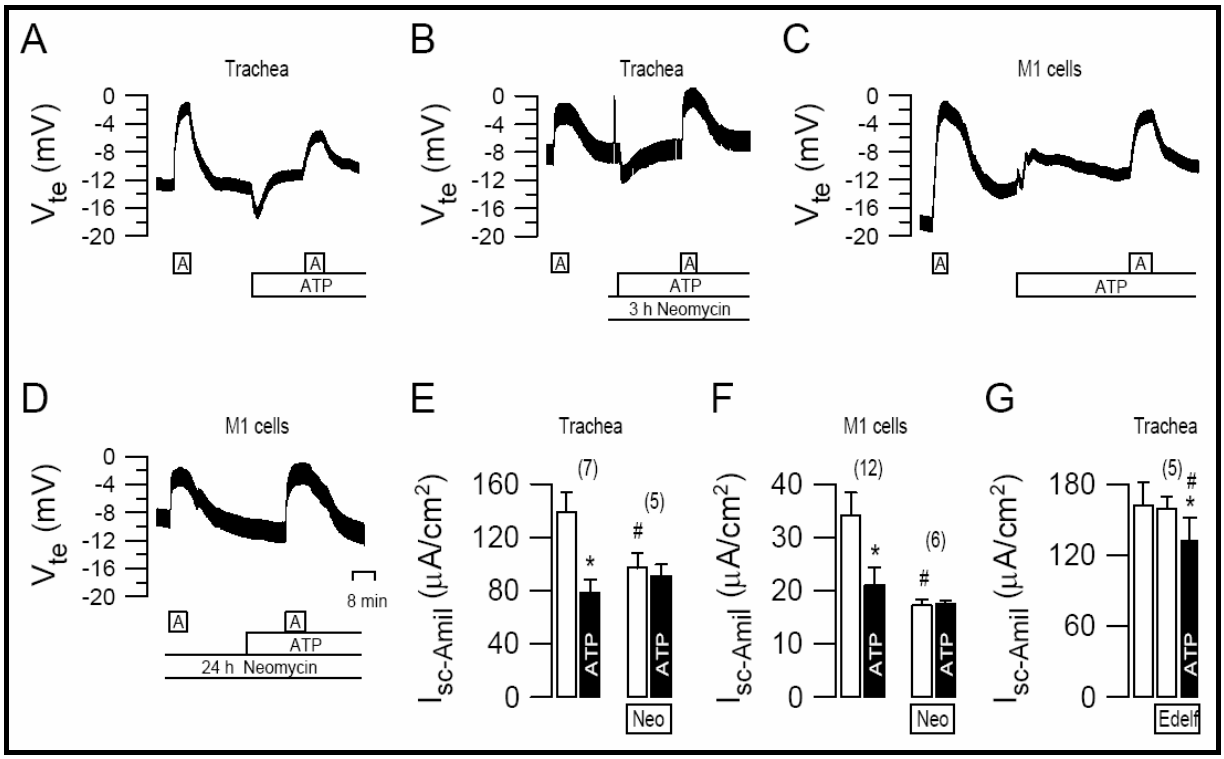

Fig. 1: Stimulation of purinergic receptors by ATP inhibits amiloride-sensitive Na^+ absorption ($I_{sc\text{-}Amil}$) in mouse trachea (A) and M1 collecting duct cells (C). Continuous recordings of the transepithelial voltage (V_{te}) in a perfused micro-Ussing chamber and effects of amiloride (A; 10 μmol/l) under control conditions (A, C) and after luminal application of ATP (100 μmol/l) (B, D). Effects of ATP after pre-incubation with neomycin (Neo, 5 mmol/l) for 3 h (trachea) and 24 h (M1), respectively. Summaries of the inhibitory effects of ATP on $I_{sc\text{-}Amil}$ in the absence or presence of neomycin (E, F). Significant inhibition of $I_{sc\text{-}Amil}$ by ATP (*paired *t*-test) and incubation with neomycin ($^{\#}$unpaired *t*-test). Incubation of mouse trachea with edelfosine (15 min, 10 μmol/l) attenuated the ATP inhibition of $I_{sc\text{-}Amil}$. Significant inhibition of $I_{sc\text{-}Amil}$ by ATP (*paired *t*-test). Attenuated effects of ATP on $I_{sc\text{-}Amil}$ in the presence of edelfosine ($^{\#}$unpaired *t*-test; G). *n*, number of experiments.

The effects of ATP on epithelial Na^+ transport in mouse trachea were reversible upon washout of ATP. Thus, within 90 min after removal of ATP, $I_{sc\text{-}Amil}$ gradually returned to resting values, which is in excellent agreement with previous kinetic analysis of receptor-activated phosphoinositide turnover (Fig. 2A and B; (68;230)). Phosphatidylinositol 4 (PI_4)-kinase is an essential enzyme of the inositol phosphate cycle necessary for resynthesis of PIP_2. The PI_4 kinase inhibitor wortmannin (10 μmol/l) blocked recovery of ATP inhibition of $I_{sc\text{-}Amil}$, similar to a recent study with neuronal M currents (Fig. 2B; (68;126;201)). Wortmannin reduced V_{te} from –10.2 ± 1.7 to –5.7 ± 0.9 mV but did not change R_{te} significantly 44.8 ± 10.2

Ωcm^2 (before wortmannin) vs. 48.3 ± 11.5 Ωcm^2 (after incubation with wortmannin). Thus, integrity of the tissue was maintained throughout the experiment.

Moreover, preincubation with wortmannin for 75 min largely reduced basal $I_{sc\text{-}Amil}$ and blocked inhibitory effects of ATP on $I_{sc\text{-}Amil}$ (data not shown). Diacylglycerol kinase is an essential enzyme for resynthesis of PIP_2. Inhibition of $I_{sc\text{-}Amil}$ by ATP in mouse trachea in the presence of R59022 (10 μmol/l), an inhibitor of the diacylglycerol kinase, was not reversible upon 90 min-washout, further supporting a role of PIP_2 hydrolysis for inhibition of Na^+ absorption (Fig. 2C; (49)). Because 10 μmol/l wortmannin may also block other enzymes, we tried to block the PI_4 kinase with phenylarsine oxide (PO; (68)). However, PO (40 μmol/l) damaged the tissue irreversibly and was therefore of no use in our study (data not shown).

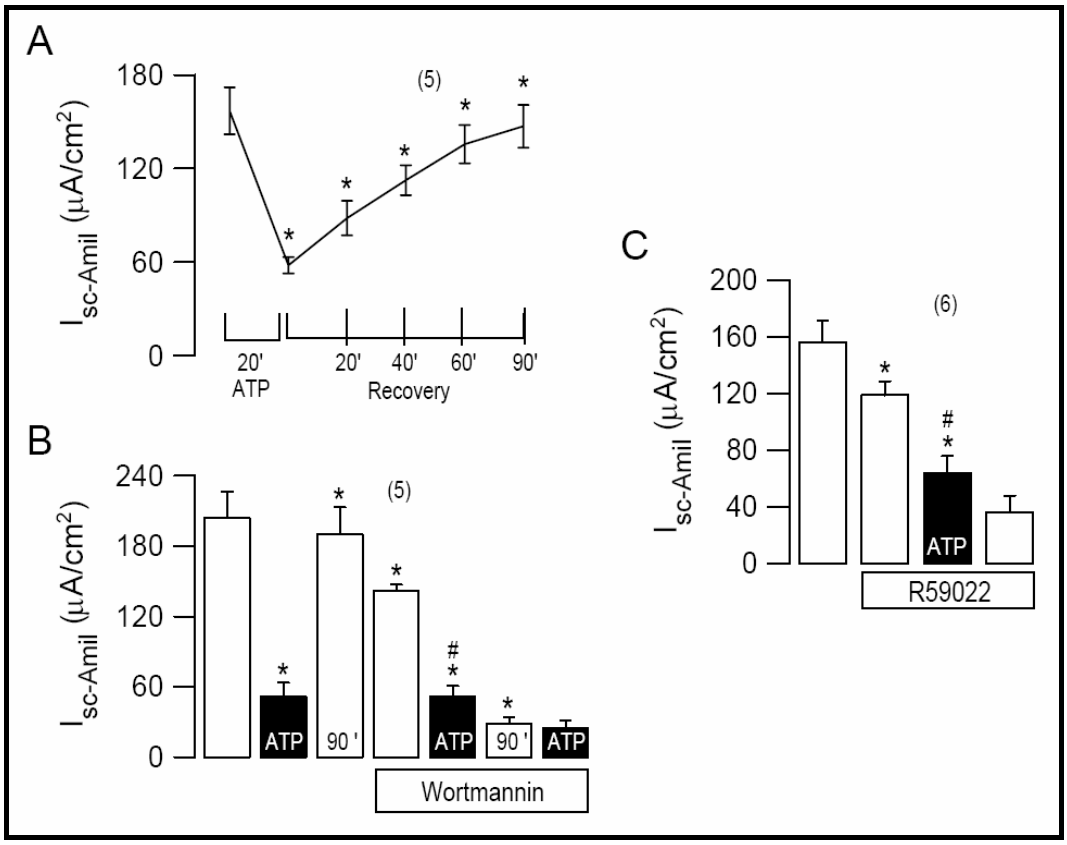

Fig. 2: Recovery of the amiloride-sensitive Na^+ absorption ($I_{sc\text{-}Amil}$) from inhibition by ATP in mouse trachea. A) Summary of $I_{sc\text{-}Amil}$ before, and during recovery from luminal application of ATP. After 90 min of washout of ATP, $I_{sc\text{-}Amil}$ has recovered almost to the same level as before application of ATP. B) Summary of experiments demonstrating inhibition of $I_{sc\text{-}Amil}$ by ATP and recovery after 90 min. Application of wortmannin (15 min, 10 μmol/l) reduces $I_{sc\text{-}Amil}$ and abolishes recovery from ATP inhibition. C) Blocking of the diacylglycerol kinase with R59022 (10 μmol/l) reduces the effects of ATP on $I_{sc\text{-}Amil}$ and abolishes recovery from the

ATP effect. *Significant difference when compared with pre-control (paired *t*-test). #Significant difference when compared with the absence of wortmannin or R59022 (unpaired *t*-test). *n*, number of experiments.

PIP_2 hydrolysis and reduced concentration of PIP_2 in the luminal membrane inhibits $I_{sc\text{-}Amil}$

The role of PIP_2 in ATP inhibition of $I_{sc\text{-}Amil}$ was examined in cells overexpressing the pleckstrin homology (PH) domain from $PLC_{\delta 3}$ fused to the green fluorescent protein (GFP). $PLC_{\delta 3}$-GFP binds to PIP_2 with high affinity, and thus PIP_2 pools can be visualized in living cells (219). In contrast, the PH domain of dynamin binds non-selectively to acidic phospholipids (240). Thus, a broader cellular staining was expected in cells transfected with dynamin-GFP. GFP fluorescence was detected in polarized grown M1 cells transiently expressing $PLC_{\delta 3}$-GFP or dynamin-GFP. In addition, parallel staining of actin filaments was performed using phalloidin-rhodamine. X/Y scans revealed staining of the plasma membrane in cells transfected with $PLC_{\delta 3}$-GFP, while dynamin-GFP transfected cells demonstrated cytosolic GFP fluorescence (Fig. 3A–C). Confocal X/Z scans indicated a predominant location of the GFP fluorescence to the luminal membrane in $PLC_{\delta 3}$-GFP transfected cells in the absence of extracellular ATP (Fig. 3A). When $PLC_{\delta 3}$-GFP transfected monolayers were pre-incubated with ATP (100 μmol/l, 30 min), GFP fluorescence in the apical membrane was reduced, which suggests ATP-induced hydrolysis of luminal PIP_2 and thus depletion of apical PIP_2 pools (Fig. 3B).

We examined the recovery of $I_{sc\text{-}Amil}$ from inhibition by ATP in M1 cells transfected with either $PLC_{\delta 3}$-GFP or dynamin-GFP (128) in Ussing chamber experiments. Baseline $I_{sc\text{-}Amil}$ was reduced in cells transfected with $PLC_{\delta 3}$-GFP but not in dynamin-GFP transfected cells. ATP stimulation further reduced $I_{sc\text{-}Amil}$ significantly in both dynamin-GFP or $PLC_{\delta 3}$-GFP expressing cells. In dynamin-GFP transfected cells, $I_{sc\text{-}Amil}$ gradually and significantly recovered from ATP-dependent inhibition within 90 min-washout, presumably due to time-dependent replenishment of apical PIP_2 pools (Fig. 3D). In contrast, in tissues transfected by the $PLC_{\delta 3}$-GFP, $I_{sc\text{-}Amil}$ did not recover from inhibition by ATP within 90 min, probably due to high-affinity binding of $PLC_{\delta 3}$-GFP to PIP_2 and delayed refilling of apical PIP_2 pools (Fig. 3E).

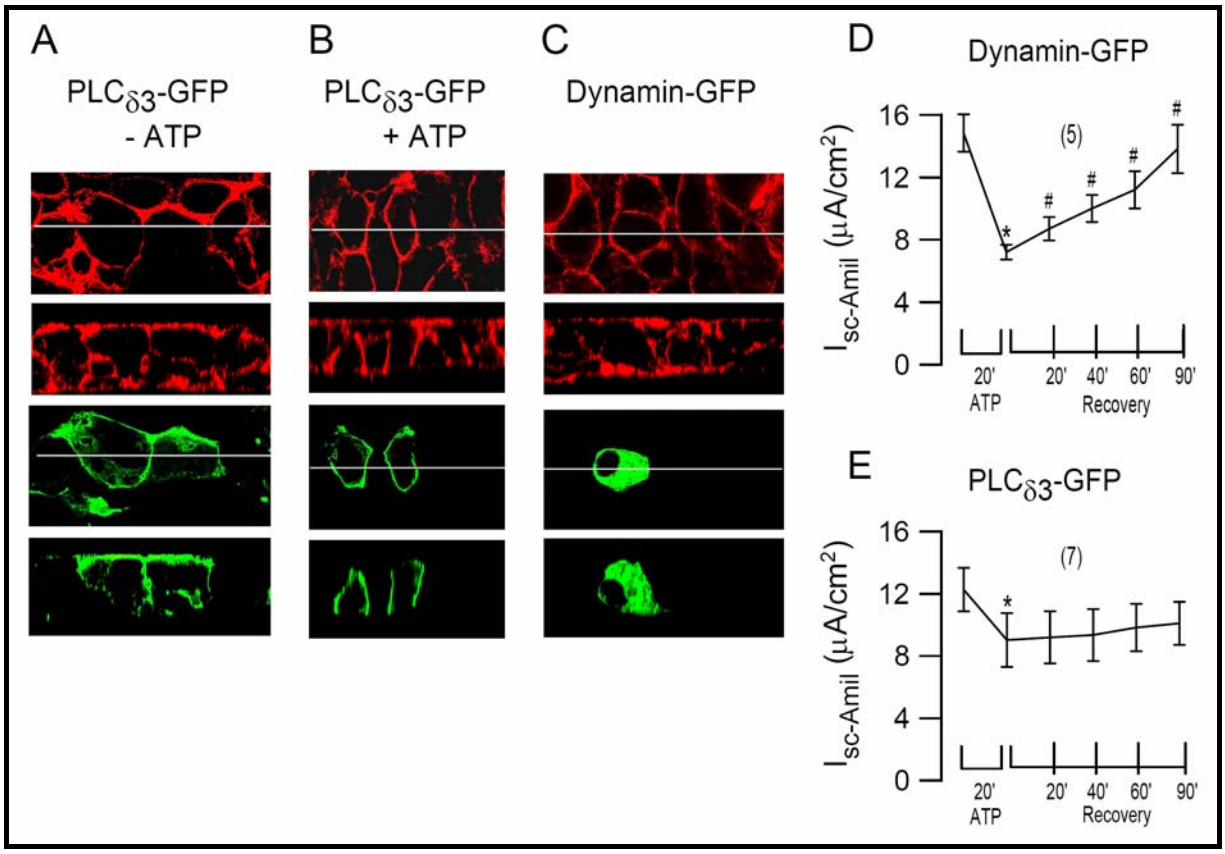

Fig. 3: Confocal microscopy of polarized grown M1 mouse collecting duct cells transiently transfected with either $PLC_{\delta 3}$-GFP cDNA or dynamin-GFP cDNA. Images are representative for *n*=3 experiments for each series. *White lines* indicate position of the XZ scan in the focal plane (XY scan). Actin filaments were stained with phalloidin-rhodamine (red). $PLC_{\delta 3}$-GFP transfected cells demonstrated staining of the cell membrane (green). A) In the absence of ATP, the luminal compartment was stained predominantly. B) Stimulation with ATP (20 min, 100 μmol/l) reduced GFP labeling of luminal but not lateral membranes. C) GFP fluorescence detected in dynamin-GFP transfected cells. D, E) Summary of amiloride-sensitive short-circuit currents $I_{sc\text{-}Amil}$ in M1 cells expressing $PLC_{\delta 3}$-GFP cDNA or dynamin-GFP, before and after stimulation with ATP (20 min, 100 μmol/l) and during 90 min-washout. *Significant inhibition of $I_{sc\text{-}Amil}$ by ATP. $^{\#}$Significant recovery from inhibition by ATP (paired *t*-test). *n,* number of experiments.

Similar to the results obtained in mouse trachea, the PI_4 kinase inhibitor wortmannin (10 μmol/l; 3 h) reduced $I_{sc\text{-}Amil}$ and the short-circuit current that is inhibited by ATP (data not shown). Taken together, these results suggest that the inhibitory effect of ATP on $I_{sc\text{-}Amil}$ is mediated by hydrolysis of PIP_2, resulting in a loss of ENaC/PIP_2 interaction.

Interaction of ENaC with PIP_2

The data point out to an interaction of the epithelial Na^+ channels with PIP_2. PIP_2 binding motifs have been identified in N termini of β- and γENaC, but not in the α subunit (235). This was further examined by immunoprecipitation of lysates isolated from M1 cells, using an anti-PIP_2 antibody (Echelon). Immunoprecipitates were detected by SDS-PAGE and Western blotting using rabbit polyclonal anti-β- or anti-γENaC antibodies. Precipitation by PIP_2 was clearly detectable for βENaC but was less obvious for γENaC (Fig. 4B). As shown in Fig. 4B (first lanes), precipitation by endogenous PIP_2 (-PIP_2) resulted in a weak band only. Immunoprecipitation was done in the presence of phosphatase inhibitor in order to avoid spontaneous hydrolysis of PIP_2. We controlled for possible effects of these inhibitors on ENaC in Ussing chamber experiments. As shown in Fig. 4C, application of the phosphatase inhibitor did not affect amiloride-sensitive Na^+ transport. Moreover, including ATP (1 mmol/l) in the buffer used for the immunoprecipitation did not affect the result (data not shown). We examined whether ATP-dependent inhibition of ENaC could be demonstrated in *Xenopus* oocytes and thus co-expressed both ENaC and $P2Y_2$ receptors. Stimulation with ATP (100 μmol/l) activated Ca^{2+}-dependent Cl^- channels and increased the whole cell current transiently. Activation of $P2Y_2$ receptors also largely reduced amiloride-sensitive currents (Fig. 4D). Effects on ENaC currents were not observed in oocytes solely expressing ENaC (Fig. 4E). Moreover, hydrolysis of PIP_2 and inhibition of ENaC in *Xenopus* oocytes was induced by injecting (1 U in 47 nl) phosphatidylinositol-specific phospholipase C from *Bacillus cereus* and by incubation with the membrane-permeable direct activator of phospholipase C, m-3M3FBS (10 μmol/l; (10)). Interfering with PIP_2 synthesis by 24 h incubation in wortmannin (10 μmol/l), injection of neomycin (1 mol/l, 47 nl), or incubation of oocytes in ND96 solution at pH 6.0 (1 h), all reduced G_{Amil}. H_2O injection (47 nl) was without effects on G_{Amil} (Fig. 4F). Phenylarsine oxide could not be used since it was toxic to oocytes. Taken together, inhibition of ENaC by ATP binding to $P2Y_2$ receptors in *Xenopus* oocytes probably occurs through PIP_2 hydrolysis.

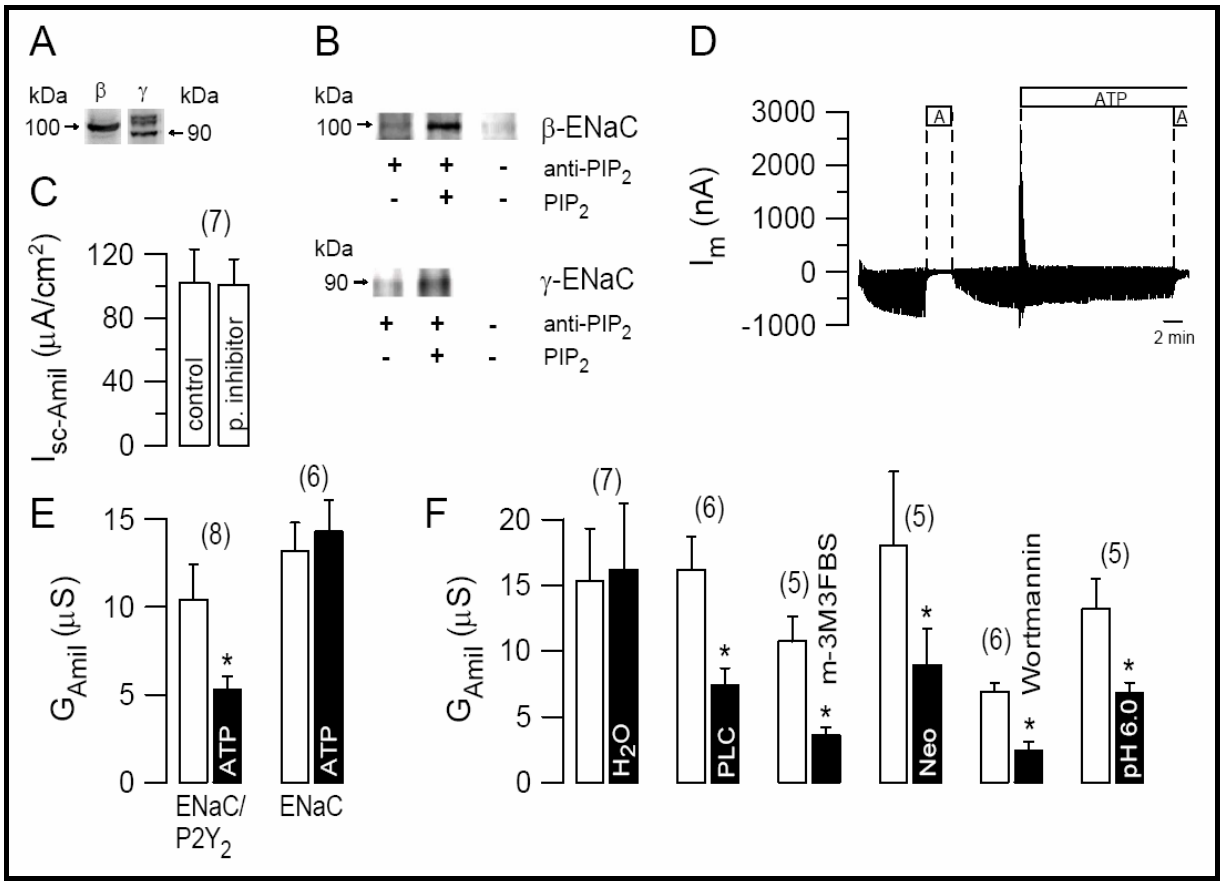

Fig. 4: A) Western blot analysis of βENaC and γENaC in M1 cells and B) co-immunoprecipitation of βENaC and γENaC with PIP_2. Cell lysates were immunoprecipitated with anti-PIP_2 antibody in the absence or presence of exogenous PIP_2 (10 μmol/l) and the immunoprecipitates resolved on gels and blots detected with subunit-specific ENaC antibodies. C) Effect of phosphatase inhibitor on $I_{sc\text{-}Amil}$ in mouse trachea. D) Inhibition of ENaC by ATP (100 μmol) in *Xenopus* oocytes co-expressing α,β,γ-wtENaC and the purinergic $P2Y_2$ receptor. Original recording showing the effects of ATP and the inhibition of the amiloride-sensitive (A, 10 μmol/l) part of the whole cell current (I_m). E) Summary of the inhibitory effects of ATP on amiloride-sensitive whole cell conductance in ENaC/$P2Y_2$ co-expressing oocytes but not in oocytes expressing ENaC only. F) G_{Amil} in ENaC expressing oocytes before and after treatment: H_2O injection (47 nl), injection of phospholipase C (PLC, 1 U in 47 nl), incubation with the PLC activator m-3M3FBS (10 μmol/l in 47 nl, 30 min), injection of neomycin (Neo, 1 mol/l, 47 nl), incubation in wortmannin (10 μmol/l, 47 nl, 25 h) and exposure to ND96, pH 6.0 (1 h). *Significant difference when compared with pre-control (paired *t*-test). *n,* number of experiments.

We tried to further verify the importance of the putative PIP_2 binding of ENaC. To that end, the binding motifs in β- and γENaC were mutated by replacing 2 (β2N, γ2N) or 4 (β4N, γ4N) positively charged amino acid residues in the N-terminal PIP_2 binding region by non-polar amino acids (cf, Fig. 5A). Wild-type and mutant ENaC proteins were expressed in oocytes and amiloride-sensitive currents were recorded. Heterotetrameric channels containing αwt,βwt,γ2N-ENaC (γ2N) and αwt,βwt,γ4N-ENaC (γ4N) produced currents indistinguishable to wild-type currents (αβ,γwt). In contrast, αwt,β2N,γwt-ENaC (β2N) produced amiloride-sensitive whole cell currents, which were significantly reduced when compared with wild-type ENaC. Replacing four charged residues (β4N) almost abolished whole cell currents (Fig. 5).

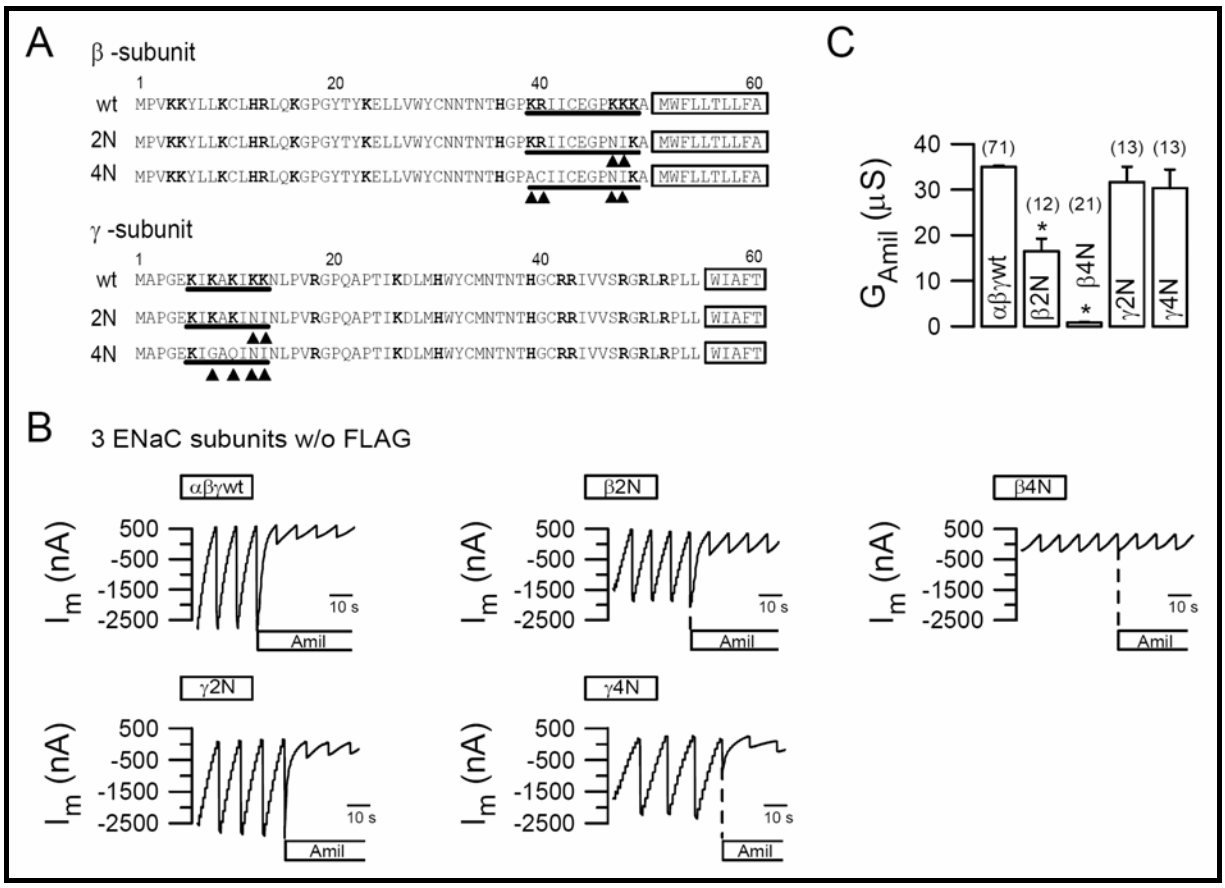

Fig. 5: The PIP_2 binding domain in βENaC is required for ENaC channel activity. A) Amino acid sequence of the putative PIP_2 binding domain in βENaC and γENaC and generated mutations. B) Original recordings of whole cell currents (I_m) in *Xenopus* oocytes expressing α,β,γ-wtENaC or ENaC in which either the β subunit (β2N, β4N) or the γ subunit (γ2N, γ4N) have been mutated. Whole cell currents were measured during continuous voltage clamp from –90 mV to +30 mV in steps of 10 mV. C) Summary of the calculated G_{Amil}. αwt,βwt,γ2N-ENaC (γ2N) and αwt,βwt,γ4N-ENaC (γ4N) produce currents indistinguishable from that of α,β,γ-wtENaC. Conductances produced by the double mutant

αwt,β2N,γwt-ENaC (β2N) were attenuated and were almost abolished for the quadruple mutant αwt,β4N,γwt-ENaC (β4N). *Indicates significant difference from βγwt (unpaired *t*-test). *n*, number of experiments.

Similar results were obtained by expression of only two subunits (Fig. 6A). Reduced current amplitudes could be due to impaired PIP_2 activation of ENaC, lower surface expression of the mutant channels, or simply by reduced expression of β2N and β4N. Using FLAG-tagged ENaC subunits (kindly provided by B. Rossier, University of Lausanne, Switzerland), we found that expression of FLAG-tagged β2N and β4N were, if at all, enhanced but not reduced (Fig. 6B). Whole cell conductances generated by FLAG-tagged subunits were comparable with that of the non-flagged subunits (Fig. 6C). Thus, loss of amiloride-sensitive Na^+ currents by mutating the PIP_2 binding domain in βENaC is due to either reduced surface expression or lower activity of the channel.

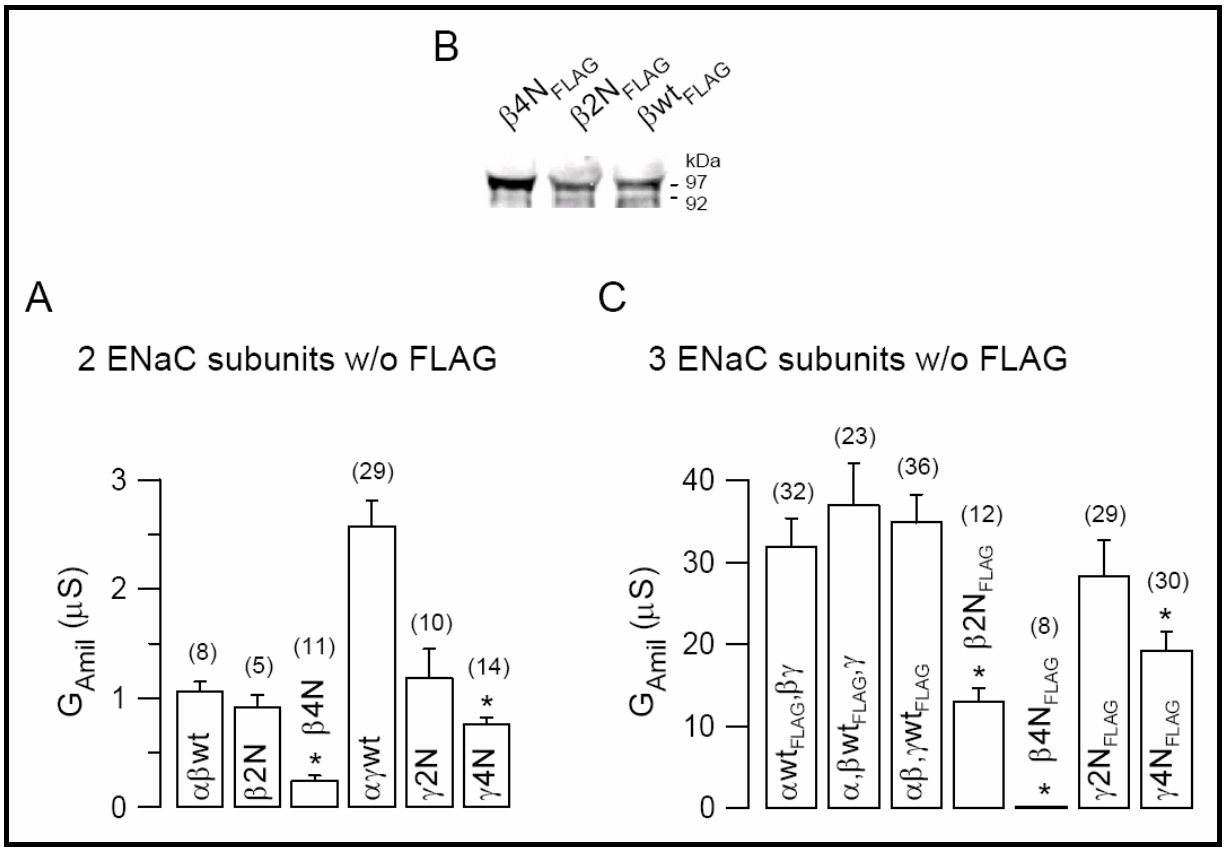

Fig. 6: *Xenopus* oocytes expressing FLAG-tagged ENaC. A) Summary of G_{Amil} generated by co-expression of only two ENaC subunits (αβENaC or αγENaC) in *Xenopus* oocytes and effects of mutations in βENaC or γENaC. B) Western blot of FLAG-tagged β4N, β2N and βwt co-expressed with wt αγENaC in *Xenopus* oocytes. C) Summary of the calculated amiloride-

sensitive whole cell conductances (G_{Amil}) generated by co-expression of non-tagged βγ-, αγ-, or αβ subunits together with wild-type and mutant FLAG-tagged α β γ subunits. *Indicates significant differences from βwt and γwt, respectively (unpaired *t*-test). *n*, number of experiments.

PIP_2 binding domain in βENaC controls channel activity rather than surface expression

By two different methods we examined whether mutations in the PIP_2 binding domain affect surface expression in *Xenopus* oocytes. Ooctyes were injected with FLAG-tagged wild-type or mutant ENaC subunits, and currents were measured in double electrode voltage clamp experiments. These oocytes were incubated first with a monoclonal anti-FLAG M2 antibody and then with a FITC-conjugated goat anti-mouse IgG_1. Little FITC fluorescence was detected in water-injected oocytes. In contrast, bright FITC fluorescence was detected in all oocytes expressing either wt or mutant β- or γ subunits (Fig. 7A). Surface expression was quantified by chemiluminescence. After oocytes were incubated with anti-FLAG M2 (clone M2, Sigma-Aldrich, Germany) and anti-mouse peroxidase-linked antibodies (Amersham Biosciences, Germany), chemiluminescence was measured for 1 s and was expressed in millivolts (mV). The signal was larger for the α_{FLAG}-injected oocytes, explained by the two α subunits present in the heterotetrameric channel, but was otherwise identical in oocytes expressing either wild-type or mutant ENaC. Thus, the reduced Na^+ conductance generated by PIP_2 binding mutants of βENaC is due to reduced channel activity rather than changes in surface expression.

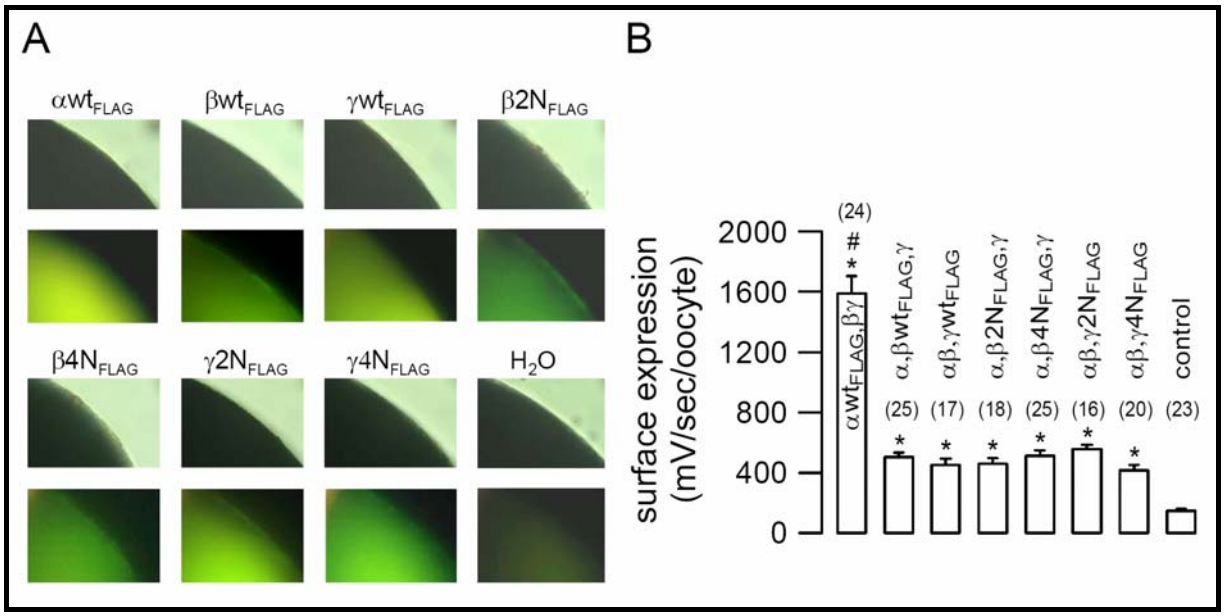

Fig. 7: A) Detection of surface expression of ENaC subunits by fluorescence labeling of ENaC subunits in intact *Xenopus* oocytes. Bright field images indicating location of the oocyte. FLAG-tagged ENaC subunits were detected by staining with primary anti-FLAG and secondary FITC-conjugated antibodies. B) Detection of surface expression of ENaC subunits by chemiluminescence measurements of intact *Xenopus* oocytes. FLAG-tagged ENaC subunits were detected by staining with primary anti-FLAG and secondary IgG peroxidase-linked antibodies. Chemiluminescence was integrated over 1 s and is expressed in mV. *,#Indicate difference from control and β- or γ FLAG-tagged subunits, respectively (unpaired *t*-test). *n*, number of experiments.

In addition, *Xenopus* oocytes co-expressing FLAG-tagged ENaC subunits together with $P2Y_2$ were stimulated with ATP (100 μmol/l). As shown in Fig. 8, surface expression of the tagged ENaC subunits remained unchanged during activation of the $P2Y_2$ receptor. Thus, purinergic inhibition of ENaC currents is due to inactivation of ENaC channels rather than channel endocytosis.

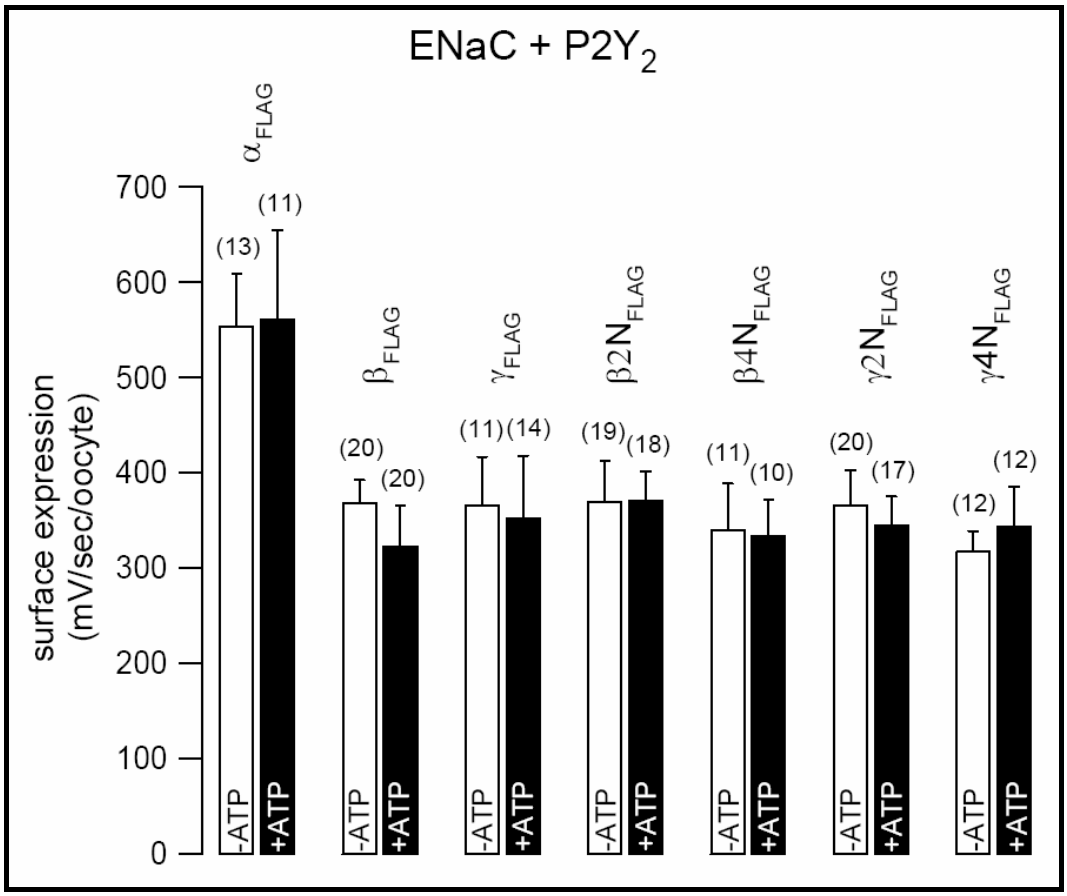

Fig. 8: *Xenopus* oocytes co-expressing FLAG-tagged ENaC together with $P2Y_2$. Detection of surface expression of ENaC subunits by chemiluminescence measurements of intact *Xenopus* oocytes. FLAG-tagged ENaC subunits were detected by staining with primary anti-FLAG and secondary IgG peroxidase-linked antibodies. Stimulation of the oocytes with ATP (100 μmol/l, *black bars*) did not change surface expression. Chemiluminescence was integrated over 1 s and is expressed in mV. *n*, number of experiments.

Discussion

A physiologically and pathophysiologically important regulation of ENaC

A role of extracellular ATP as important signalling molecule has been proposed. Luminal purinergic receptors along the nephron may control cell volume during solute transport (127;194). Compartmentalized autocrine signalling activates Cl^- secretion in the respiratory tract and is thought to resemble a mechanism to “flush” noxious particles away from airway surfaces (90). The present findings may be of potential interest for a novel pharmacological approach to cystic fibrosis. In recent years, it has been demonstrated that activation of purinergic receptors in airway epithelia by extracellular nucleotides improves mucus clearance in CF. This is due to activation of Ca^{2+}-dependent Cl^- channels and attenuation of

excessive Na^+ absorption. Clinical trials are underway to test the effects of synthetic purinergic compounds on the progression of lung disease in CF patients (122). The present data indicate a strong regulatory impact of PIP_2 on ENaC. Thus, compounds that interfere with the PIP_2 metabolism and deplete airway epithelial cells of PIP_2 could be used for deactivation of ENaC and inhibition of Na^+ absorption.

How is ENaC regulated by PIP_2?

Phospholipid regulation of ion channels has unmasked a functional link between membrane metabolism and ion channel activity (83). A metabolism-excitation coupling has been described for K_{ATP} channels, where PIP_2 largely controls the nucleotide sensitivity of the K_{ATP} channel (12;199). Mechanosensitivity of GIRK K^+ channels has been shown to be mediated by PKC-dependent channel-PIP_2 interaction (239). A protein kinase-independent activation of CFTR Cl^- channels has been found in one but not in another study (83;85). For transient receptor potential like (TRPL) channels, inhibitory and activatory effects of PIP_2 have been found (132). PIP_2 activates K_{ATP} channels as well as the delayed rectifier potassium channel KCNQ1/KCNE1 and KCNQ2/KCNQ3 channels, forming the M current in neuronal cells (89;134;238). Incubation of neuronal cells with wortmannin prevented recovery from receptor-mediated inhibition of M currents and blocked PIP_2 replenishment of the cell membrane. Recovery of ENaC currents from ATP inhibition was also abolished after treatment with wortmannin, which inhibits conversion of phosphatidylinositol to PI(4)P by the PI_4 kinase. Similar to that, wortmannin caused a rapid loss of the hormone-sensitive PIP_2 pool after angiotensin II stimulation of glomerulosa cells (167). Thus, the present data indicate upregulation of ENaC activity by PIP_2, probably due to an increase in the open probability of ENaC as suggested earlier (137;235). Further experiments will have to elucidate the impact of PIP_2 on channel kinetics and may identify a possible stabilization of the channel open state, as suggested for both K_{ATP} and KCNQ1/KCNE1 channels (61;134).

PIP_2 regulation of ENaC in lipid rafts?

The present results trigger the challenging question whether purinergic and thus PIP_2-dependent regulation of ENaC in the luminal membrane of epithelial cells takes place in lipid rafts. This is not unlikely because localization of ENaC in cholesterol and PIP_2-rich microdomains has been shown recently (84). For inhibition of ENaC to take place, PIP_2 hydrolysis should occur in close proximity to the channel, and thus co-localization of ENaC and $P2Y_2$ in lipid rafts would offer an ideal platform for receptors/channel interaction. Membrane staining by binding of $PH_{PLC\delta}$-GFP to PIP_2 in the inner leaflet of non-polarized cells has been shown recently (48). PLC activation through ionomycin-induced hydrolysis of PIP_2 and redistributed GFP fluorescence to the cytosolic compartment (2). The present data

show location of PIP_2 predominantly in the luminal membrane of polarized M1 epithelial cells and suggest emptying of these apical PIP_2 pools by stimulation with ATP. PIP_2 turnover requires permanent resynthesis by ATP-consuming kinases. A rundown of ENaC activity is often observed in ENaC expressing oocytes or during patch clamp experiments and inclusion of ATP into the patch pipette prevents channel rundown (94;224). This was explained by a direct non-hydrolytic action of ATP on ENaC. However, rundown of ENaC activity in the absence of ATP may also be explained by dephosphorylation and loss of PIP_2 (137).

A binding pocket for PIP_2 in ENaC?

PIP_2 binding domains from various proteins, including K_{ATP} channels, contain a lipid interaction domain with conserved structural features. This domain is formed by clustered positively charged residues in a β-strand binding pocket, such as formed by the intracellular COOH terminus of K_{ATP}. It probably mediates electrostatic interaction with the negatively charged phosphates of PIP_2 (48;57;62;217). However, highly conserved positively charged amino acids were also localized in the NH_2 terminus of the channel, which are crucial for PIP_2 binding and changes in pH and ATP sensitivity (12;57;62;217). Thus, both NH_2 and COOH termini participate in the control of K_{ATP} channel activity by PIP_2. Because similar could hold true for the PIP_2-dependent regulation of ENaC, we analyzed the distribution of positively charged amino acids in β- and γ subunits of ENaC. In fact, COOH termini in both β- and γ subunits contain numerous arginine residues, which could serve as potential sides for PIP_2 interaction. In additional experiments we generated COOH truncation mutants of β (βV561X, βR561X)- and γ (γS608X, γR565X) ENaC but found no change in amiloride-sensitive whole cell currents after expression in *Xenopus* oocytes (unpublished from the author's laboratory).

According to our data, the N terminus of γENaC does not participate in PIP_2-dependent regulation. Moreover γENaC was only weakly co-immunoprecipitated by PIP_2. Lack of importance of γENaC for PIP_2-dependent regulation is further supported by chimeric subunit, in which the initial 95 amino acids in the N terminus of γENaC were replaced by the N terminus of αENaC. This α/γ chimera produced normal ENaC currents upon co-expression with α- and β subunits. In contrast, elimination of the N terminus in βENaC abolished Na^+ currents almost completely (unpublished from the author's laboratory). These results suggest that PIP_2-dependent regulation of ENaC is limited to the putative PIP_2 binding side in the NH_2 terminus of βENaC. Thus, the COOH terminus of ENaC determines surface expression of the channel, whereas the NH_2 terminus regulates channel activity, probably by controlling the single channel open probability.

Chapter 3

Cl^- interference with the epithelial Na^+ channel ENaC

Abstract

The cystic fibrosis transmembrane conductance regulator (CFTR) is a protein kinase A and ATP-regulated Cl^- channel that also controls the activity of other membrane transport proteins, such as the epithelial Na^+ channel ENaC. Previous studies demonstrated that cytosolic domains of ENaC are critical for downregulation of ENaC by CFTR, while others suggested a role of cytosolic Cl^- ions. We therefore examined in detail the anion-dependence of ENaC and the role of its cytosolic domains for the inhibition by CFTR and the Cl^- channel CLC-0. Co-expression of rat ENaC with human CFTR or the human Cl^- channel CLC-0 caused inhibition of amiloride-sensitive Na^+ currents after cAMP-dependent stimulation and in the presence of a 100 mM bath Cl^- concentration. After activation of CFTR by 3-isobutyl-1-methylxanthine and forskolin or expression of CLC-0, the intracellular Cl^- concentration was increased in *Xenopus* oocytes in the presence of a high bath Cl^- concentration, which inhibited ENaC without changing surface expression of $\alpha\beta\gamma$ENaC. In contrast, a 5 mM bath Cl^- concentration reduced the cytosolic Cl^- concentration and enhanced ENaC activity. ENaC was also inhibited by injection of Cl^- into oocytes and in inside/out macropatches by exposure to high cytosolic Cl^- concentrations. The effect of Cl^- was mimicked by Br^-, NO_3^- and I^-. Inhibition by Cl^- was reduced in trimeric channels with a truncated COOH terminus of βENaC and γENaC, and it was no longer detected in dimeric $\alpha\Delta C\beta$ ENaC channels. Deletion of the NH_2 terminus of α-, β-, or γENaC, mutations in the NH_2-terminal phosphatidylinositol-bisphosphate binding domain of βENaC and γENaC and activation of phospholipase C, all reduced ENaC activity but allowed for Cl^--dependent inhibition of the remaining ENaC current. The results confirm a role of the carboxyl terminus of βENaC for Cl^--dependent inhibition of the Na^+ channel, which, however, may only be part of a complex regulation of ENaC by CFTR.

Introduction

The cystic fibrosis transmembrane conductance regulator (CFTR) is a cAMP-regulated Cl^- channel and a regulator of other channels. A large number of membrane proteins and cellular processes are reported to be controlled by CFTR (117;193). Most work has been devoted to the inhibitory effect of CFTR on the epithelial Na^+ channel ENaC. Missing inhibition of ENaC by defective CFTR in cystic fibrosis (CF) is regarded as an important reason for the enhanced epithelial Na^+ conductance detected in the airways of CF patients (31;120;138). A regulatory relationship has been shown for CFTR and ENaC in human and murine airway and intestinal epithelia (138;139), and enhanced Na^+ absorption has been demonstrated in airways and colonic epithelia carrying the CF defect (31). Subsequent studies showed that the epithelial Na^+ channel is inhibited in recombinant and native cells during activation of CFTR (34;95;98;111;129;138;139;142;210).

Studies were performed to uncover the mechanism of the reciprocal interaction between CFTR and ENaC. Two-hybrid analysis and co-immunoprecipitation suggested a direct molecular interaction between CFTR and αENaC, and the first nucleotide binding domain of CFTR was found to be crucial for inhibition of ENaC (97;121;191). Another study found a role of the carboxyl terminus of βENaC for downregulation of ENaC by activation of CFTR in *Xenopus* oocytes (97). When CFTR and ENaC were reconstituted in a cell-free planar lipid bilayer, carboxyl-terminal domains of β- and γENaC were found to modulate the kinetics of the channel, whereas the NH_2 terminus β- and γENaC were in charge of CFTR-dependent regulation of heterodimeric αβ- and αγENaC but not in heterotrimeric αβγENaC (18). We and others found that truncations or Liddle's disease mutations in the COOH terminus of α-, β- and γENaC do not abolish CFTR-dependent inhibition of ENaC in trimeric channels (86;110). However, the COOH-terminal 20 amino acid residues of αENaC conferred species specificity of ENaC inhibition by CFTR in another study (231). Most studies agreed that CFTR affects ENaC channel kinetics and open probability rather than surface expression of ENaC (18;97;110). For mutant CFTR, which is unable to inhibit ENaC, genistein was shown to restore the functional interaction between CFTR and ENaC (142;211;212). Interestingly, the reverse namely an upregulation of CFTR currents by ENaC co-expression, has also been observed (98;111).

Possible contributions by additional proteins and factors to the CFTR regulation of ENaC has been examined in subsequent studies. CFTR carries a so-called PDZ-binding domain, a common site for protein interaction at the COOH terminus, which binds regulatory proteins such as NHERF (225). This PDZ domain is essential for proper expression of CFTR in the

apical plasma membrane of polarized cells (162;163). Whereas in *Xenopus* oocytes this domain was neither important for expression of CFTR nor for inhibition of ENaC by CFTR, in polarized epithelial cells NHERF affects expression of both CFTR and ENaC (33;190). Other mechanisms were excluded, such as release of ATP by CFTR, followed by purinergic inhibition of ENaC (108). Also changes in cell volume, which may occur during activation of Cl^- conductances, are unlikely to explain the negative effects of CFTR on ENaC (192). However, independent reports demonstrated a role of Cl^- ions (97;109). It has known for some time that Na^+ and Cl^- conductances are controlled by the cytosolic Cl^- concentration in intralobular duct cells of the mouse mandibular gland (54). Subsequent studies demonstrated that the control of ENaC currents by intracellular anions is mediated by G proteins in salivary duct cells, but not in *Xenopus* oocytes (53;91). Different mechanisms have been shown for inhibition of ENaC by cytosolic Na^+ and Cl^- (107). Our initial work suggested that influx of Cl^- into the oocyte rather than the efflux is inhibiting ENaC (34). Although a role of Cl^- for the inhibition of ENaC by CFTR was not found in all studies (42;110), subsequent work in both epithelial tissues and *Xenopus* oocytes confirmed that intracellular Cl^- ions decrease expression of ENaC protein (169) and acutely inhibit ENaC currents (97;109;190;229). Recent studies with polarized epithelial cells expressing ENaC along with CFTR and Ca^{2+}-activated Cl^- channels, demonstrate an increase in intracellular Cl^- by stimulation of CFTR or Ca^{2+}-dependent Cl^- channels (1). This increase in intracellular Cl^- is paralleled by inhibition of amiloride-sensitive Na^+ conductance. Amiloride-sensitive Na^+ currents are also inhibited in patch clamp experiments, when high Cl^- concentrations are present on the cytosolic side (1;190). These results strongly suggest a role of Cl^- ions for inhibition of ENaC by CFTR or other Cl^- channels. These channels cause an increase in the intracellular Cl^- concentration when a large parallel Na^+ conductance is present (118). We therefore tried in the present study to identify a Cl^--sensitive side in ENaC. We found that amino and carboxyl termini of α-, β-, and γENaC control ENaC activity and show a role of the COOH terminus of βENaC for inhibition by Cl^-.

Material and Methods

Ussing chamber experiments

Mouse M1 collecting duct cells were grown to confluence on permeable supports and were mounted into a modified Ussing chamber with a circular aperture of 0.95 mm^2. M1 cells are derived from mouse cortical collecting duct and have properties of principal cells (kindly provided by C. Korbmacher, Physiologisches Institut, Universität Erlangen, Germany). Luminal and basolateral sides of the epithelium were perfused continuously at a rate of 10 ml/min (chamber volume 2 ml). The bath solution had the following composition (mmol/l): NaCl 145,

KH_2PO_4 0.4, K_2HPO_4 1.6, D-glucose 5, $MgCl_2$ 1, HEPES 5, Ca-gluconate 1.3. pH was adjusted to 7.4. Bath solutions were heated to 37°C using a water jacket. Experiments were carried out under open-circuit conditions. Values for transepithelial voltages (V_{te}) were referred to the serosal side of the epithelium. Transepithelial resistance (R_{te}) was determined by applying short (1 s) current pulses (ΔI=0.5 μA) and the resistance of the empty chamber was subtracted. R_{te} was calculated according to Ohm's law ($R_{te}=\Delta V_{te}/\Delta I$). The equivalent short-circuit current (I_{sc}) was calculated ($I_{sc}=V_{te}/R_{te}$) and the amiloride-sensitive I_{sc} ($I_{sc\text{-}Amil}$) is used to express the amount of equivalent short-circuit current that is inhibited by 10 μmol/l amiloride. Tissue preparations were only accepted if the transepithelial resistance exceeded that of an empty chamber at least by a factor of 3. The transepithelial resistance of filter grown M1 cells was 387 ± 39 Ωcm^2 (*n*=20).

cRNAs for ENaC subunits, CFTR and CLC-0 and ENaC mutants

cDNAs encoding rat αβγENaC (kindly provided by Prof. Dr. B. Rossier, Pharmacological Institute of Lausanne, Switzerland) and the Cl^- channels CFTR or CLC-0 were linearized in pBluescript or pTLN (105) with *Not*I or *Mlu*I, and *in vitro* transcribed using T7, T3 or SP6 promotor and polymerase (Promega, USA). For some experiments cDNAs of FLAG-tagged αβγENaC subunits were used (kindly provided by Prof. B. Rossier, University of Lausanne, Switzerland) (67). Isolation and microinjection of oocytes have been described in a previous report (142). In brief, after isolation from adult *Xenopus laevis* female frogs (*Xenopus* express, South Africa and Kähler, Germany), oocytes were dispersed and defolliculated by a 45 min-treatment with collagenase (type A, Boehringer, Germany). Subsequently, oocytes were rinsed and kept at 18°C in NMDG/ND96 buffer (in mmol/l): NMDG 96, HCl 80, KCI 2, $CaCl_2$ 1.8, $MgCl_2$ 1, HEPES 5, sodium pyruvate 2.5, pH 7.55, supplemented with theophylline (0.5 mmol/l) and gentamycin (5 mg/l). Mutations in the NH_2-terminal phosphatidylinositol-bisphosphat PIP_2 binding domains of β- and γENaC were generated by replacing 2 (β2N, γ2N) and 4 (β4N, γ4N) positively charged amino acids by non-polar (N) amino acids as described in Ref. 119. αΔN, βΔN and γΔN indicate that the NH_2 terminus of α-, β-, and γ subunits was shortened by removing the first 94, 50, and 94 initial amino acids, respectively, and in some cases replaced by other N-terminal subunits (116). All other mutations and truncations (αP671A, αΔC=αH647X, βΔC=βR561X and βV554X, γΔC=γS608X and γR565X) have been generated by PCR techniques and correct sequences were verified by sequencing.

Double electrode voltage clamp

Oocytes were injected with cRNA (1–10 ng) after dissolving in 47 nl double-distilled water (Nanoliter Injector WPI, Germany). Water-injected oocytes served as controls. 2–4 days after

injection, oocytes were impaled with two electrodes (Clark instruments) that had a resistance of <1 MΩ when filled with 2.7 mol/l KCI. Using two bath electrodes and a virtual-ground headstage, the voltage drop across R_{serial} was effectively zero. Membrane currents were measured by voltage clamping of the oocytes (Warner oocyte clamp amplifier OC725C) in intervals from –90 to +30 mV, in steps of 10 mV, each 1 s. Conductances were calculated according to Ohm's law and amiloride-sensitive conductances (G_{Amil}) were used in the present report to express the amount of whole cell conductance that is inhibited by 10 μmol/l amiloride. During the whole experiment, the bath was continuously perfused at a rate of 5–10 ml/min. All experiments were conducted at room temperature (22°C).

Chemiluminescence measurements

Oocytes were incubated for 60 min at 4°C in ND96 media (in mM: 96 NaCl, 2 KCl, 1.8 $CaCl_2 \cdot 2\ H_2O$, 1 $MgCl_2 \cdot 6\ H_2O$, 5 HEPES, 2.5 sodium pyruvate, adjusted to pH 7.5 with NaOH) with 1% bovine serum albumin (BSA) to block non-specific binding of antibodies. Afterwards oocytes were incubated for 60 min at 4°C with 1 μg/ml mouse monoclonal anti-FLAG M2 antibody (clone M2, Sigma) in 1% BSA/ND96, washed eight times at 4°C with 1% BSA/ND96, and incubated with sheep anti-mouse IgG peroxidase-linked whole antibody (Amersham Biosciences) diluted 1:20000 in 1% BSA/ND96 for 40 min at 4°C. Then oocytes were washed for 60 min at 4°C in 1% BSA/ND96 and in ND96 (60 min, 4°C) and placed separately in 50 μl ECL Plus Western Blotting Detection Reagents (Amersham Biosciences). After an incubation period of 5 min at room temperature, chemiluminescence was measured in a BioOrbit 1250 Luminometer (Turku, Finland). The integration period was 1 s and the results were obtained in millivolts (mV).

Fluorescence measurements

Oocytes were incubated for 60 min at 4°C in ND96 media (in mM: 96 NaCl, 2 KCl, 1.8 $CaCl_2 \cdot 2\ H_2O$, 1 $MgCl_2 \cdot 6\ H_2O$, 5 HEPES, 2.5 sodium pyruvate, adjusted to pH 7.5 with NaOH) with 1% BSA to block non-specific binding of antibodies. Afterwards oocytes were incubated for 60 min at 4°C with 1 μg/ml mouse monoclonal anti-FLAG M2 antibody in 1% BSA/ND96, washed eight times at 4°C with 1% BSA/ND96 and incubated with goat anti-mouse IgG_1 fluorescein isothiocyanate (FITC)-conjugated (Santa Cruz Biotechnology) in 1% BSA/ND96 for 60 min at room temperature and in the dark. Oocytes were washed for 60 min at room temperature and in the dark in 1% BSA/ND96 and then under the same conditions for 60 min in ND96. Images were obtained using a Zeiss Axiovert 35 inverted microscope with a × 3.2 objective and digitized with a Nikon D100 camera.

Macropatch

Xenopus oocytes expressing ENaC were defolliculated and were placed on the stage of an inverted microscope (IM35, Zeiss, Oberkochen, Germany). The bath was continuously perfused with Ringer solution at a rate of about 10 ml/min. Patch clamp experiments were performed in cell-excised inside/out and outside/out configurations. The patch pipettes had an input resistance of 2–4 MΩ when filled with a solution containing (mmol/l) 96 NaCl, 2 KCl, 1.8 $CaCl_2 \cdot 2\ H_2O$, 1 $MgCl_2 \cdot 6\ H_2O$, 5 HEPES, 2.5 sodium pyruvate, 1 diphenylcarboxylate at pH 7.5. Currents (voltage clamp) and voltages (current clamp) were recorded using a patch clamp amplifier (EPC 9, HECA, Lambrecht, Germany) and data were stored continuously on a computer hard disc. In regular intervals, membrane voltages (V_C) were clamped in steps of 10 mV from –50 mV to +50 mV. G was calculated from the measured I and V_C values according to Ohm's law.

Materials and statistical analysis

All compounds were of highest available grade of purity. Nystatin, amiloride, NMDG, PIP_2, phosphatidylinositol-specific phospholipase C from *Bacillus cereus* and ATP were from Sigma. U73122 was from Calbiochem. The anti-PIP_2 antibody was from Echelon. Student's *t*-test *P* values <0.05 were accepted to indicate statistical significance. *n* indicates the number of experiments.

Results

Whole cell currents produced by the epithelial Na^+ channel ENaC were partially inhibited by activation of CFTR through stimulation with IBMX (1 mmol/l) and forskolin (2 μmol/l). Inhibition was reversible when extracellular (bath) Cl^- concentration was reduced from 100 to 5 mM. This is shown as a continuous whole cell current recording of an oocyte co-expressing CFTR and ENaC (Fig. 1A) and is summarized in Fig. 1B. In oocytes expressing ENaC only, the amiloride-sensitive conductance (G_{Amil}) of 59.2 ± 7.9 microsiemens was not changed when the extracellular Cl^- concentration was reduced to 5 mmol/l (G_{Amil}=59.9 ± 8.2 μS; *n*=9). All experiments were performed using a bath clamp, which minimizes voltage drops along the series resistances. However, we included two sets of control experiments. (i) We permeabilized ENaC expressing oocytes with 10 μM nystatin, which induced a non-selective conductance without affecting amiloride-sensitive membrane currents (Fig. 1D). G_{Amil} was 19.3 ± 2.7 and 23.3 ± 3 μS (*n*=7) in the absence and presence of nystatin, respectively. (ii) ENaC was co-expressed with K_VLQT1 K^+ channels, and amiloride-sensitive currents were assessed in the absence or presence of the K^+ channel blocker Ba^{2+} (5 mM), which did not affect Na^+ transport (Fig. 1E): G_{Amil} was 7.9 ± 1.3 and 7.5 ± 1.1 μS (*n*=9) in the absence and presence of

Ba^{2+}, respectively. Thus, additional currents do not compromise the measurement of ENaC currents in our setup. Cl^- currents generated by CFTR but not non-selective currents or K^+ currents inhibited ENaC.

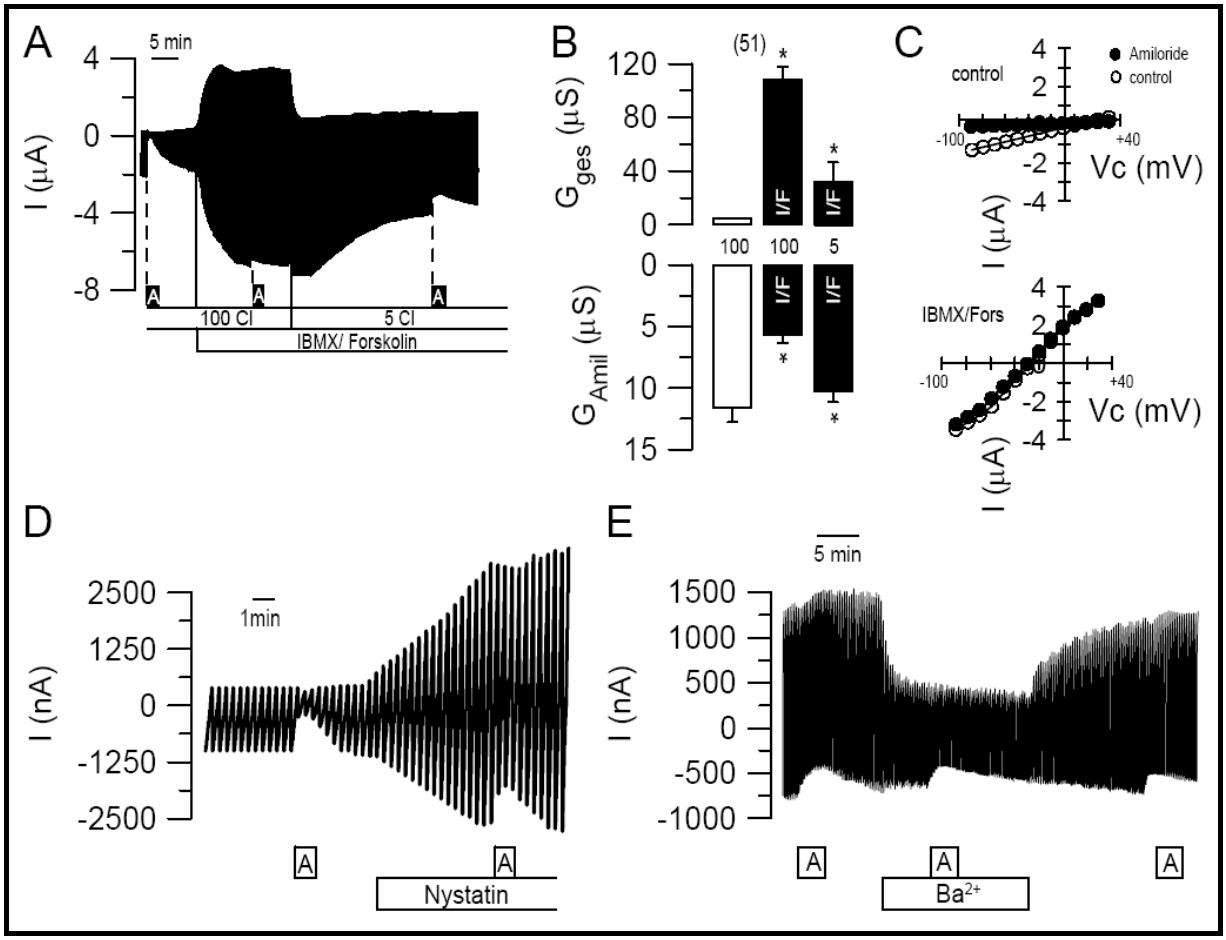

Fig. 1: CFTR inhibits ENaC in *Xenopus* oocytes. A) Original recording of the whole cell current in a *Xenopus* oocyte co-expressing rat αβγENaC together with human CFTR. Whole cell currents were measured during continuous voltage clamp from –90 mV to +30 mV in steps of 10 mV. CFTR Cl^- currents were activated by IBMX/forskolin (1 mM/2 μM) and were measured in the presence of a high (100 mM) or low (5 mM) bath Cl^- concentration. The effects of amiloride (A, 10 μM) on whole cell currents were largely inhibited after activation of CFTR and in the presence of high bath Cl^- concentration. B) Summary of the effects of IBMX/forskolin (I/F) on amiloride-sensitive conductance (G_{Amil}) in co-expressing oocytes. C) Typical current/voltage relationships of co-expressing oocytes before and after stimulation with IBMX/forskolin and the effect of amiloride. D) Original recording of the whole cell current in an ENaC expressing oocyte and the effect of amiloride before and after inducing a non-selective conductance with nystatin (10 μM). E) Original recording of the whole cell current in

a *Xenopus* oocyte co-expressing rat $\alpha\beta\gamma$ENaC together with human K_VLQT1 K^+ channels. *Indicates significant difference (paired *t*-test). *n*, number of experiments.

We examined the Cl^--dependence of the CFTR effect on ENaC in more detail and found that in oocytes, in which CFTR had been activated by IBMX/forskolin, a gradual increase in the bath Cl^- concentration from 2 to 100 mM, gradually inhibited ENaC currents, in parallel to the increase of CFTR Cl^- currents (Fig. 2A and C). Moreover, we co-expressed the Cl^- channel CLC-0 together with ENaC and found a comparable decrease of ENaC currents with increasing bath Cl^- concentrations (Fig. 2B and D). Thus, Cl^- ions play an essential role in both CFTR, and CLC-0 induced inhibition of ENaC. When ENaC was inhibited by amiloride, oocyte membranes are dominated by a Cl^- conductance. Thus it is possible to measure the Cl^- diffusion potential and to calculate for the apparent intracellular Cl^- concentration. We found that in the presence of activated CFTR or when CLC-0 was co-expressed, increase in bath Cl^- from 5 to 100 mM resulted in a change of the apparent intracellular Cl^- concentration from about 10 to roughly 60 mM (Fig. 2E and F). In parallel, ~ 50% of the initial amiloride-sensitive Na^+ current was inhibited, indicating that an increase in cytosolic Cl^- inhibits ENaC. We observed a recovery of amiloride-sensitive conductances over the time course of 30 min, when bath Cl^- was reduced from 100 to 5 mM in ENaC/CLC-0 co-expressing oocytes. Finally, injection of 23 nl of 50 mM NaCl also inhibited ENaC, whereas injection of water or 5 mM NaCl had no effect (data not shown). In summary, increase in intracellular Cl^- inhibits ENaC, which may be in charge of the inhibitory effects of CFTR or CLC-0 on ENaC.

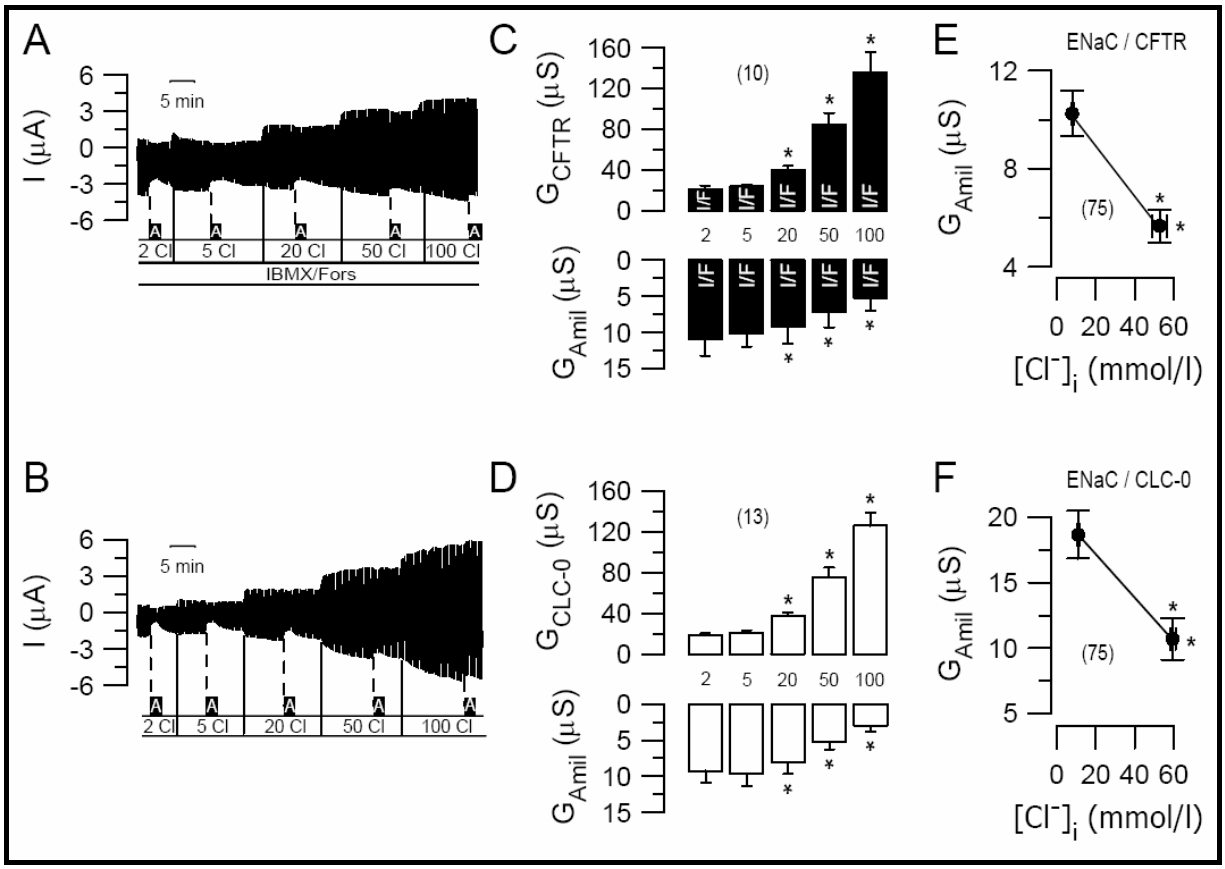

Fig. 2: Cl^--dependent inhibition of ENaC by CFTR and CLC-0. Original recording of the whole cell current in *Xenopus* oocytes co-expressing αβγENaC together with CFTR (A) or CLC-0 (B). Whole cell currents were measured during continuous voltage clamp from –90 mV to +30 mV in steps of 10 mV. CFTR Cl^- currents were activated by IBMX/forskolin (1 mM/2 µM). Inhibition of whole cell currents by amiloride (A, 10 µM) was examined in the presence of bath Cl^- concentrations ranging from 2 to 100 mM. Summary of the CFTR (C) and CLC-0 (D) induced whole cell conductances and amiloride-sensitive whole cell conductances at different bath Cl^- concentrations. Relationship between amiloride-sensitive whole cell conductance and calculated intracellular Cl^- concentration in CFTR (E) and CLC-0 (F) expressing oocytes. *Indicates significant difference (paired *t*-test). *n*, number of experiments.

This was further confirmed in experiments with macropatches from ENaC expressing oocytes, after verifying expression by double electrode voltage clamp. Patch pipettes were filled with 1 mM diphenylcarboxylate, to minimize endogenous Cl^- currents. A current noise was recorded from excised inside/out macropatches, which was largely increased when the cytosolic Cl^- concentration was reduced from 100 to 5 mM (Fig. 3A and B). 95 mM Na^+ were replaced by $NMDG^+$ in the presence of low or high bath Cl^-. We found that the $NMDG^+$ that inhibited Na^+

conductance in macropatches was 86.2 ± 6.2 μS in the presence of 5 mM cytosolic Cl^-, which was significantly larger when compared with that observed at 100 mM Cl^- (27.3 ± 2.1 μS). We then exposed the cytosolic side of the macropatches to different Cl^- concentrations, ranging from 5 to 100 mM. As shown in Fig. 3B, a gradual increase in cytosolic Cl^- inhibited the conductance of excised inside/out membrane patches. Finally, we confirmed expression of ENaC in excised outside/out patches and found inhibition of membrane conductance by amiloride (10 μM) from 228 ± 70 to 140 ± 60 μS (*n*=5). Thus ENaC may be directly inhibited by Cl^- ions or attached Cl^--sensitive proteins control ENaC activity.

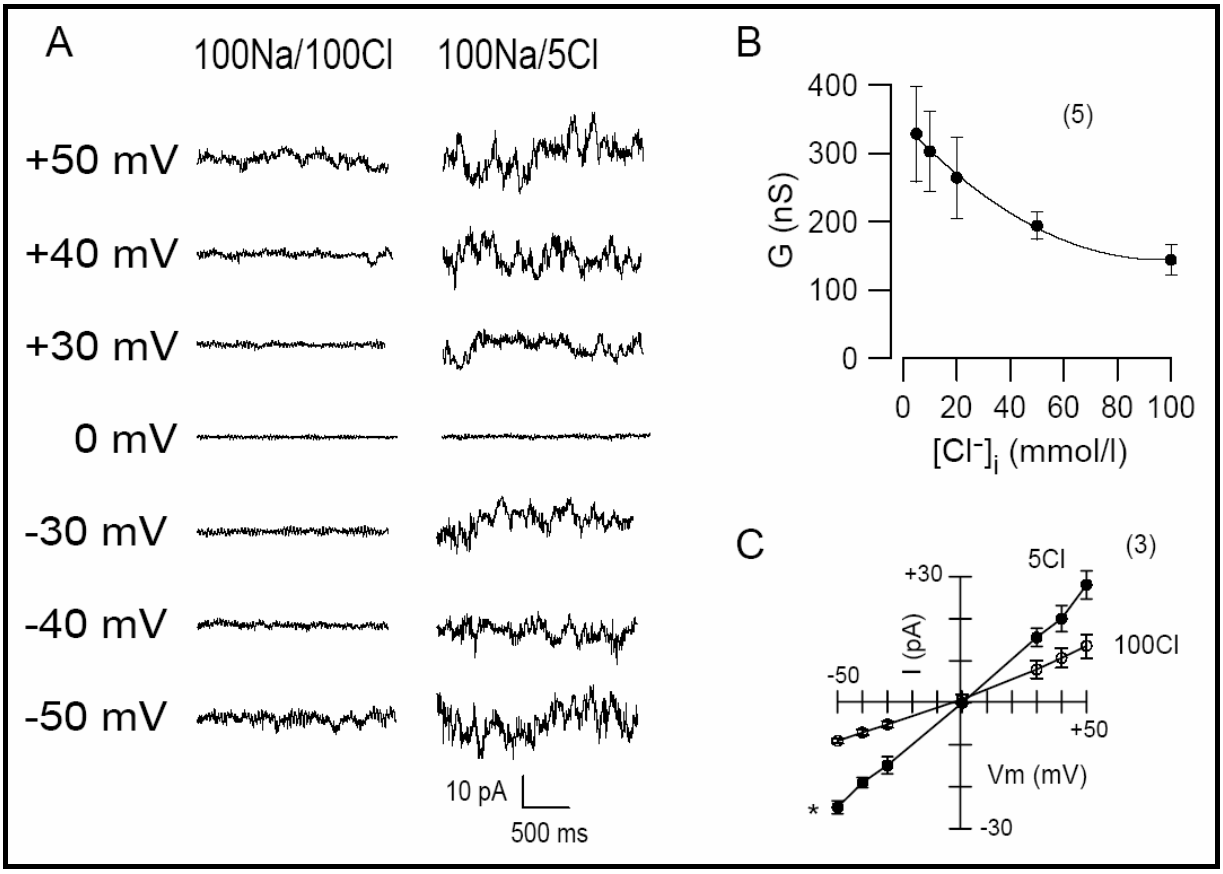

Fig. 3: Cl^--dependent inhibition of ENaC in macropatches. A) Current noise in an inside/out macropatch of an ENaC expressing oocyte at different clamp voltages and in the presence of high (100 mM) or low (5 mM) cytosolic Cl^- concentration. B) Cl^--dependence of the conductance of inside/out macropatches of ENaC expressing oocytes. C) Current/voltage relationships of the current noise in inside/out macropatches of ENaC expressing oocytes in the presence of low or high cytosolic Cl^- concentration. *n*, number of experiments.

We examined if the change in cytosolic Cl^- affects membrane expression of ENaC. To that end, we expressed FLAG-tagged ENaC subunits together with CFTR or CLC-0 and exposed the oocytes to 5 or 100 mM bath Cl^- concentration. For these experiments CFTR had been pre-activated by IBMX and forskolin. FLAG-tagged ENaC subunits were detected by staining with primary anti-FLAG and secondary fluorescein isothiocyanate-conjugated antibodies. There was no obvious change in fluorescence during exposure to high or low extracellular Cl^- (data not shown). We quantified surface expression of individual ENaC subunits by chemiluminescence and found no change in membrane expression in ENaC/CFTR (Fig. 4A) or ENaC/CLC-0 (Fig. 4B) co-expressing oocytes, during change of the bath Cl^- concentration from 5 to 100 mM Cl^-. Chemiluminescence was also measured for βENaC and γENaC mutants, in which 2 (β2N, γ2N) or 4 (β4N, γ4N) positively charged amino acids in the NH_2 terminus have been replaced by neutral amino acids. These amino acids are located in PIP_2 binding sides of βENaC and γENaC and control ENaC activity (119;137;235). However, membrane expression of the mutant ENaCs was not affected by changes in the bath Cl^- concentration (Fig. 4A and B).

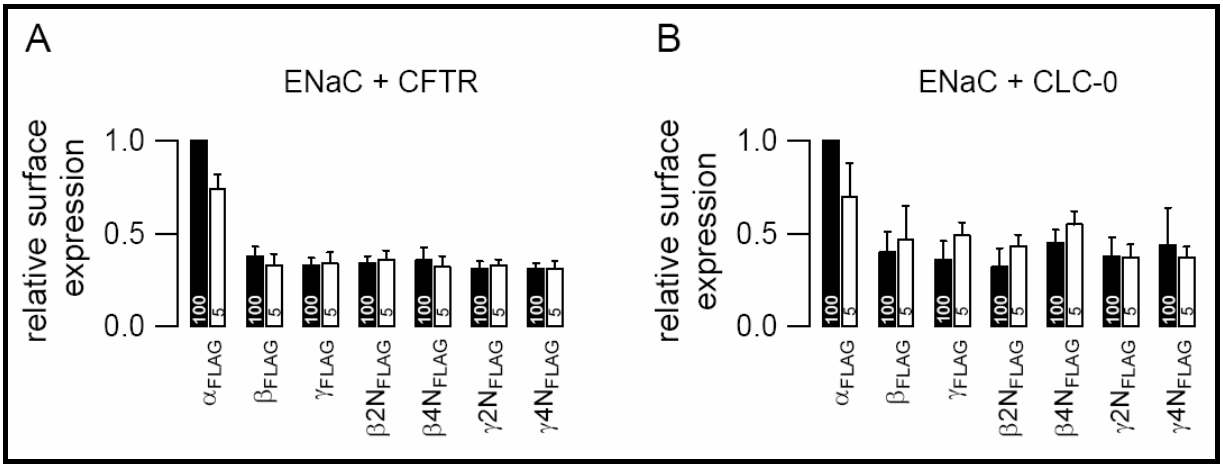

Fig. 4: Expression of FLAG-tagged ENaC subunits. A) Detection of surface expression of ENaC subunits by chemiluminescence in ENaC/CFTR (A) or ENaC/CLC-0 (B) co-expressing oocytes. FLAG-tagged ENaC subunits were detected by staining with a primary anti-FLAG and secondary IgG peroxidase-linked antibody. Chemiluminescence was integrated over 1 s and is expressed as surface expression relative to that of αENaC at 100 mM Cl^-. Chemiluminescence was assessed in a bath solution containing 100 mM (*black bars*) or 5 mM (*white bars*) Cl^-. β2N, γ2N and β4N, γ4N indicate that 2 or 4 positively charged amino acids have been removed from the NH_2 terminus of either βENaC or γENaC. The number of experiments was for each series between 5 and 15.

To further validate the chemiluminescence methods used here, we expressed FLAG-tagged ENaC subunits, which were truncated at the COOH terminus of either βENaC (R561X, βΔC) or γENaC (S608X, γΔC). These truncations have been shown to lead to enhanced membrane expression of ENaC. In fact, expression of βΔC and γΔC was enhanced 1.70 ± 0.2 (*n*=15)- and 1.73 ± 0.3 (*n*=15)-fold, respectively, when compared to wt βENaC and wt γENaC. Moreover, when βΔC and γΔC were co-expressed together with CLC-0 or CFTR, membrane expression was not affected by a change of bath Cl^- from 5 to 100 mM (*n*=15 for all series, data not shown).

The role of Cl^- for inhibition of ENaC was further confirmed by blocking CLC-0 channels with 500 μM Zn^{2+} (44). Zn^{2+} inhibited about 50% of the CLC-0 conductance in 100 mM extracellular Cl^- and enhanced amiloride-sensitive conductance (18.3 ± 4.3 vs. 26.3 ± 4.5 μS). Zn^{2+} applied in a low bath Cl^- concentration abolished CLC-0 conductance completely and further enhanced ENaC conductance (29.1 ± 4.4 μS, *n*=9). Zn^{2+} itself had no effects on ENaC. We examined if the effect of Cl^- on ENaC can be mimicked by other anions and therefore replaced bath Cl^- by equimolar concentrations of NO_3^-, I^-, or Br^- (Fig. 5A). CFTR conductance and inhibition of ENaC were detected in the presence of the different anions, but were both reduced in the presence of extracellular I^- (Fig. 5B and C). ENaC is inhibited by increase in intracellular Na^+ (54). This was reported as feedback inhibition and is abolished by ENaC mutations occurring in Liddle's disease (86). Since both intracellular Cl^- and Na^+ may change in parallel, we examined if Cl^--dependent inhibition of ENaC is also observed with ENaC carrying Liddle's disease mutations or truncations in the COOH terminus of all three subunits (Fig. 5D and E). The ENaC mutants were co-expressed either with CFTR (Fig. 5D) or with CLC-0 (Fig. 5E). The summaries show that the mutant channels were also inhibited by Cl^- in a concentration-dependent manner, although inhibition appeared somewhat reduced when compared with wtENaC. Thus, Cl^--dependence can be clearly separated from Na^+-dependent inhibition.

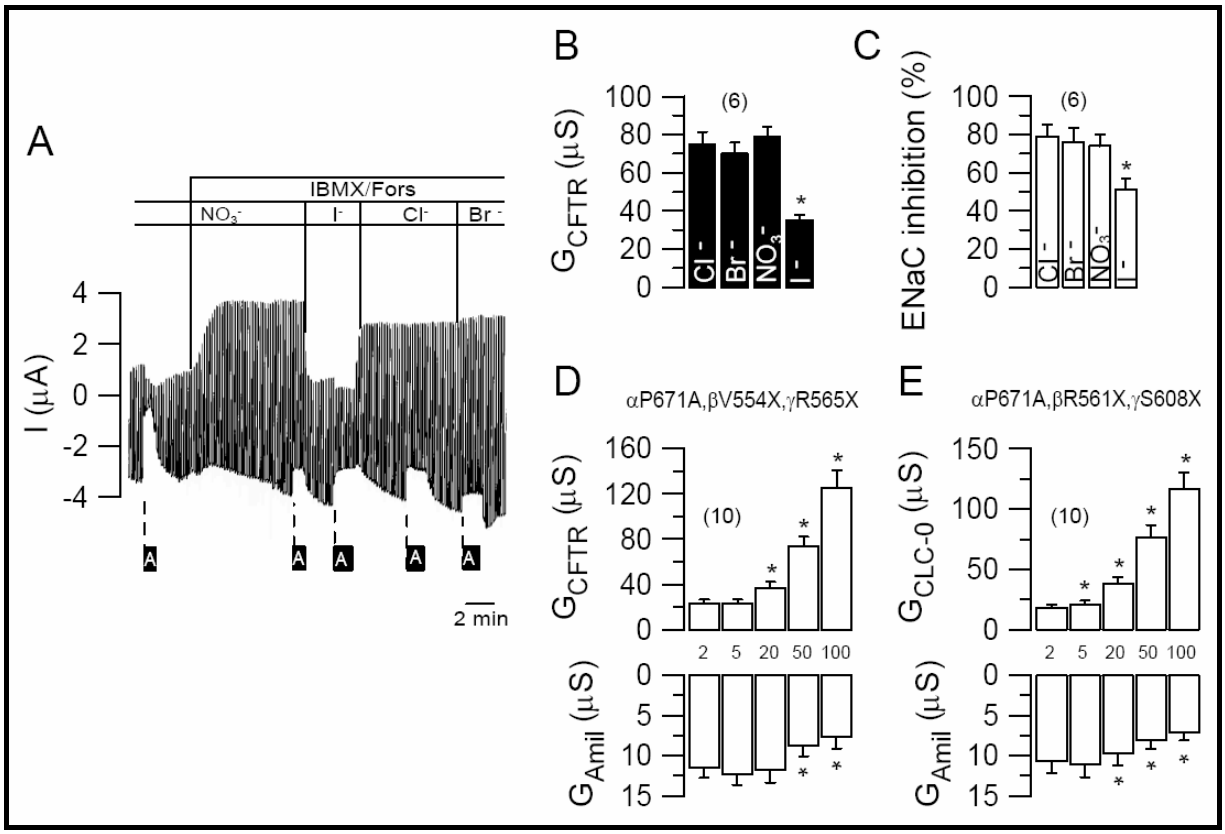

Fig. 5: Anion-dependent inhibition of ENaC. A) Original recording of the whole cell current in an oocyte co-expressing ENaC and CFTR and the effect of amiloride in the presence of different anions in the bath. Summary of the CFTR conductance (B) and inhibition of amiloride-sensitive Na^+ conductance (C) in the presence of different anions in the bath. D) Summary of the CFTR conductance and inhibition of little mutants of the amiloride-sensitive Na^+ channel in the presence of different bath Cl^- concentrations. E) Summary of the CLC-0 conductance and inhibition of little mutants of the amiloride-sensitive Na^+ channel in the presence of different bath Cl^- concentrations. *Indicates significant difference (paired *t*-test). *n*, number of experiments.

ENaC is inhibited by CFTR and by stimulation of puringeric receptors with ATP or UTP, which leads to hydrolysis of PIP_2 via activation of phospholipase C_β (119). We previously found a Cl^--dependence also for purinergic inhibition of ENaC (123) and therefore asked whether both mechanisms are additive. To that end, we measured Na^+ absorption in polarized epithelial cells of the collecting duct, which express CFTR, ENaC and Ca^{2+}-activated Cl^- channels along with purinergic receptors. ENaC was shown to be controlled by CFTR and purinergic receptors in these cells (47;119;129). In Ussing chamber experiments we observed attenuation of amiloride-sensitive transport after activation of CFTR by IBMX and forskolin, indicating inhibition of ENaC by CFTR (Fig. 6A). After pre-inhibition of ENaC by purinergic stimulation,

the amiloride-sensitive short-circuit current was further reduced by 1.6 ± 0.3 μA/cm^2 when CFTR was activated. This, however, was significantly less than inhibition of ENaC by CFTR without purinergic pre-stimulation (3.9 ± 0.4 μA/cm^2, *n*=6). Moreover when phospholipase C_β was inhibited by U73122 (10 μM), inhibition of amiloride-sensitive transport by CFTR was significantly enhanced (7.8 ± 0.9 μA/cm^2, *n*=8). This data suggest that both inhibitory mechanisms are additive. The NH_2 terminus of β- and γENaC play a central role for the purinergic regulation of ENaC and may also participate in CFTR and Cl^--dependent control of ENaC. We examined this issue in ENaC and CLC-0 expressing *Xenopus* oocytes and performed maneuvers, which have been shown to affect PIP_2 binding and thus ENaC activity (119). Injection of PIP_2 (30 μM, 30 nl) slightly but significantly enhanced amiloride-sensitive whole cell currents. This additional current was inhibited by increase in intracellular Cl^- (Fig. 6B). Control injection of oocytes with water had no effects. In contrast, injection of a PIP_2 antibody (1:100, 30 nl) slightly reduced G_{Amil} and the remaining current was inhibited by Cl^- to the same level as before injection (Fig. 6C). Moreover, both injection of phospholipase C_β (2 U/mg, 30 nl) or incubation of the oocytes in pH 6.0 for 1 h largely reduced G_{Amil} and the amount of G_{Amil} blocked by Cl^- (Fig. 6D and E). These results suggest that PIP_2 binding of β- and probably γENaC determines the amount of ENaC current inhibited by Cl^- ions.

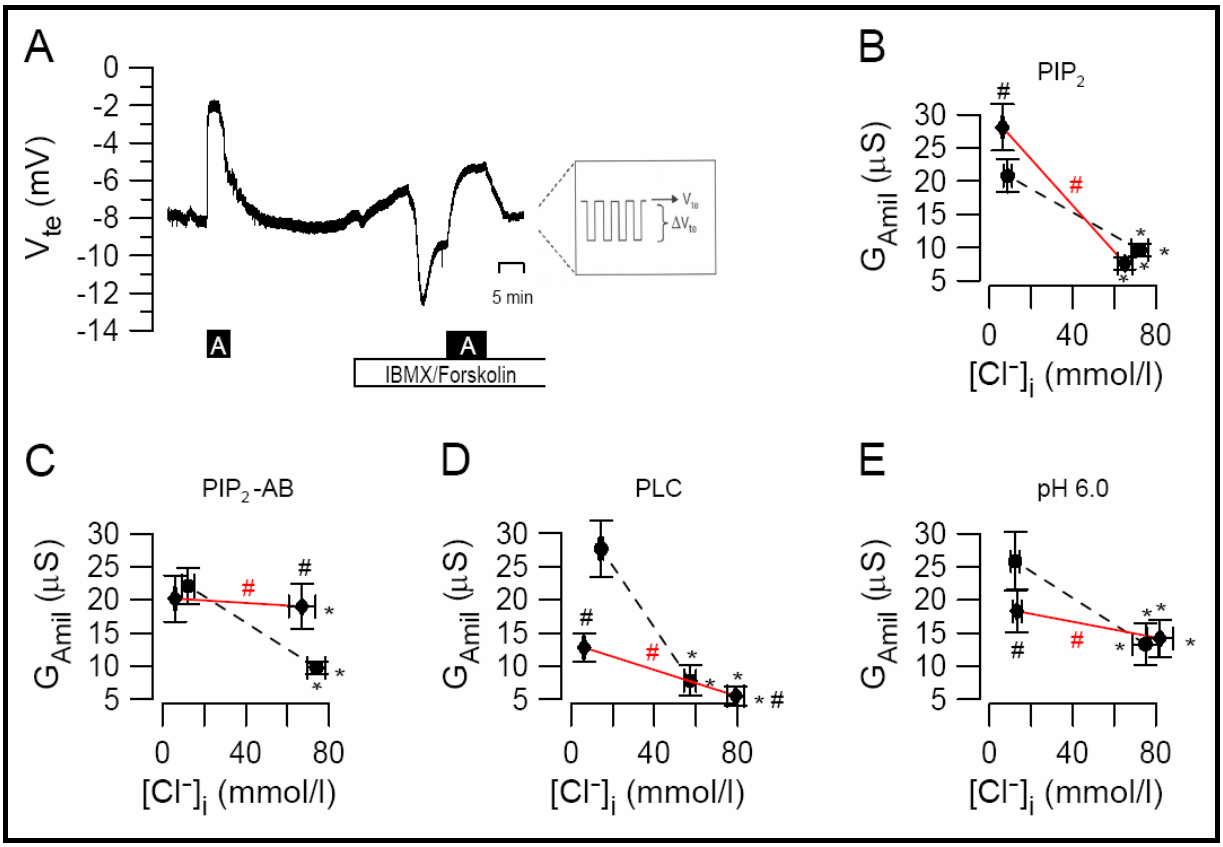

Fig. 6: Inhibition of ENaC by ATP and Cl^-. Continuous recording of the transepithelial voltage (V_{te}) of M1 collecting duct cells in a perfused micro-Ussing chamber and effects of amiloride (A; 10 µmol/l) under control conditions and after activation of CFTR by IBMX and forskolin. B–E) Change in the intracellular Cl^- concentration $[Cl^-]_i$ by an increase in the bath Cl^- concentration from 5 to 100 mM in CLC-0/ENaC co-expressing oocytes and change in the amiloride-sensitive Na^+ conductance. Effects of injection of PIP_2 (23 nl, 25 µM, *n*=16) (B), injection of PIP_2 antibody (23 nl, 1:100, *n*=6) (C), injection of PLC (23 nl, 2 U/ml, *n*=9) (D) or incubation for 30 min at pH 6.0; *n*=26 (E). *Dashed lines* indicate inhibition of ENaC by increase in $[Cl^-]_i$ in control oocytes (*n*=10–26). *Indicates significant difference (paired *t*-test). #Indicates significant difference in Na^+ conductance and slope for Cl^--dependent inhibition (unpaired *t*-test).

We further tried to identify the ENaC subunits and cytosolic domains that participate in Cl^--dependent regulation. To that end, αβγ subunits were truncated at amino (ΔN) or carboxyl (ΔC) termini and co-expressed in various combinations. Moreover, PIP_2 binding domain mutants of β- and γENaC were generated by eliminating 2 or 4 positively charged amino acids (β2N, β4N, γ2N, γ4N) (119). ENaC subunits were co-expressed together with CLC-0 or CFTR, activated with IBMX and forskolin. The whole cell currents generated by CLC-0 or CFTR in the

presence of 100 mM extracellular Cl^- were between 5 and 10 μA and were reduced by replacing extracellular Cl^- by gluconate (data not shown). Because virtually identical results were obtained for co-expression of ENaC with CLC-0 and CFTR and for αwt, αΔC, αP671A, the data are not listed separately. Fig. 7A shows the ratio of G_{Amil} generated by mutant ENaC to G_{Amil} produced by wtENaC at low (5 mM) bath Cl^- (*black bars*). The *white bars* indicate the ratio of the inhibition of mutant ENaC to inhibition of wtENaC by an increase in bath Cl^- to 100 mM (*white bars*). It is shown that individual truncations (ΔC) of the carboxyl terminus of α-, β-, and γENaC in trimeric channels lead to enhanced Na^+ currents compared with wtENaC, but attenuated downregulation by Cl^- only for βΔC. Interestingly, the double mutant βΔCγΔC showed reduced ENaC currents and downregulation by Cl^-. In contrast, truncation of the amino terminus reduced (βΔN, γΔN) or even abolished (αΔN) ENaC currents. Individual mutations in the PIP_2 binding domain (β2N, β4N, γ2N and γ4N) inhibited ENaC currents, particularly in βENaC, but did not affect Cl^- inhibition. The double mutant β4Nγ4N did not produce significant whole cell currents. As further shown, expression of various other combinations of double mutants showed compromised inhibition of ENaC by Cl^-, when the carboxyl terminus of βENaC was truncated.

Expression of αENaC alone generated a small but significant Na^+ current, which was not downregulated by Cl^- (Fig. 7B). Additional mutations in the carboxyl terminus of αENaC did not change Cl^- sensitivity (data not shown). ENaC currents were reduced in dimeric channels formed by αENaC together with βENaC or γENaC, but were all inhibited by Cl^-, except of the dimeric channel containing βΔC (Fig. 7B). Taken together, the results suggest that (i) αENaC does not participate in the control of ENaC by intracellular Cl^-, (ii) the COOH terminus of βENaC confers Cl^- sensitivity and has a central role for the regulation of ENaC by CFTR, and (iii) both NH_2 termini of βENaC and γENaC containing the PIP_2 binding motif determine the activity of ENaC, and the amount of ENaC controlled by Cl^-.

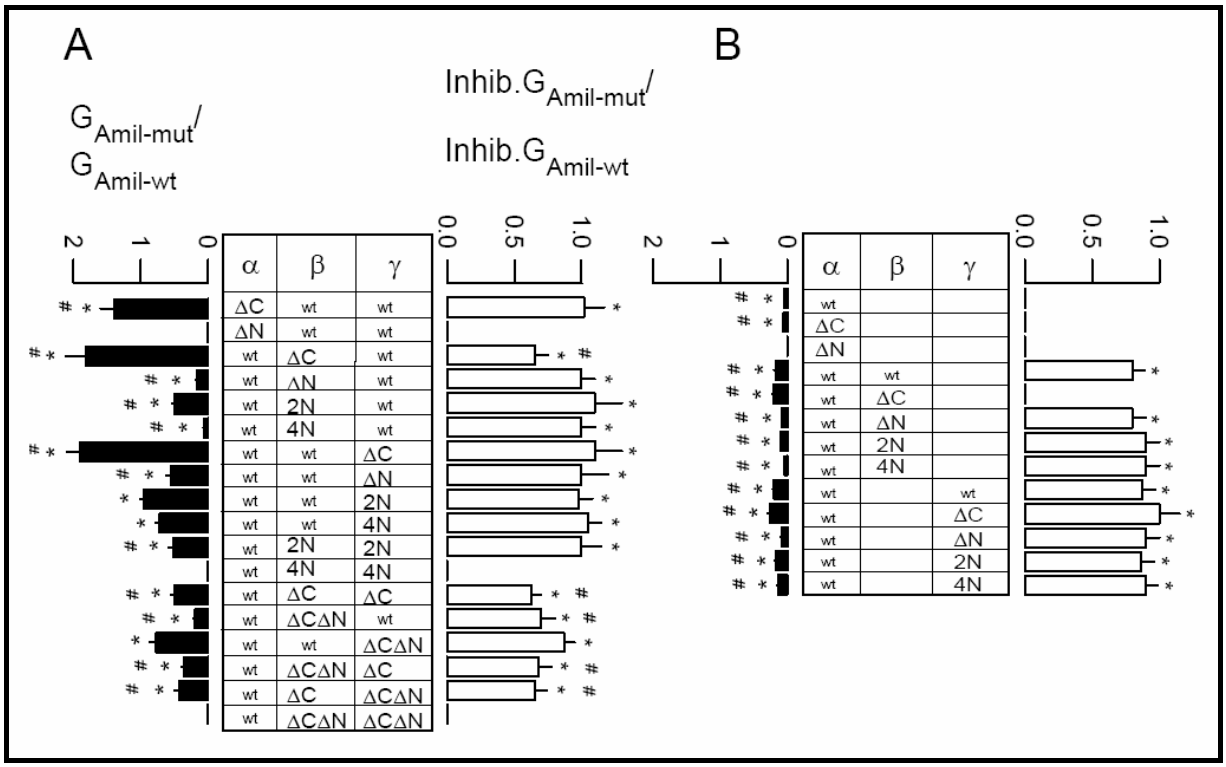

Fig. 7: Summary of double voltage clamp experiments with oocytes co-expressing wtENaC or various ENaC mutants in different combinations together with CFTR or CLC-0. CFTR was pre-activated with IBMX (1 mM) and forskolin (2 μM). *Black bars* indicate the ratio of the conductance generated by mutant ENaC to that produced by wtENaC at low (5 mM) bath Cl^- concentration. *White bars* indicate the ratio for the inhibition of mutant ENaC to that of wtENaC by an increase of bath Cl^- from 5 to 100 mM. A) All three αβγENaC subunits were co-expressed to/from trimeric channels. B) Monomeric channels were formed by αENaC only, or dimeric channels were formed by αβENaC or αγENaC. *Indicates significant effects of amiloride (*black bars*) and significant inhibition of ENaC during an increase of Cl^- from 5 to 100 mM (*white bars*; paired *t*-test). #Indicates significant difference in the amplitude of amiloride-sensitive currents generated by mutant ENaC when compared with wtENaC (*black bars*) and significantly attenuated inhibition of mutant ENaC by Cl^- (*white bars*, unpaired *t*-test). The number for each series of experiments was *n*=6–36.

Discussion

The present results clearly demonstrate inhibition of amiloride-sensitive Na^+ currents by activation of CFTR or CLC-0 Cl^- channels. In contrast, ENaC currents were not affected by a parallel K^+ conductance or by a non-selective conductance induced by nystatin. Inhibition of ENaC by CFTR has been questioned in two studies and it was suggested that the inhibitory

effect of CFTR on ENaC could be attributed to problems arising from high levels of channel expression and suboptimal recording conditions, such as a large series resistance and/or insufficient feedback voltage gain (165;166). However, several facts argue against the possibility of a series resistance error as an explanation for the present and previous results: (i) In contrast to Refs. 166 and 165, CFTR and ENaC currents were of a much smaller amplitude in the previous reports (33;34;42;86;97;98;109;121;123;142;191). (ii) Inhibition of ENaC by CFTR was observed at whole cell currents as low as 1.5 μA (34;108;142;192), which is roughly 10-fold below the currents reported in Refs. 166 and 165. (iii) Experiments were performed with large dimension, low resistance KCl electrodes, avoiding a significant artificial voltage drop along series resistances (34;121;142;191). (iv) Experiments performed with different oocyte voltage clamp amplifiers and two bath electrodes with compensation circuit confirmed previous results (33;109;123;212). (v) Including the present report, a roughly 50% inhibition of ENaC currents by activation of CFTR was found in most of the previous studies (34;86;97;109;110;142;190;231). (vi) Co-expression of large K^+ conductances together with ENaC should exert the same artifact as activation of CFTR Cl^- currents according to Ref. 165. This, however, was not observed in the present and a previous report (110). (vii) Partial permeabilization of oocytes with amphotericin B, which induced a large leak conductance did not compromise detection of G_{Amil} (109). (viii) Partial permeabilization of oocytes with nystatin in the present study, or co-expression of another parallel K^+ conductance did not compromise the measurement of G_{Amil}. Taken together, it is rather unlikely that the reported inhibition of ENaC by CFTR is a result from compromised measurements of whole cell currents in *Xenopus* oocytes.

It was discussed that in epithelial tissues such as the reabsorptive sweat duct, where both CFTR and ENaC reside in the same apical membrane, the absence of CFTR necessarily reduces absorption of Na^+ because of coupled movement of both Cl^- and Na^+ (165;166;183). Whereas this may accurately describe the situation for a tight epithelium such as the sweat duct, where all electrolyte transport occurs transcellularly, the situation is quite different for the airways, which is a leaky epithelium unable to maintain larger osmotic gradients (30;147). Additional Na^+ conductance, as present in the airways of cystic fibrosis patients, will necessarily lead to an increase in Na^+ and Cl^- absorption, with consecutive loss of airway surface liquid and reduced mucociliary clearance. This has been convincingly demonstrated in a novel transgenic mouse model with airway-specific overexpression of ENaC. In contrast to CFTR-transgenic animals, these mice reproduce a lung disease with all typical features of a CF lung, including an increased salt absorption and reduced airway surface liquid (140). Thus, enhanced electrolyte absorption because of increased Na^+ conductance in the airways takes place even in the absence of an additional Cl^- selective shunt.

As outlined above, an inhibitory effect of CFTR on ENaC has been detected under very different experimental conditions and accordingly enhanced Na^+ absorption has been detected in CF tissues, including human airways and intestine (31;32;120;138;139). In contrast, CFTR knock-out mice do not demonstrate a CF lung disease (78). In the mouse, expression of CFTR takes place in the nasal epithelium, but is essentially irrelevant in trachea and more distal airways (186). Mouse airways are obviously dominated by a Ca^{2+}-activated Cl^- conductance and thus lack of CFTR does not affect ion transport in the airways, except the nasal epithelium. Consequently, enhanced Na^+ absorption is found in CFTR knock-out mice only in the nasal epithelium, but not in the remaining airways (79;170). A thorough analysis of the CFTR expression in human airways using a new high affinity CFTR antibody revealed that CFTR protein is expressed in the apical membrane of ciliated cells within the superficial epithelium and in gland ducts, but hardly detectable in the gland acinus and alveolar epithelium. This suggests an essential role of CFTR for the regulation of Na^+ absorption (113).

The present results demonstrate an increase in the intracellular Cl^- concentration in ENaC expressing oocytes, when a parallel Cl^- conductance and a high bath Cl^- concentration is present. This is not surprising, because a large Cl^- shunt allows for electroneutral uptake of NaCl into the oocyte. The results show that Cl^- or other anions have an inhibitory effect on ENaC, when accumulating on the cytosolic side. It should be pointed out that this inhibitory effect of Cl^- ions on epithelial Na^+ channels confirms results from earlier studies on mandibular duct cells, which shows an inhibitory effect of Cl^- on epithelial Na^+ conductance (53;54;91). Our results are also in excellent agreement with a previous report showing that deletion of the cytoplasmic NH_2 terminus of α-, β- and γENaC dramatically reduces G_{Amil} (43). The present results confirm that the carboxyl terminus of βENaC is crucial for downregulation of ENaC by CFTR (97). We conclude that the inhibitory effect of CFTR on ENaC is at least in part Cl^- mediated. Evidence is presented that cytosolic domains of ENaC, in a complex and not yet fully understood, participate in this regulation, not excluding the possible role of partner proteins. Moreover, it is possible that additional partner proteins may form a complex together with ENaC and CFTR, possibly in raft-like lipid platforms (84;112). Although participation of some anion-sensitive proteins has been excluded recently (91;123), others have not yet been examined. In this regard, the recently discussed metabolic coupling of ENaC and CFTR via AMP-activated protein kinases would provide a good candidate (40;152).

Chapter 4

Establishment and characterization of a novel polarized MDCK epithelial cellular model for CFTR studies

Abstract

F508del is the most common mutation in the cystic fibrosis transmembrane conductance regulator (CFTR) gene that is responsible for the genetic disease Cystic Fibrosis (CF). It results in a major failure of CFTR to traffic to the apical membrane of epithelial cells, where it should function as a chloride (Cl^-) channel. Most studies on localization, processing and cellular trafficking of wild-type (wt) and F508del-CFTR have been performed in non-epithelial cells. Notwithstanding, polarized epithelial cells possess distinctly organized and regulated membrane trafficking pathways. We have used Madin-Darby canine kidney (MDCK) type II cells (proximal tubular cells, which do not express endogenous CFTR) to generate novel epithelial, polarized cellular models stably expressing wt- or F508del-CFTR through transduction with recombinant lentiviral vectors. Characterization of these cell lines shows that wt-CFTR is correctly processed and apically localized, producing a cAMP-activated Cl^- conductance. In contrast, F508del-CFTR is mostly detected in its immature form, localized intracellularly and producing only residual Cl^- conductance. These novel cell lines constitute *bona fide* models and significantly improved resources to investigate the molecular mechanisms of polarized membrane traffic of wt- and F508del-CFTR in the same cellular background. They are also useful to identify/validate novel therapeutic compounds for CF.

Introduction

Cystic fibrosis (CF), a clinically complex disease known as the most common lethal inherited disorder among Caucasians, is caused by mutations in the cystic fibrosis transmembrane conductance regulator (CFTR) gene, which encodes a membrane protein that functions as a cAMP-activated chloride (Cl^-) channel. CFTR is expressed in a wide variety of epithelial cells, including those lining sweat ducts, small pancreatic ducts, airways surface and submucosal gland, intestinal surface and crypts, and kidney tubules (46;56;60).

A high number of different loss-of-function gene variants causes distinct cellular defects on the resulting protein. However, one single mutation, the deletion of phenylalanine residue at position 508 (F508del) of CFTR, occurs in about 90% of CF patients. It is believed that deletion of Phe-508 causes a protein folding defect (45;135;179;237) and the resulting abnormal CFTR conformation is recognized as such by the endoplasmic reticulum (ER) quality control that targets most of it for degradation via the ubiquitin-proteasome pathway (96;226).

A limited amount of cAMP Cl^- conductance, however, is detected at the epithelia surface of F508del-homozygous patients and mice, suggesting that the ER retention is not absolute in native tissues (21;144;220). Consistently, minor expression of F508del-CFTR can be detected at the cell surface in recombinant cells, CF primary airway cells, and CF native tissues using a large variety of anti-CFTR antibodies (55;99;174;188;236).

Polarized monolayers of human airway epithelial cells are thus the desirable model to study CFTR traffic and indeed there is a number of human airway epithelial cell lines from CF patients that are able to polarize in culture (for a review see (80)). These immortalized cell lines are of significant importance to study CFTR because the scarcity of material provided by native tissues and primary cell systems causes major limitations to the feasibility of the experiments that can actually be carried out (80). However, they are often difficult to maintain in culture and to keep consistent and reproducible transepithelial resistance (R_{te}) values. Moreover, their CFTR expression levels have been observed to decrease with increasing number of passages (80).

Therefore, the majority of studies on the traffic and processing of wt- and F508del-CFTR have been conducted in heterologous, non-epithelial or non-polarized/epithelial cellular systems. Because the efficiency of CFTR processing has also been shown to be widely cell-type- and polarization-dependent, with endogenous epithelial CFTR maturation patterns

differing from those reported in overexpressing systems (16;218), our aim was to generate novel epithelial, polarized cellular models stably expressing wt- or F508del-CFTR.

We have thus herein established and characterized two novel cellular models by stably transducing MDCK type II cells with wt- or F508del-CFTR recombinant lentivirus. MDCK type II cells were the model of choice due to their reported absence of endogenous CFTR protein expression and cAMP-stimulated Cl^- conductance (159).

These models are characterized here for their CFTR expression at the RNA and protein levels as well as regarding the intracellular localization of the respective transgene product and also in terms of their transepithelial electric properties. Results presented demonstrate that these novel epithelial/polarized cell lines are *bona fide* models to investigate the differences in wt- and F508del-CFTR polarized expression and traffic on the same cellular background, being thus relevant tools to elucidate the basic cellular mechanisms of CF disease.

Material and Methods

MDCK type II cells

Derived by SH Madin and NB Darby from the kidney tissue of an adult female cocker spaniel, MDCK cells were originally produced in September 1958 and ever since have been commonly used as a general model to study protein traffic in epithelial cells (153;161;200). MDCK cells are easy to maintain, form highly polarized monolayers of epithelial cells when grown on filters, with microvilli in the apical surface and with the basolateral membrane interdigitating with the filter. Moreover, their membrane trafficking pathways have been thoroughly characterized (for a review see (161)). Cultured monolayers of MDCK cells display many features of *in vivo* epithelia and their growth on permeable substrates also allows measurement of electrophysiological parameters (158).

However, MDCK cells were previously shown to be heterogeneous in nature, with marked differences reported between type I and type II cultures. It is believed that the two MDCK strains consist in distinct cell populations derived from the same initial pool of cells, being strain I cells derived from the distal collecting duct, while strain II cells are most probably derived from the proximal tubule (184). Some authors, however, suggests that MDCK II may be of thick ascending limb origin (168). MDCK type II cells used here were obtained from the ATCC (Rockville, MD, USA).

Viral transduction

MDCK type II cells were transduced to overexpress CFTR (Tranzyme Corporation from Birmingham, Alabama, USA). Cells were infected with HIV-based translentiviral recombinant vectors containing the human wt- or F508del-CFTR cDNAs, as previously described (13;101). Cells were maintained in DMEM/F12 medium supplemented with 10% (v/v) fetal bovine serum (FBS) and 1% glutamine (both from Invitrogen, Carlsbad, CA, USA) at 37°C in a humidified incubator in 5% (v/v) CO_2 and selection was performed with 2 μg/ml of blasticidin S (Sigma, St Louis, MI, USA) for MDCK wt-CFTR cells and 4 μg/ml of puromycin (Invitrogen) for MDCK F508del-CFTR cells. Following transfection of MDCK II cells (that do not express endogenous CFTR) with HIV-based translentiviral vectors, clones were selected and characterized for CFTR expression (by reverse transcription polymerase chain reaction, RT-PCR and Western blotting, WB), subcellular localization (by immunofluorescence) and for transepithelial electric properties (through Ussing chamber measurements).

Cell culture conditions

Cells were grown on 24 mm polyester Transwell filter supports (Corning Costar, Cambridge, MA, USA), with an area of 4.7 cm^2 and a pore size of 0.4 μm. R_{te} was measured using an EVOMX Epithelial Ohmmeter with a STX2 electrode (WPI, Sarasota, FL, USA).

CFTR transcript analysis by RT-PCR

Total RNA was isolated using the RNeasy extraction kit (Qiagen, Hilden, Germany) according to the manufacturer's instructions. Total RNA concentration was determined by measurement of A_{260} and 1μg was treated with 1 U of RNAse-free DNAse I (Invitrogen) for 15 min at room temperature to eliminate contamination with genomic DNA. DNAse-treated RNA was used for the synthesis of complementary DNA (cDNA). RNA was annealed to 100 pmol of random hexamers (Invitrogen), the mixture was incubated for 10 min at 60°C and then chilled on ice. Following the addition of 5 × first strand buffer (Invitrogen), 0.1M DTT (Invitrogen), 25 mM dNTP mix (Amersham Biosciences, Uppsala, Sweden) and 20 U RnaseOut (Roche, Basel, Switzerland), contents were incubated for 2 min at 42°C. SuperScript II RNaseH-reverse transcriptase (RT) (200 units; Invitrogen) was then added and the final mixture was incubated for 60 min at 42°C for reverse transcription. The RT enzyme was inactivated by heating at 70°C for 15 min. The PCR amplification of the cDNA products was carried out in a reaction that contained 5 μl of cDNA, 10 × PCR buffer, 25 mM dNTP mix (Amersham), 10 pmol of each primer and 1 U *Taq* polymerase (Perkin Elmer, Norwalk, CT, USA). Three sets of primers were used for the PCR amplification:

– “universal mammalian” CFTR primers amplifying from 5´ of exon 22 to 3´ of exon 23 (~ 200 bp fragment) (221): forward primer 5´-CTAAGCCATGGCCACAAGCA-3´ (positions 4168–4187 of human CFTR mRNA, GenBank Accession Number M28668) and reverse primer 5´-CATTGCTTCTATCCTGTGTT-3´ (4353–4372),

– human CFTR primers amplifying a fragment spanning exons 8 to 10 (391 bp fragment) (180): forward primer 5´-AATGTAACAGCCTTCTGGGAG-3´ (1318–1338 of human CFTR mRNA) and reverse primer 5´-GTTGGCATGCTTTGATGACGCTTC-3´ (1685–1708),

– β-actin primers amplifying a fragment spanning exon 8 to 10 (227 bp fragment) (157): forward primer 5´-GCACTCTTCCAGCCTTCC-3´ (positions 852–869 of human β-actin mRNA, GenBank Accession Number BC014861) and reverse primer 5´-GCGCTCAGGAGGAGCAAT-3´ (1079–1062).

For the mammalian CFTR and human β-actin set of primers, cDNA samples were heated at 94°C for 5 min and then subjected to 35 amplification cycles of denaturation at 94°C for 1 min, primer annealing at 57°C for 1 min, and extension at 72°C for 2 min, followed by a final extension at 72°C for 12 min. For the human CFTR set of primers, the only difference was the annealing temperature, which was 60°C. DNA fragments were visualized after agarose gel electrophoresis by staining with ethidium bromide. The following negative controls were included: water instead of RNA and no RT.

Automatic sequencing

PCR products were purified with the JetQuick kit (Genomed, Lohne, Germany) and sequencing was performed on a 3100 Genetic Analyser (Applied Biosystems, Norwalk, CA, USA), using the ABI PRISM™ Dye Terminator Cycle Sequencing kit (Applied Biosystems) according to the manufacturer’s procedure.

Western blotting and treatment with glycosidases

Protein quantification, WB and treatment with glycosidases were performed as previously described (63;64).

Antibodies

For immunofluorescence subcellular localization, all antibodies (Abs) were diluted in 0.5% (w/v) BSA in PBS and for WB in 5% (w/v) skimmed milk in PBS. The following Abs, previously shown to specifically recognize CFTR (154), were used: monoclonal (mAb) 24-1

(R&D Systems; Abington, UK) raised against amino acid (aa) residues 1377–1480 (99) 1:20, polyclonal (pAb) MPCT-1 (a kind gift from Dr. R. Dormer; University of Wales, Cardiff, UK) raised against the C terminus (55) 1:100 and M3A7 mAb (Chemicon, Temecula, CA, USA) raised against aa residues 1370–1380 (102) 1:2000.

Other primary Abs were anti-Rab4 pAb (Stressgen, Victoria, BC, Canada), 1:250; anti-GM130 mAb (BD Transduction, San Jose, CA, USA), 1:250; anti-E-cadherin (BD), 1:100; anti-α/β-tubulin mAb (Amersham), 1:100; anti-cytokeratin18/19 mAb (Roche, Basel, Switzerland), 1:1500. Secondary Abs were: FITC-conjugated, anti-rabbit IgG (Amersham), 1:50; FITC-conjugated anti-mouse IgG (Roche), 1:60; TRITC-conjugated, anti-mouse IgG (Sigma), 1:600 and HRP-conjugated anti-mouse IgG (Amersham), 1:3000.

Subcellular localization by immunofluorescence

Cells grown on 8-well chamber slides (Nalge Nunc, Roskilde, Denmark) or on Transwell filters were incubated for 18 h with 5 mM sodium butyrate, an inhibitor of histone deacetylases (HDACs) and thus a transcriptional activator of non-housekeeping genes (160), for enhancement of CFTR expression. Slides/filters were rinsed twice with cold PBS and fixed in ice-cold methanol for 10 min. After two washes with PBS, cells were permeabilized with 0.2% (v/v) Triton X-100 in PBS for 15 min, washed 3 times in PBS, and blocked with 1% (w/v) BSA/PBS for 30 min prior to incubation with the primary Ab for 90 min at room temperature. Cells were then washed three times with PBS and incubated with the secondary Ab for 30 min at room temperature. Slides were mounted with Vectashield (Vector Laboratories, Burlingame, CA, USA) containing DAPI (Sigma). Immunofluorescence staining was observed and recorded on an Axioskop fluorescence microscope (Zeiss, Jena, Germany) equipped with a cooled CCD camera (Photometrics, Tucson, AZ, USA). Images were processed with the Power Gene 810/Probe software system (PSI, Chester, UK). Confocal images were obtained in a MRC-600 laser confocal imaging system with the Comos software package (BioRad, Hercules, CA, USA).

Transepithelial short- and open-circuit measurements

For short-circuit current measurements, filters were mounted in modified Ussing chambers (Jim's Instruments, Iowa City, IA, USA) and bathed on both sides with identical HEPES-buffered saline solutions that contained (mM) 130 NaCl; 5 sodium pyruvate; 4 KCl; 1 $CaCl_2$; 1 $MgCl_2$; 5 glucose and 5 HEPES-NaOH (pH 7.4). Bath solutions were gassed with room air. Solution temperature was maintained at 37°C. Short-circuit current (I_{sc}) measurements were obtained by using an epithelial voltage clamp (VCC-600; Physiologic Instruments, San Diego, CA, USA). Forskolin (Fsk) (20 μM) was added to the bathing solution to stimulate

cAMP-mediated Cl^- secretion. Cl^- secretory currents were identified on the basis of activation by forskolin and by sensitivity to basolateral glibenclamide (Glib) (200 μm).

For open-circuit measurements MDCK cells were grown for 3–12 days on permeable supports (MilliporeMA, Germany) coated with rat-tail collagen (Roche, Germany). The resistances of the monolayers were checked every day using a volt-Ω-meter (Millicell-ERS, Millipore, Germany) and typically reached values between 600 and 1800 Ωcm^2. Apical and basolateral surfaces of the epithelium were perfused continuously at a rate of 10 ml/min (chamber volume 2 ml). The bath solution contained (mM): 145 NaCl; 0.4 KH_2PO_4; 1.6 K_2HPO; 5 D-glucose; 1 $MgCl_2$; 5 HEPES and 1.3 Ca-gluconate (pH 7.4). Bath solutions were maintained at 37°C. The transepithelial resistance (R_{te}) was determined by applying short (1 s) current pulses (I=0.5 μA).

Results

CFTR transcript analysis

Firstly, CFTR expression in the transduced MDCK cells was characterized by RT-PCR analysis with two different pairs of CFTR primers (mammalian and human-specific, respectively). The “universal mammalian” primers amplified a 200 bp fragment spanning the region between exons 22–23 and were selected due to their reported success in amplifying CFTR transcripts from seven different mammalian species (221). The human-specific primers amplifying a fragment of 391 bp spanning exons 8–10 were previously described (180). Samples were also amplified for the housekeeping gene β-actin as a control (157). As shown in Fig. 1A, CFTR transcripts were amplified by the two different sets of primers in the three cell lines tested: the parental MDCK II (PAR), MDCK wt-CFTR and MDCK F508del-CFTR, showing that the human-specific primers can also amplify canine CFTR transcripts. However, results show that for a similar intensity of the β-actin-specific band, significantly lower levels are obtained for the CFTR-specific band in parental cells in comparison to wt- or F508del-CFTR transfected cell lines (compare lane 2 to lanes 3 and 4 in Fig. 1A).

Sequencing of these RT-PCR amplification products and nucleotide alignment analysis with human CFTR (Fig. 1B), revealed that in both wt- and F508del-CFTR transfected cell lines, transcripts correspond to CFTR of human origin (i.e., expressed from the transgene) whereas transcripts detected in the parental line correspond to canine CFTR, i.e., resulting from endogenous expression.

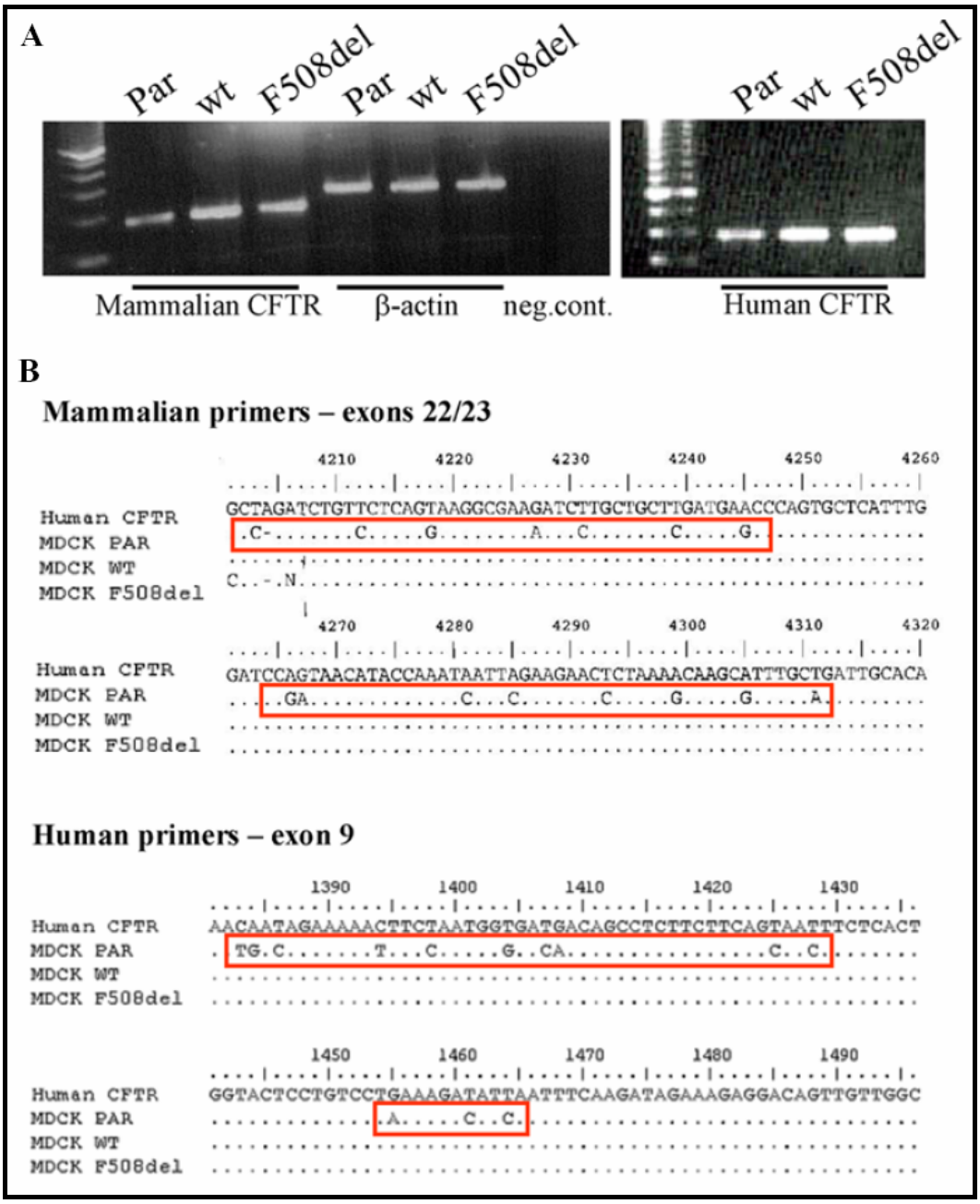

Fig. 1: CFTR transcript analysis in MDCK II cells. A) RT-PCR analysis of CFTR transcripts in MDCK II cells. Total RNA was prepared from parental and CFTR-transfected MDCK II cells. Samples of 1.0 μg of total RNA were reverse-transcribed to cDNA and PCR-amplified with mammalian or human-specific CFTR primers. β-actin-specific primers were used as a positive control for the RT-PCR and a reaction with no RNA was the negative control. B) Sequence alignment of the RT-PCR products from parental and CFTR-transfected MDCK II cells with human CFTR mRNA (GenBank Accession Number M28668), using the BioEdit software package (Tom Hall, Ibis Therapeutics, Carlsbad, CA, USA). In red boxes are marked the differences between the MDCK parental endogenous CFTR transcript and human CFTR.

We have submitted the sequences of these canine CFTR transcripts to the EMBL Nucleotide Sequence database, as expressed sequence tags (EST) with accession numbers: AJ810177, (EST resulting from exons 22/23 amplification, clone CFTR22) and AJ8110178 (EST from exons 8/10, clone CFTR8).

Expression of CFTR protein by MDCK cells

In order to assess expression of CFTR protein, total protein extracts from parental, wt-CFTR and F508del-CFTR MDCK cells were analysed by WB (Fig. 2A). To enhance CFTR expression levels, cells were incubated with sodium butyrate, an inhibitor of HDACs and thus a transcriptional activator of non-housekeeping genes (160) (see Methods). Results in Fig. 2A show that CFTR is not detected in MDCK parental cells and is only detected in transfected cell lines when incubated with butyrate. To confirm the nature of the bands detected, Western blot analysis combined with digestion with two glycosidases, Endo H and PNGase F was also performed (Fig. 2B). Results show that in wt-CFTR transfected MDCK cells the protein is fully-glycosylated, as demonstrated by the presence of the typical two-band pattern: the mature, Endo H-resistant and PNGase F-sensitive band C and the immature, Endo H- and PNGase F-sensitive band B. In contrast, F508del-CFTR is only detected as the immature ER-characteristic form (band B) that is sensitive to both glycosidases (63).

Since expression of membrane proteins is known to depend on the degree of polarization of epithelia, we examined here whether expression of CFTR is altered in MDCK II cells under highly polarized conditions. MDCK cells were maintained on permeable filter supports for 10 days to induce polarization, and WB analysis (Fig. 2C) shows that when these cell lines polarize, expression levels of wt- and F508del-CFTR are significantly increased in comparison to non-polarized cells.

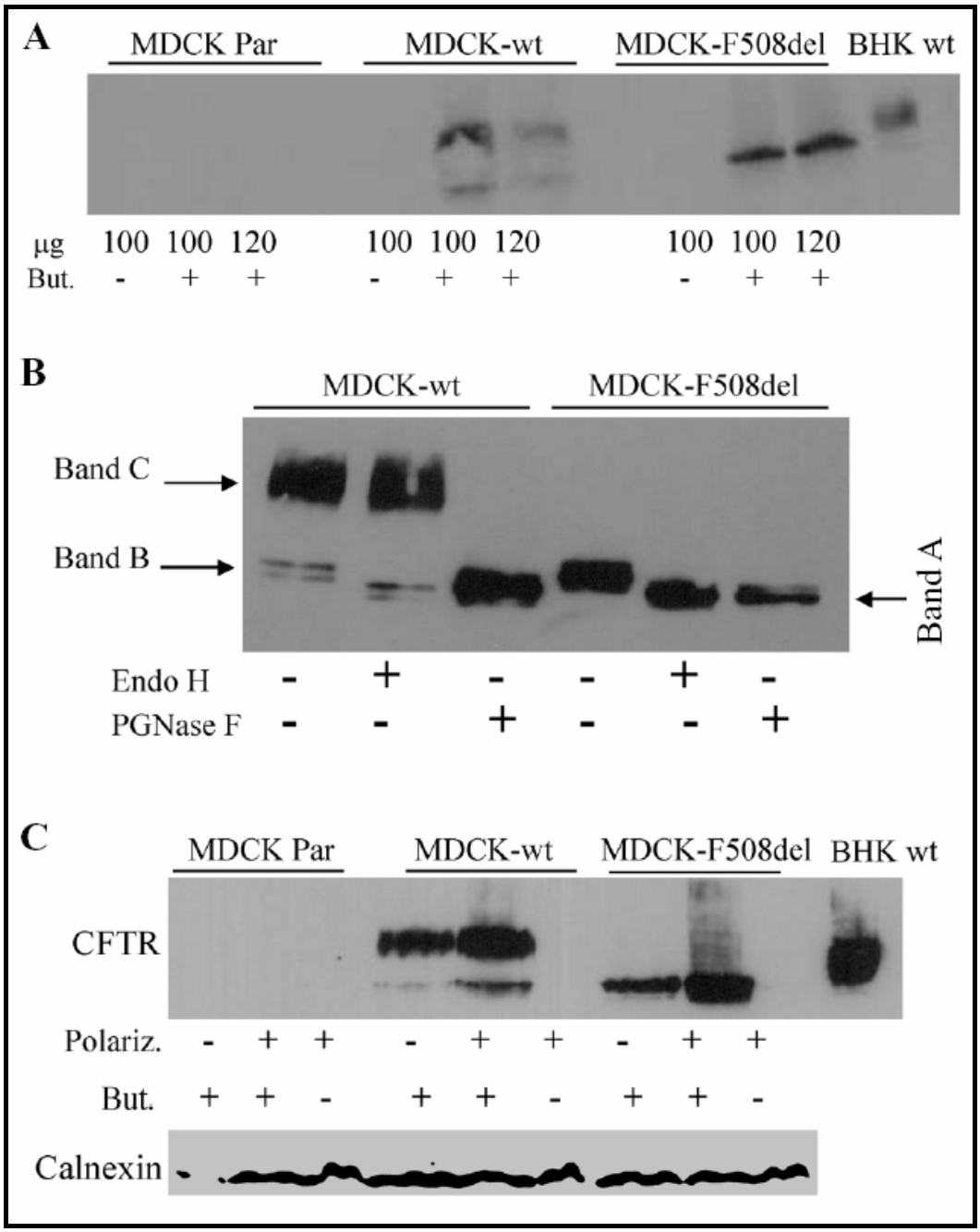

Fig. 2: Characterization of CFTR protein expression. A) Western blot of total protein extracts from parental (PAR), wt-CFTR and F508del-CFTR MDCK cells. Cells were grown on plastic dishes and incubated with 5 mM sodium butyrate for 18 h (but.). Cell lysates were prepared (µg of protein indicated) and resolved on a SDS-polyacrylamide gel before electrophoretic transfer to nitrocellulose for immunodetection of CFTR, using M3A7 Ab. Wt-CFTR baby hamster kidney cells (BHK) were used as a positive control. B) Western blot analysis combined with digestion with Endo H and PNGase F of total protein extracts from wt-CFTR and F508del-CFTR MDCK cells. Cells were grown on plastic dishes and incubated with 5 mM sodium butyrate for 18 h to enhance expression. Cell lysates (150 µg) were treated with the Endo H and PNGase F glycosidases, as indicated, proteins precipitated and

resolved on a SDS-polyacrylamide gel before electrophoretic transfer to nitrocellulose for immunodetection of CFTR, using M3A7 Ab. C) Western blot of total protein extracts (250 μg) from parental, wt-CFTR and F508del-CFTR cells. Cells were grown on plastic dishes (polariz -) or on filters (polariz +) and incubated with 5 mM sodium butyrate for 18 h. Proteins were resolved on a SDS-polyacrylamide gel before electrophoretic transfer to nitrocellulose for immunodetection of CFTR and calnexin, which was used as an internal control. Wt-CFTR baby hamster kidney cells (BHK) were used as a positive control.

Subcellular localization of CFTR

In order to evaluate the localization of CFTR in MDCK transfected cells, immunofluorescence microscopy was performed with two different anti-CFTR Abs (see Methods), namely: mAb 24-1 (Fig. 3A–C) and pAb MPCT1 (Fig. 3D–F). Results show that wt-CFTR exhibits membrane localization (Fig. 3B and E, compare with Fig. 4B), whereas F508del-CFTR is localized intracellularly (Fig. 3C and F), in an ER-like staining pattern (compare with Fig. 4A). No specific CFTR labelling was detected in MDCK II parental cells (Fig. 3A and D).

To characterize the localization of CFTR in polarized cells, MDCK wt- and MDCK F508del cells were grown on filters, immunostained with 24-1 anti-CFTR mAb and analysed by confocal microscopy. Sections on the *z* plane of the cells, from the apical to the basal membrane were acquired. While wt-CFTR localized predominantly in the apical region (Fig. 3G), F508del-CFTR showed mostly an intracellular, perinuclear distribution (Fig. 3H). These results are consistent with those evidencing wt- and F508del-CFTR localization in non-polarized cells (Fig. 3A–F).

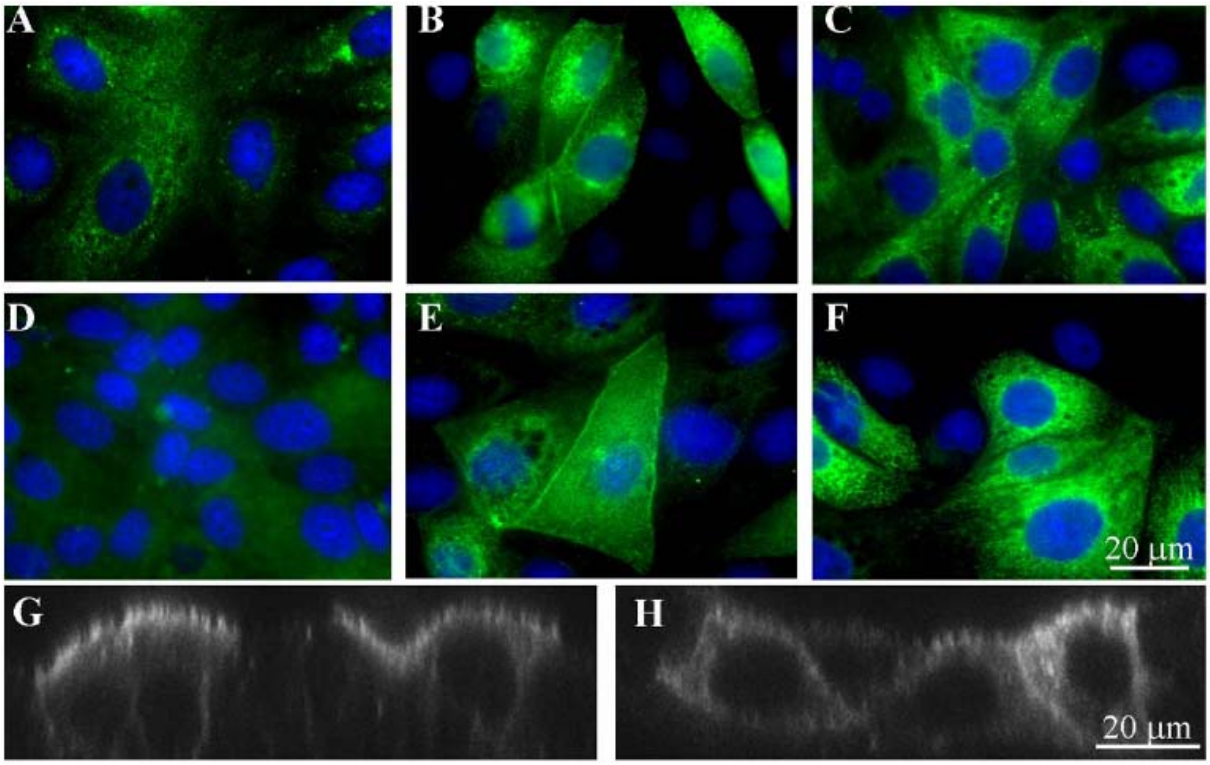

Fig. 3: Immunolocalization of CFTR in parental, wt-CFTR and F508del-CFTR MDCK cells. Cells were grown in 8-well chamber slides and analysed by immunofluorescence using the 24-1 mAb (A–C) or the MPCT1 (D–F) pAb against CFTR. F508del-CFTR (C and F) is detected strictly in the cytoplasm, while wt-CFTR (B and E) is located at the plasma membrane. No specific CFTR labelling was detected in MDCK II parental cells (A and D). Confocal fluorescence micrographs (*z* axis) of wt-CFTR (G) and F508del-CFTR (H) detected in polarized MDCK cells grown on filters and analysed by immunofluorescence using the anti-CFTR 24-1 mAb. *Bar*=20 µm.

Immunolocalization of several organelle markers was also performed, showing that non-polarized MDCK II cells present a diffuse ER staining pattern (Fig. 4A), a perinuclear Golgi localization (Fig. 4C) and a well-differentiated cytoskeleton network (panels E and F). E-cadherin was chosen as a membrane marker (Fig. 4D), while Rab4, a marker for the early endosomes, exhibits a localization that seems almost juxtaposed to the membrane (Fig. 4B).

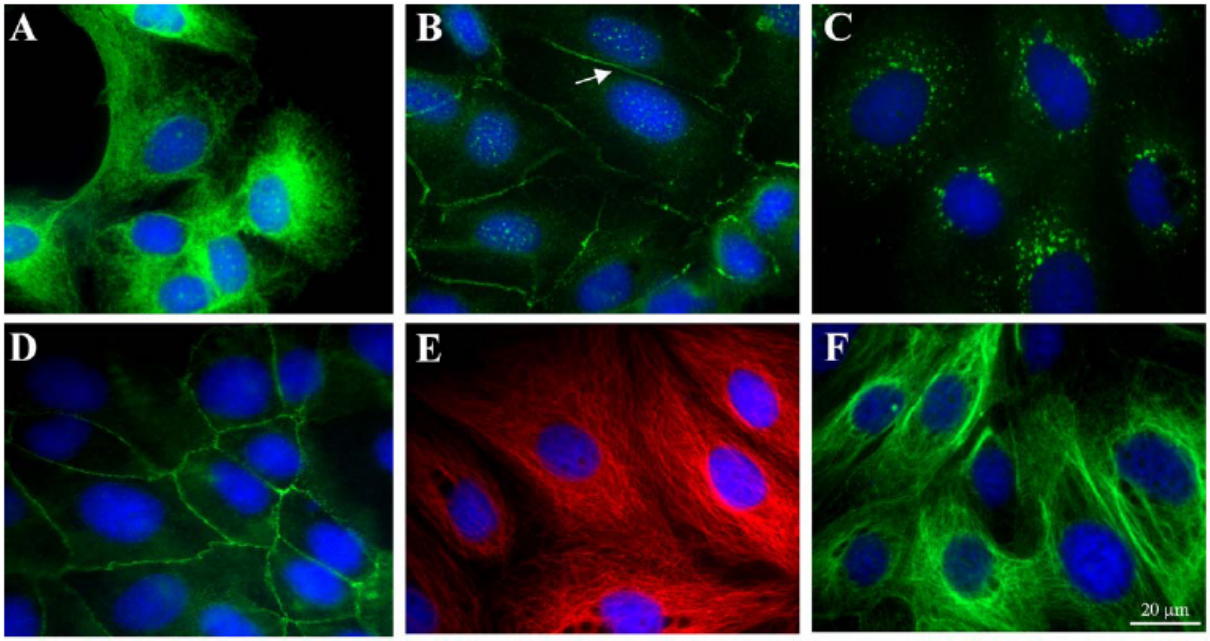

Fig. 4: Immunolocalization of several organelle markers in parental MDCK cells. Cells were analysed by immunofluorescence using the following Abs: A) anti-calnexin for ER staining; B) anti-Rab4 for early endosomes (arrow shows perimembranar localization); C) anti-GM130 for Golgi; D) anti-E-cadherin for plasma membrane; E) anti-tubulin for microtubules and F) anti-cytokeratin 18/19 for intermediate filaments of epithelial cells. *Bar*=20 µm.

CFTR functional analysis

Functional expression of CFTR in the transfected cell lines was assessed through transepithelial open- and short-circuit current measurements. Under short-circuit conditions, secretory CFTR currents were identified on the basis of activation by forskolin (Fsk, 20 µM) and inhibition by glibenclamide (Glib, 200 µM). Fsk-stimulated Cl^- secretion was clearly detected in wt-CFTR expressing cells (Fig. 5A), while MDCK F508del-CFTR only evidenced residual Fsk response when grown at 37°C (Fig. 5B). However, when F508del-CFTR cells were incubated at 27°C for 24 h, the Fsk response and inhibition by Glib was increased.

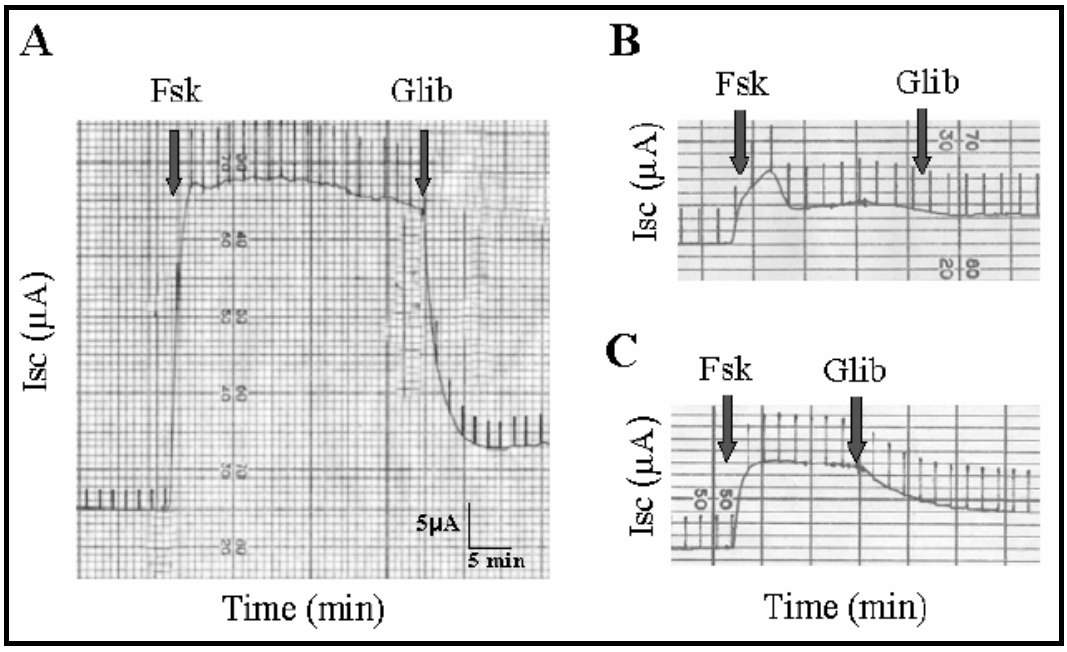

Fig. 5: Functional analysis of CFTR in short-circuit measurements. A) Original recording of the short-circuit current induced by forskolin (Fsk, 20 µM) and inhibited by glibenclamide (Glib, 200 µM) in MDCK wt-CFTR cells. B) A modest and transient increase in I_{sc} was also detected upon addition of forskolin to F508del-CFTR MDCK cells, which was enhanced following a 24 h-incubation at 27°C (C). Arrows indicate time of addition of forskolin or glibenclamide, respectively.

Open-circuit conditions (Fig. 6) confirmed these results and showed a large increase in the transepithelial conductance (G_{te}) of wt-CFTR cells upon stimulation with 3-isobutyl-1-methylxanthine (IBMX) and forskolin (I/F; 100 µM/2 µM) and just a minor increase in F508del-CFTR cells. Parental cells did not respond at all (Fig. 6A). Amiloride-sensitive Na^+ transport was not detected in any of the three cell lines and could not be induced by dexamethasone (5 days/0.1 µM) (data not shown). Moreover, we examined Ca^{2+}-activated transport by stimulation of luminal purinergic receptors with ATP (A, 100 µM). Large changes in transepithelial voltage and an increase in transepithelial conductance upon ATP stimulation were detected in early cultures (4 days) of all three cell lines, while Ca^{2+}-activated Cl^- conductance was progressively lost during continuous culture on permeable supports (12 days) (Fig. 6B and C).

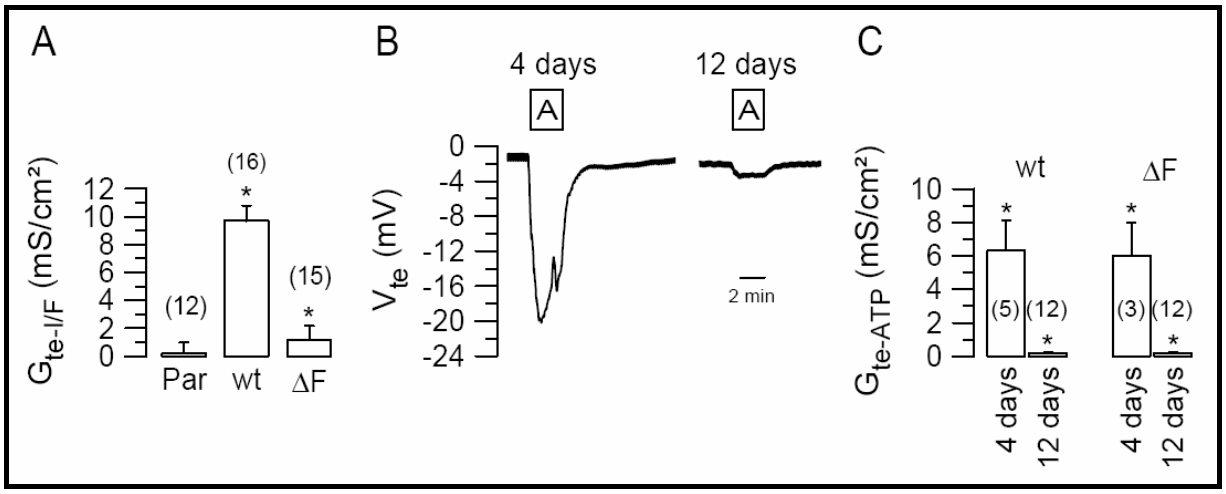

Fig. 6: Functional analysis of CFTR in open-circuit measurements. A) Summary of the transepithelial conductances (G_{te}) activated by IBMX and forskolin (I/F; 100 μM/2 μM) under open-circuit conditions in parental (PAR), wt-CFTR (wt) and F508del-CFTR (ΔF) cells. B) Original recording of the transepithelial voltage (V_{te}) and changes induced by ATP (A, 100 μM) in an early (4 days) and a late (12 days) culture of wt-CFTR cells. C) Summary of the transepithelial conductances activated by ATP in early and late cultures of wt-CFTR and F508del-CFTR cells. *Indicates significant effects of I/F and ATP, respectively (paired *t*-test). *n*, number of experiments.

Discussion

It is well known that protein trafficking is largely dependent on the polarization status of the epithelium and yet there are multiple examples of CFTR trafficking studies performed in non-epithelial/non-polarized cells, mainly due to difficulties in culture of primary cultures and to the fact that CFTR expression is progressively lost by immortalized cell cultures (80). Examples of studies carried out in non-epithelial/non-polarized cells include descriptions of a non-conventional biosynthetic trafficking pathway (11;234); a late quality control mechanism operating at early endosomes (195); characterization of ER-to-proteasome sorting in yeast cells (69).

The need and importance of appropriate epithelial polarized cellular models to finely investigate both the processing mechanisms and the trafficking pathways of wt- and F508del-CFTR in the same background, led us to produce the two novel cellular models described here.

We had first attempted to produce the cell lines stably expressing wt- and F508del-CFTR by transfection using cationic liposomes. Expression of CFTR was characterized in such cell lines at the level of transcripts and protein, total and at the membrane. However, after several reproducible experiments, a rapid decrease in CFTR protein expression occurred in those stable lipofectin-transfected MDCK II cell lines (F. Mendes, unpublished results), similarly to what is above described for immortalized primary cultures.

Since virally-transduced cell lines are generally described to exhibit very stable transgene expression (209) such an approach was also adopted here. We therefore, used an HIV-based lentivirus to transduce MDCK II cells with wt- and F508del-CFTR as transgenes and thus generate the stable expression systems herein described. Characterization of such cell lines at CFTR mRNA level evidenced that MDCK II parental cell line solely transduced with the lentiviral vector (i.e., with no transgene) already exhibits detectable levels of CFTR transcripts through the sensitive RT-PCR analysis employed here. This was unexpected since MDCK II cells had been previously reported to lack CFTR expression (159). These apparent contradictory results suggest that either the sensitivity of our RT-PCR protocols is higher or that the viral transduction somehow activated the endogenous canine CFTR gene. Indeed, sequencing of the respective CFTR RT-PCR product from the parental MDCK cells confirmed that it is not of human origin. Additionally, we cannot exclude the possibility that the MDCK II cells used here for lentiviral transduction differed from those used by the other authors. Notwithstanding, since no CFTR protein could be detected in the MDCK parental cell line, at least using the anti-CFTR Abs tested here (see below), we still regard this MDCK II cellular system as a good parental line for CFTR transduction.

Results from CFTR protein analysis of MDCK wt-CFTR and MDCK F508del-CFTR cell lines evidenced that wt-CFTR is detected mostly as the fully-glycosylated form (band C), typical of post-ER cellular compartments, being thus correctly processed, whereas F508del-CFTR could only be detected as the immature, core-glycosylated protein (band B) that is characteristic of the ER. These biochemical results were confirmed by immunofluorescence subcellular localization data, which revealed an apical membrane localization for wt-CFTR and most F508del-CFTR localized intracellularly in these cellular systems. Additionally, expression levels of both wt-CFTR and F508del-CFTR proteins in these MDCK II cells detected by WB at steady-state were shown to be increased when cells are polarized.

Comparison of CFTR expression results in the lentiviral transduced MDCK cells with those previously obtained for liposome-transfected MDCK cells, evidenced significantly higher expression levels of the CFTR transgene in the transduced cells and, most importantly,

sustained expression after a relatively high number of passages (F. Mendes, unpublished results).

Functional analysis of the transduced MDCK cell lines by transepithelial open- and short-circuit current measurements clearly identified secretory CFTR currents (IBMX/forskolin-activated, glibenclamide inhibited) in MDCK wt-CFTR cells, while MDCK F508del-CFTR cells only showed residual Cl^- currents in response to IBMX/forskolin when grown at 37°C. Parental cells did not respond at all. The Cl^- currents of MDCK F508del-CFTR cells were, however, increased following a 24 h-incubation at 27°C, consistently with the rescuing effect of low temperature described for F508del-CFTR in other cellular systems.

There was no evidence for Na^+ transport mediated by the epithelial Na^+ channel (ENaC) in these cell lines, as none of them evidenced amiloride-sensitive luminal currents, nor could these be detected following dexamethasone induction. This observation is not surprising since MDCK type II cells are derived from the kidney proximal tubule (184) (see Methods). As a consequence of the lack of expression of ENaC channels, the transepithelial voltage of the epithelium was close to zero mV in the absence of any stimulation However, upon stimulation of luminal purinergic receptors with ATP, Ca^{2+}-activated Cl^- transport was clearly detected in early cultures (4 days) of all three cell lines, which was progressively lost with prolonged (12 days) culture of polarized cells. This progressive loss of Ca^{2+}-activated Cl^- secretion during prolonged cell culture has also been observed for other epithelial cell lines such as M1 (collecting duct cells) or 16HBE (bronchial epithelial cells), and appears to reflect changes during differentiation (unpublished observations, K Kunzelmann).

MDCK type I cells transfected with wt- and F508del-CFTR have been used previously (133;164), but those systems have the disadvantage of expressing endogenous canine wt-CFTR protein in significant amounts (14;159). To circumvent the caveats of endogenous CFTR expression, the 27-kDa green fluorescent protein (GFP) tag was added at the N terminus of CFTR (133). However, this tag most plausibly disrupts the interaction of CFTR with other proteins that have been shown to be critical for its membrane traffic in epithelial cells, namely components of the SNARE machinery (reviewed in (4)).

Recent studies carried out using such MDCK I cells include the characterization of GFP-tagged F508del-CFTR trafficking to the plasma membrane under low temperature (213) and the identification of the C terminus of CFTR as a PDZ interacting apical membrane retention motif (213). MDCK II cells expressing FLAG-CFTR were used to show that CFTR is not

involved in the regulation of organelle pH nor on protein post-endocytic traffic (76) and that cAMP stimulates the apical recruitment of CFTR (87).

We believe that the novel cellular models produced here are more appropriate to investigate polarized membrane trafficking pathways of CFTR. Moreover, they allow comparison of such pathways between wt- and F508del-CFTR in the same cellular background. These models can also be useful to confirm/discard previously described mechanisms shown to occur in non-polarized cells regarding biogenesis, degradation, processing and traffic of CFTR (reviewed in (4)) and for the development of pharmacological therapies, namely by high-throughput screening strategies, aimed at identifying new drugs for the treatment of CF.

We conclude that these novel cell lines constitute *bona fide* models that mimic wt- and F508del-CFTR traffic, processing and function occurring in native polarized epithelial systems and provide significantly improved resources for cellular studies focused on the pathology or treatment of devastating genetic disorder.

Chapter 5

Regulation of the epithelial Na^+ channel by protein kinase CK2

Abstract

CK2 is an ubiquitous, pleiotropic and constitutively active Ser/Thr protein kinase that controls protein expression, cell signalling and ion channel activity. Phosphorylation sites for CK2 are located in the C terminus of both β- and γ subunits of the epithelial Na^+ channel (ENaC). We examined the role of CK2 towards the regulation of ENaC endogenous to native murine epithelia and in *Xenopus* oocytes expressing rENaC. In Ussing chamber experiments with mouse airways, colon and cultured M1 collecting duct cells, amiloride-sensitive Na^+ transport was inhibited dose-dependently by the selective CK2 inhibitor 4,5,6,7-tetrabromobenzotriazole (TBB). TBB, the structurally unrelated inhibitors heparin and poly E:Y all inhibited ENaC current in oocytes. Expression of a trimeric channel that lacks of both CK2 sites ($\alpha\beta_{S631A}\gamma_{T599A}$) produced a largely attenuated amiloride-sensitive whole cell conductance and rendered the mutant channel insensitive to CK2. Immunocytochemistry demonstrated translocation of CK2 to the cell membrane upon expression of wtENaC but not $\alpha\beta_{S631A}\gamma_{T599A}$ENaC. Chemiluminescence measurements suggested that phosphorylation by CK2 is essential for ENaC activity, but not for membrane expression of the three ($\alpha\beta\gamma$) ENaC subunits. Channels lacking the Nedd4-2 binding motif in βENaC (R561X, Y618A) no longer required the CK2 site for channel activity, implying an action of CK2 through inhibition of the Nedd4-2 pathway. We propose that the C terminus of βENaC is targeted by this essential, conserved pleiotropic kinase that directs its constitutive activity towards many cellular protein complexes.

Introduction

Electrogenic Na^+ absorption across the apical membrane of epithelia utilizes an amiloride-sensitive channel (ENaC) composed of three ($\alpha\beta\gamma$) subunits produced from different genes (38). In kidney collecting duct, distal colon, airway, secretory ducts from a variety of organs and the absorptive sweat duct, ENaC is regulated by an interaction between the β- and γ subunits (at each C terminus) and the ubiquitin ligase Nedd4-2. The WW domains of Nedd4-2 bind proline-rich PY motifs in each subunit leading to channel ubiquitination, internalization and degradation or channel inactivation (50;156). In turn, the Nedd4-2 interaction with ENaC is controlled by phosphorylation of either Nedd4-2, or the C termini of both β- and γENaC. Accordingly, the aldosterone induced serum- and glucocorticoid-dependent kinase, SGK1, phosphorylates Nedd4-2 on serine 444 and 338 and thereby reduces its interaction with the channel (50;204). Apart from this, SGK1 also phosphorylates ENaC directly at ser 621 (51). Protein kinase A, which is known to activate ENaC in alveolar epithelial cells, sweat duct and kidney, was also shown to phosphorylate Nedd4-2 (at ser 221, 246 and 327) and to reduce binding to ENaC (203). Thereby PKA prevents inhibition of ENaC due to phosphorylation at thr 613 by the extracellular regulated kinases (ERK) (232). Phosphorylation of thr 613 in βENaC and thr 623 in γENaC was shown to increase the channel's affinity towards Nedd4-2, and thereby downregulates channel activity (197).

Thus differential phosphorylation of both β- and γ subunits either enhances or reduces the affinity of ENaC for destruction by Nedd4-2, thereby controlling ENaC activity. Along this line the G protein-coupled receptor kinase 2 (Grk2) was found recently to upregulate the activity of ENaC in salivary duct cells (52). Grk2 acts twenty amino acids downstream of ERK on S633 in the C terminus of βENaC. It increases the activity of ENaC by rendering the channel insensitive to Nedd4-2 (52). Notably, an increased Grk2 activity has been reported to be associated with hypertension in humans and in animal models (65). Therefore imbalance in ENaC channel regulation by activatory or inhibitory pathways may lead to inappropriate Na^+ absorption, hypertension or cystic fibrosis-like phenotype (125).

Additional phosphorylation sites for the pleiotropic but essential protein casein kinase 2 (CK2) are located in the C terminus of the β- and γ subunits of ENaC (198). It has been demonstrated that CK2 specifically binds to and phosphorylates the carboxy termini of both these ENaC subunits. As found for the CK2 site (S633) in βENaC a pair of CK2 phosphorylation sites (βS631 and γT599) are located in close proximity to their respective PY motifs. CK2 is not easy to study as siRNA approaches invariably impact on multiple pathways due to its multiplicity of targets in signal pathways coupled to its essential function

for cell survival. Although no contribution of CK2 to regulation of ENaC followed single site mutation of putative CK2 targets in a previous study (198), we nevertheless investigated a role for CK2 towards ENaC function in native epithelia from airway and colon as well as *Xenopus* oocytes expressing rat ENaC. We found that constitutive CK2 phosphorylation maintains not only ENaC activity but also controls membrane subunit expression.

Material and Methods

Ussing chamber experiments

Tracheas and distal colon were removed from mice euthanased by ethically approved institutional procedures (C57BL/6, Charles Rivers, Germany). Tissues were put immediately into ice cold buffer solution of the following composition (mmol/l): NaCl 145, KCl 3.8, D-glucose 5, $MgCl_2$ 1, HEPES 5, Ca-gluconate 1.3. After stripping the colonic mucosa and opening tracheas by a longitudinal cut, the tissues were mounted into a micro-Ussing chamber with a circular aperture of 0.95 mm^2. Mouse M1 collecting duct cells (kindly provided by C. Korbmacher, Physiologisches Institut, Universität Erlangen, Germany) were grown to confluence on permeable supports and mounted into the Ussing chamber (9). Luminal and basolateral sides of the epithelium were perfused continuously at a rate of 5 ml/min. The bath solution containing (mmol/l) NaCl 145, KH_2PO_4 0.4, K_2HPO_4 1.6, D-glucose 5, $MgCl_2$ 1, HEPES 5, and Ca-gluconate 1.3, was heated to 37°C, and pH was adjusted to 7.4. Experiments were carried out under open-circuit conditions. Values for transepithelial voltages (V_{te}) were referred to the serosal side of the epithelium. Transepithelial resistance (R_{te}) was determined by applying short (1 s) current pulses (ΔI=0.5 μA) and after subtracting the resistance of the empty chamber, using Ohm's law ($R_{te}=\Delta V_{te}/\Delta I$). Transepithelial resistances were 63 ± 3.8 Ωcm^2; *n*=12 (trachea), 31 ± 2.1 Ωcm^2; *n*=13 (colon) and 669 ± 45 Ωcm^2; *n*=38 (M1).

cRNAs for ENaC subunits and CFTR

cDNAs encoding rat (FLAG-tagged or non-tagged) $\alpha\beta\gamma$ENaC (kindly provided by Prof. Dr. B. Rossier, Pharmacological Institute of Lausanne, Switzerland (67)) and the Cl^- channel CFTR were linearized in pBluescript with *Not*I or *Mlu*I, and *in vitro* transcribed using T7, T3 or SP6 promotor and polymerase (Promega, USA). Isolation and microinjection of oocytes have been described in details elsewhere (9). The ENaC mutants β_{S631A}, γ_{T599A}, β_{R561X}, β_{Y618A}, and β_{S633A} were generated by PCR and correct sequences were verified by sequencing.

Double electrode voltage clamp

Oocytes were injected with cRNA (10 ng, 47 nl double-distilled water). Water injected oocytes served as controls. 2–4 days after injection, oocytes were impaled with two electrodes (Clark instruments), which had a resistance of <1 MΩ when filled with 2.7 mol/l KCI. Using two bath electrodes and a virtual-ground headstage, the voltage drop across R_{serial} was effectively zero. Membrane currents were measured by voltage clamping (Warner oocyte clamp amplifier OC725C) in intervals from –90 to +30 mV, in steps of 10 mV, each 1 s. The bath was continuously perfused at a rate of 5 ml/min. All experiments were conducted at room temperature (22°C).

Chemiluminescence measurements

Oocytes were fixed for 60 min at room temperature with 3% paraformaldehyde (in TBS, pH 8.0) and washed with Tris buffered saline (TBS; (mM) 50 Tris, 138 NaCl, 2.7 KCl, pH 8.0) at room temperature. Then oocytes were incubated for 60 min in TBS with 1% bovine serum albumin (BSA), another 60 min with 1 μg/ml mouse monoclonal anti-FLAG M2 antibody in 1% BSA/TBS at 4°C (Sigma-Aldrich, Taufkirchen, Germany), washed at 4°C with 1% BSA/TBS and incubated with sheep anti-mouse IgG peroxidase-linked whole antibody (Amersham Biosciences, Freiburg, Germany) diluted 1:20000 in 1% BSA/TBS for 40 min at 4°C. Afterwards oocytes were washed for 60 min at 4°C in 1% BSA/TBS and finally in TBS (60 min, 4°C). Oocytes were placed separately in 50 μl ECL Plus Western Blotting Detection Reagents (Amersham). After incubation for 5 min at RT, chemiluminescence was measured in a BioOrbit 1250 Luminometer (Turku, Finland) and an integration period of 1 s was allowed.

Oocyte staining

Oocytes were incubated for 60 min in ND96, fixed for 60 min with 3% paraformaldehyde (in TBS, pH 8.0) and washed in TBS. After embedding in optimum cutting temperature compound (Sakura Finetek Europe, Zoeterwoude, NL), oocytes were cut to 20 μm slices with a cryostat (Leica CM3050 S, Wetzlar, Germany). Sections were put in either TBS or phosphate buffered saline (PBS; (mM) 137 NaCl, 1.8 KH_2PO_4, 10.3 Na_2HPO_4, pH 7.4), incubated for 5 min in 0.1% SDS in PBS and washed 2 times with either TBS or PBS. Sections were incubated for 60 min in TBS or PBS (5% bovine serum albumin) and for 60 min at 37°C with the anti-FLAG M2 antibody diluted 1:50 in 2% BSA/TBS or a goat polyclonal casein kinase IIα antibody (Santa Cruz Biotechnology, Heidelberg, Germany) diluted 1:25 in 2% BSA/PBS. Afterwards sections were washed twice in PBS and incubated for 1 h with secondary antibodies (donkey anti-mouse IgG-Alexa Fluor 488 conjugated and donkey anti-

goat IgG-Alexa Fluor 546 conjugated; Molecular Probes, Eugene, OR) at a dilution of 1:1000 in 2% BSA/PBS. Sections were washed 2 times with PBS for 5 min and covered with DakoCytomation fluorescent mounting medium (DakoCytomation, Inc., Carpinteria, CA). Images were obtained using a Zeiss Axiovert 200M microscope with a × 63 objective (Carl Zeiss, Inc., Jena, Germany).

Materials and statistical analysis

All compounds used were of highest available grade of purity. Amiloride, 2-dimethylamino-4,5,6,7-tetrabromo-1H-benzimidazole (DMAT), forskolin, IBMX=3-isobutyl-1-methylxanthine, heparin, okadaic acid, poly E:Y peptide and poly K were from Sigma. 4,5,6,7-tetrabromobenzotriazole (TBB) was a generous gift from Prof. L. Pinna (Department of Biological Chemistry, University of Padua, Italy). Student's *t*-test was used for statistical analysis. A *P* value of <0.05 was regarded as significant.

Results

CK2 phosphorylation sites in βENaC and γENaC are necessary for ENaC activity

We examined the contribution of CK2 to regulation of epithelial Na^+ channels in native epithelia from mouse trachea and colon. In Ussing chamber experiments we explored CK2-selective concentrations of the specific inhibitor TBB (4,5,6,7-tetrabromobenzotriazole), which was shown to have no effect on over 30 other kinases. TBB selectivity depends on its ability to bind an unusual hydrophobic ATP binding site that differs from the equivalent in conventional kinases. Electrogenic Na^+ transport in mouse trachea was assessed by inhibition of ENaC with amiloride (10 μM) (Fig. 1A). TBB (10 μM) reduced the transepithelial voltage V_{te} and attenuated amiloride-sensitive short-circuit currents ($I_{sc\text{-}amil}$) in a dose-dependent manner (Fig. 1A and B). Similarly, TBB blocked amiloride-sensitive Na^+ transport in mouse distal colon (Fig. 1C and D). This effect could be reproduced in cultured mouse M1 collecting duct cells, grown on permeable supports (Fig. 1E and F). The combined results suggested that endogenous epithelial Na^+ channels expressed in epithelial tissues are maintained in an active state by constitutively active CK2.

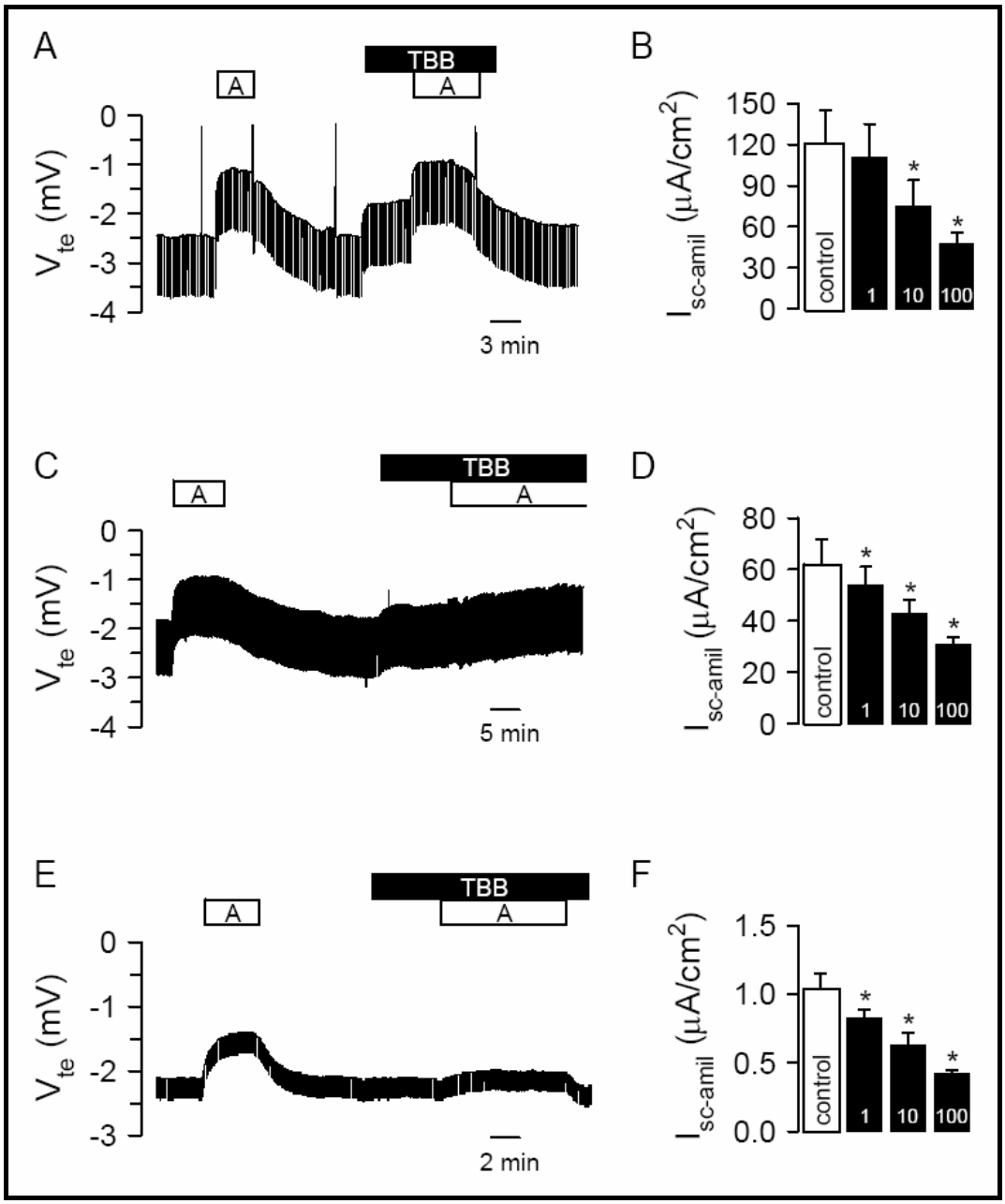

Fig. 1: CK2 activates ENaC in epithelia. Original Ussing chamber recordings of the transepithelial voltages V_{te} detected in mouse trachea (A), mouse colon (C) and M1 cells (E). Effects of amiloride (A, 10 μM) and the CK2 inhibitor TBB (10 μM). Concentration-dependence of the effects of TBB on amiloride-sensitive transport in trachea (B), colon (D), and M1 cells (F). *Indicates significant effects of TBB (paired *t*-tests). Number of experiments 9–13 for each series.

To further confirm regulation of epithelial Na^+ channels by CK2, the three ($\alpha\beta\gamma$) ENaC subunits were expressed in *Xenopus* oocytes and examined in double electrode voltage clamp experiments. As shown in the original recording in Fig. 2A, expression of the three

ENaC subunits produced a large current, which was inhibited by amiloride (A, 10 μM). CK2 structure is virtually identical in oocytes compared to mammals and TBB (10 μM) significantly reduced amiloride-sensitive whole cell currents and conductance (G_{amil}), respectively (Fig. 2A and B). Another compound, 2-dimethylamino-4,5,6,7-tetrabromo-1H-benzimidazole (DMAT), has recently been shown to inhibit CK2 with higher inhibitory potency but it has limited efficacy *in vivo* due to rapid metabolism (LA Pinna, personal communication). At 2 μM, we did not observe inhibition of ENaC currents by DMAT in *Xenopus* oocytes, however, 5 μM reduced amiloride-sensitive ENaC conductance significantly from 31.9 ± 6.8 to 25.7 ± 4.1 μS (*n*=5). Regulation of ENaC by CK2 was further validated using the structurally-unrelated peptide inhibitor of CK2, poly E:Y and conversely, by activating CK2 with polylysine (poly K) (149;216). The peptides were injected into oocytes at final concentrations between 10 and 100 μM, and amiloride-sensitive Na^+ conductances were compared before and 1–5 h after injection. During these few hours, ENaC conductance further increased almost doubling in water injected controls (Fig. 2C), However, this time-enhanced Na^+ conductance was nevertheless inhibited by poly E:Y and was further activated through stimulation of CK2 by poly K (Fig. 2C). CK2 is known to associate with protein phosphatase 2A (PP2A). To confirm phosphorylation-dependent activation of ENaC, ooctyes were exposed to a PP2A-specific concentration of okadaic acid (10 nM), which further increased amiloride-sensitive Na^+ transport (Fig. 2D and E). Thus ENaC appears to be activated by constitutively active CK2 with counter regulation by PP2A-like inhibition. As a further check for CK2 function, injection of the non-specific CK2 inhibitor heparin (10 μM) also reduced Na^+ conductance in *Xenopus* oocytes (Fig. 4).

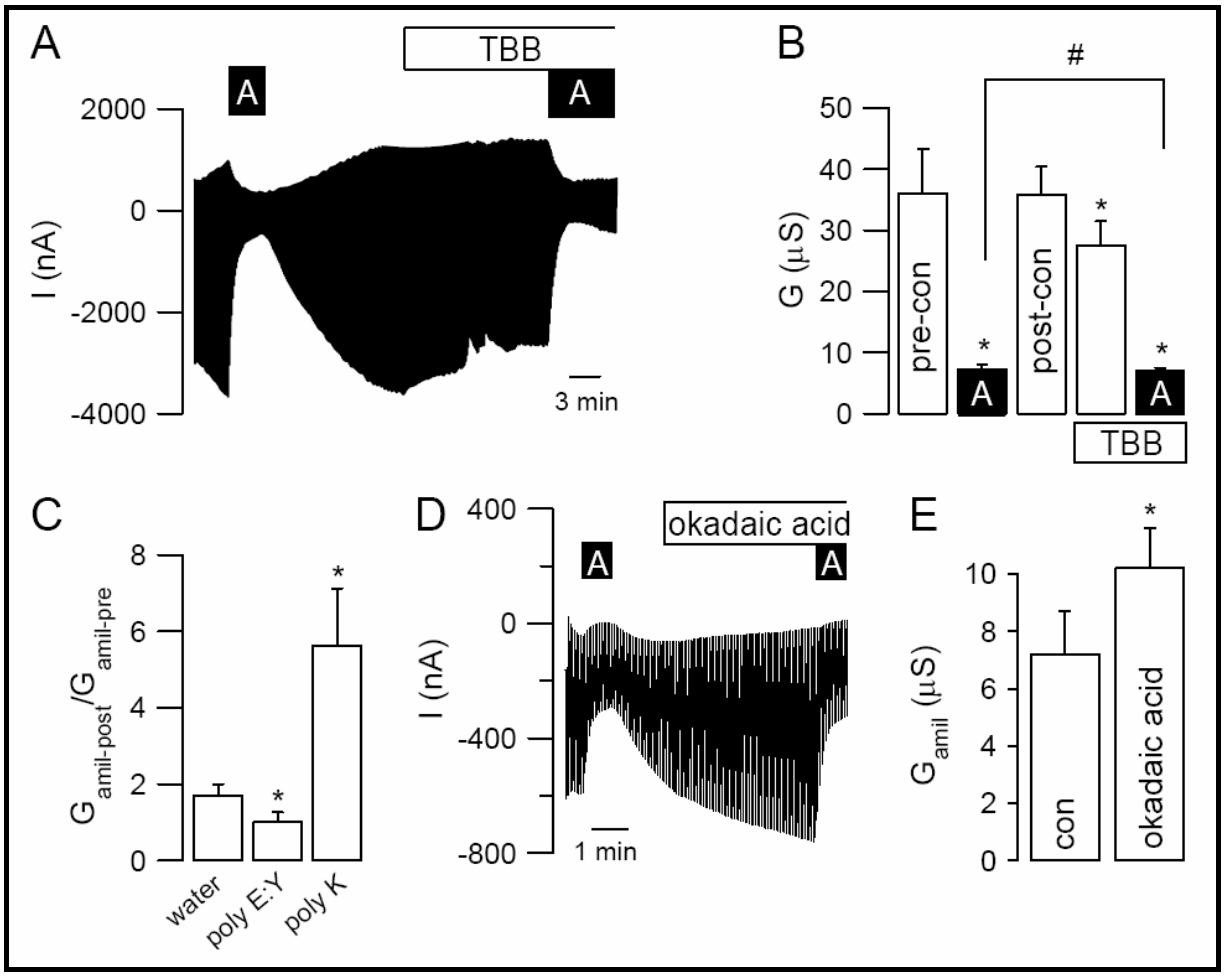

Fig. 2: CK2 activates ENaC in *Xenopus* oocytes. A) Current recording from a *Xenopus* oocyte expressing αβγENaC and effects of amiloride (10 μM) and TBB (10 μM). B) Summary of the effects of amiloride and TBB on whole cell conductance in ENaC expressing oocytes. C) Summary of the change of amiloride-sensitive conductance (G_{amil}) after injection of water, the CK2 inhibitor poly E:Y (50 μM) and CK2 activator poly K (50 μM), respectively. D) Current recording of an ENaC expressing oocyte and the effects of amiloride (A, 10 μM) and okadaic acid (100 nM). E) Summary of the effect of okadaic acid on the amiloride-sensitive whole cell conductance measured in oocytes. *Indicates significant effects (paired *t*-test). #Indicates significant difference for the effects of amiloride before and after incubation with TBB (paired *t*-test). 6–25 experiments for each series.

Removal of CK2 sites inhibits amiloride-sensitive Na^+ conductance and renders ENaC insensitive towards TBB

Similar to endogenous Na^+ currents present in epithelial tissues (Fig. 1), ENaC expressed exogenously in *Xenopus* oocytes was inhibited by TBB in a dose-dependent manner (Fig. 3A

and C). ENaC contains two phosphorylation sites for CK2, in βENaC (serine 631) and γENaC (threonine 599). Changing both CK2 sites to alanines ($\alpha\beta_{S631A}\gamma_{T599A}$), virtually eliminated Na^+ conductance and rendered residual conductance of the doubly mutated channel insensitive to TBB (Fig. 3B and D). Trimeric Na^+ channels carrying only one mutation in either βENaC or γENaC ($\alpha\beta_{S631A}\gamma$, $\alpha\beta\gamma_{T599A}$), produced more measurable but still significantly attenuated Na^+ conductances when compared to wtENaC (Fig. 3E). Moreover, the remaining amiloride-sensitive Na^+ conductances formed by dimeric αβENaC and αγENaC channels were further reduced by β_{S631A} and γ_{T599A}, respectively (Fig. 3F). Taken together, these results demonstrate that phosphorylation of β_{S631} and γ_{T599} is essential for an active ENaC.

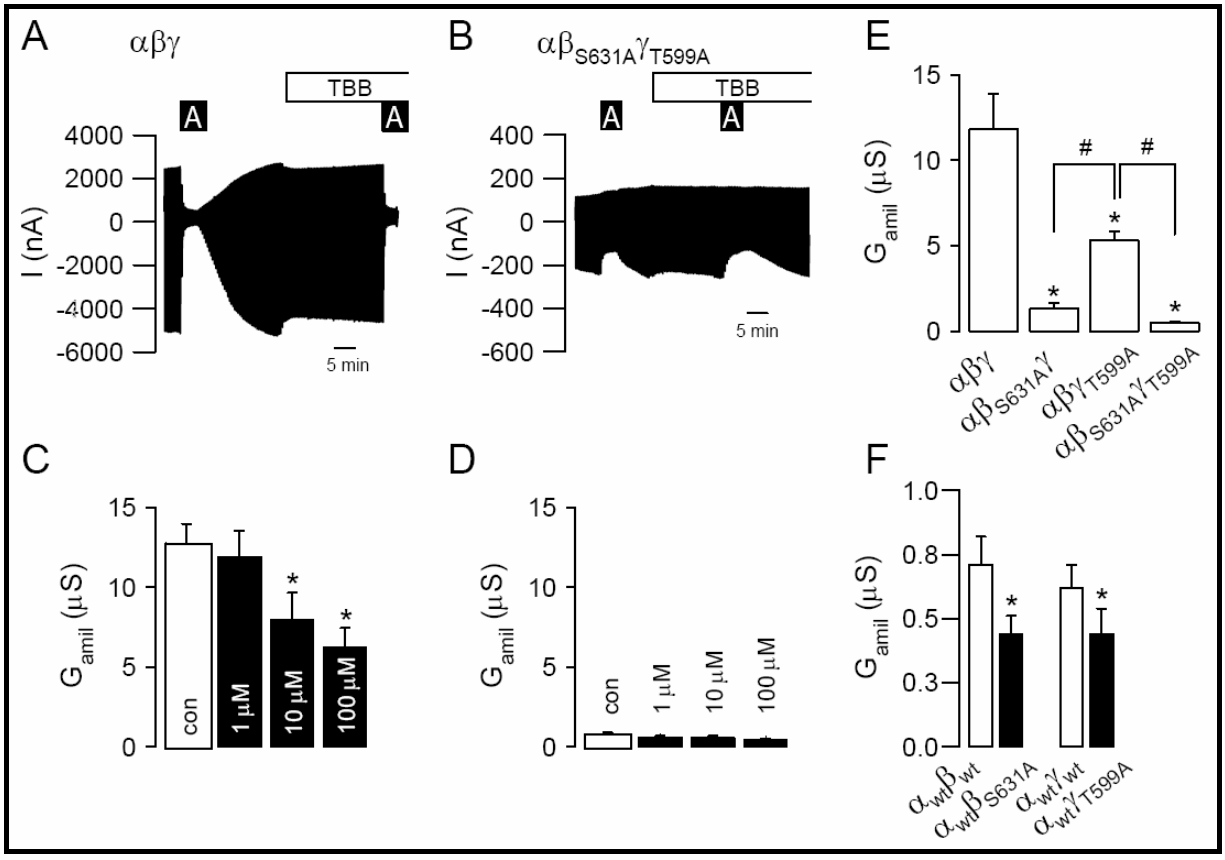

Fig. 3: Elimination of CK2 sites inhibits ENaC. A) Current recording from a *Xenopus* oocyte expressing αβγENaC and effects of amiloride (10 μM) and TBB (10 μM). B) Current recording from a *Xenopus* oocyte expressing $\alpha\beta_{S631A}\gamma_{T599A}$ENaC and effects of amiloride (10 μM) and TBB (10 μM). C and D) Summaries of the effects of amiloride and TBB on G_{amil} generated by αβγENaC and $\alpha\beta_{S631A}\gamma_{T599A}$ENaC. E) Comparison of G_{amil} produced by wt (αβγ)-, single mutants ($\alpha\beta_{S631A}\gamma$, $\alpha\beta\gamma_{T599A}$)- and a double mutant ($\alpha\beta_{S631A}\gamma_{T599A}$) ENaC. F) Summaries of G_{amil} produced by dimeric wt (αβ, αγ)- and mutant ($\alpha\beta_{S631A}$, $\alpha\gamma_{T599A}$) ENaC channels. $^{*,\#}$Indicate significant difference (paired *t*-test). 13–25 experiments for each series.

CK2 controls ENaC activity and membrane expression of αENaC

In order to examine whether CK2 phosphorylation controls membrane expression of ENaC, Flag-tagged αENaC was co-expressed with non-flagged βγENaC in *Xenopus* oocytes. Appearance of α_{Flag}ENaC in the cell membrane was monitored by chemiluminescence, during an observation period of 40–48 h (cf Methods). In parallel, amiloride-sensitive Na^+ conductance was assessed at corresponding intervals. When $\alpha_{Flag}\beta\gamma$ENaC was allowed to express in ND97 control buffer, G_{amil} and membrane expression continuously increased (Fig. 4A and B). In contrast, when oocytes were kept in 10 μM TBB containing buffer, amiloride-sensitive Na^+ conductance was completely abolished and membrane expression was significantly reduced. Moreover, co-injection of αβγENaC-cRNAs together with the CK2 inhibitors heparin (final concentration 10 μM) or the peptide inhibitor poly E:Y (final concentration 50 μM) also inhibited Na^+ conductance along with membrane expression of αENaC (Fig. 4C–F). Finally M1 cells were grown on permeable supports, in the absence or presence of 10 μM TBB. As observed in oocytes, TBB reduced amiloride-sensitive transport from 2.05 ± 0.35 μA/cm^2 (*n*=19) to 1.52 ± 0.25 μA/cm^2 (*n*=16). Thus CK2 phosphorylation differentially controls membrane expression of αENaC and ENaC activity. The inhibitory effect of conductance (3–5-fold) was significantly greater than on the attenuated expression (typically 2-fold).

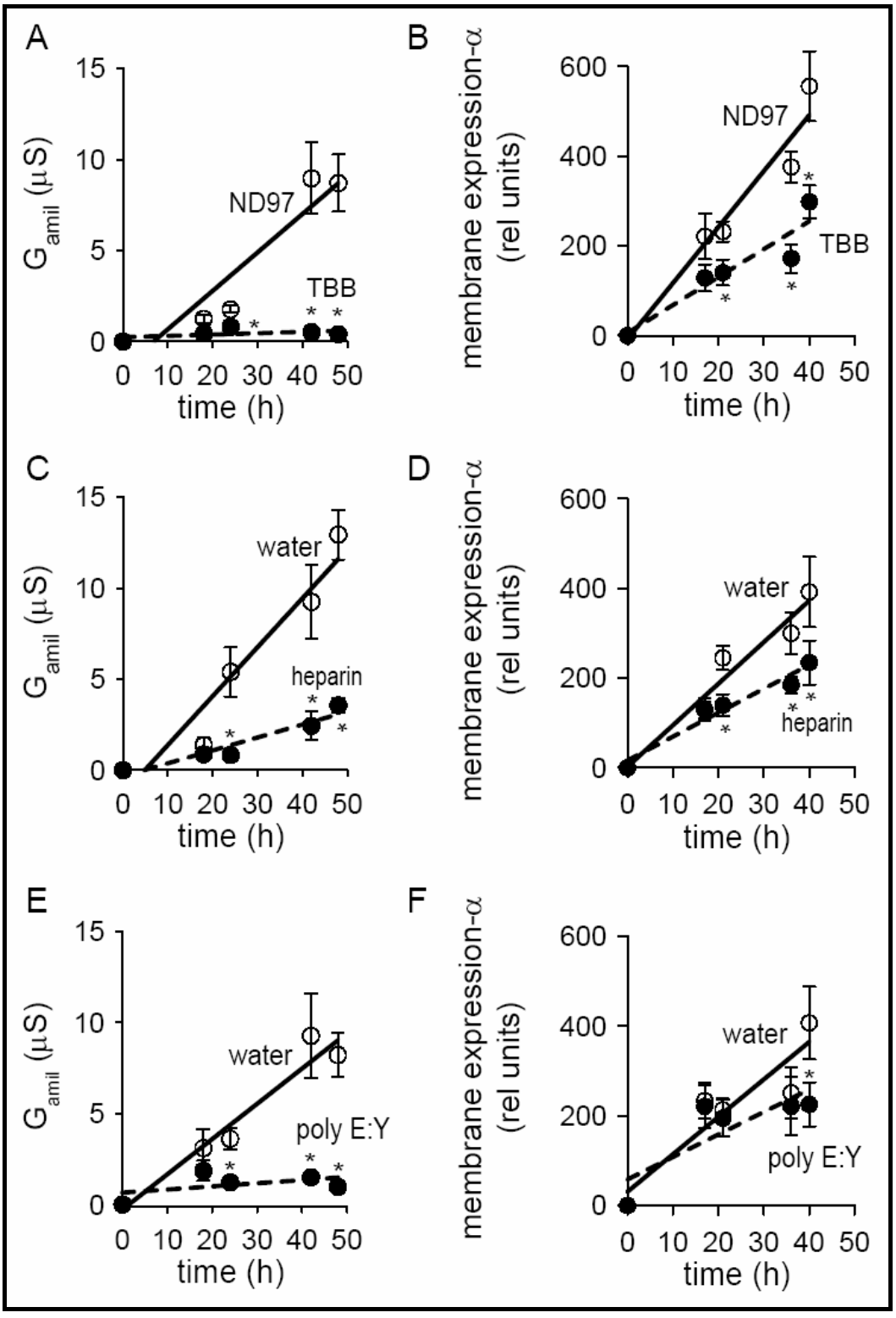

Fig. 4: CK2 controls maturation of ENaC in *Xenopus* oocytes. Time course for the expression of G_{amil} (A, C, E) and membrane expression of α_{Flag}ENaC (B, D, F). Ooctyes were kept in ND97 or in ND97 containing TBB (10 µM), or were injected with heparin (10 µM), poly E:Y (50 µM) or equal amounts (30 nl) of water. *Indicates significant difference when compared to ND97 or water (unpaired *t*-tests). 6–13 experiments for each series.

CK2 is essential for ENaC activity but not for membrane expression of αENaC

The contribution of both CK2 phosphorylation sites in βENaC and γENaC, to membrane expression of αENaC was further examined by expressing single mutants ($\alpha_{Flag}\beta_{S631A}\gamma$ENaC or $\alpha_{Flag}\beta\gamma_{T599A}$ENaC) or the double mutant ($\alpha_{Flag}\beta_{S631A}\gamma_{T599A}$ENaC). For the sake of simplicity, we only show (relative to wild-type) the data for membrane expression and ENaC conductance reached after 40 h of expression. Importantly, single mutations in βENaC or γENaC largely reduced the Na^+ conductance but did not affect membrane expression. Notably, elimination of both CK2 sites in βENaC and γENaC also showed no effects on membrane expression of αENaC, but nevertheless eliminated the inhibitory effects of TBB (Fig. 5 upper panel). Amiloride-sensitive Na^+ conductances were strongly reduced for the double mutant (Fig. 5 lower panel). These data suggest that single site mutation and double site mutation create different effects on ENaC such that TBB significantly reduces αENaC expression only when one or other CK2 site is intact. The reason why expression of αENaC is unaffected by double mutation is unclear at present.

Since nearby located Grk2 phosphorylation site S633 was reported to control Nedd4-2 binding to ENaC (52), we explored whether similar may hold true for CK2. To that end, we compared whole cell conductances of several mutants compared to wtENaC. A mutation in the Nedd4-2 binding site (β_{Y618A}) increased whole cell conductance relative to the wild-type and eliminated the inhibitory effect of S631A on ENaC conductance (Fig. 5B). This strongly suggests that CK2 phosphorylation at S631 antagonizes the inhibitory action of Nedd4-2 in ENaC (197) (Fig. 8). Similarly, when we expressed the truncated $\alpha\beta_{R561X}\gamma$ENaC channel we found that amiloride-sensitive whole cell conductance was largely increased (64.5 ± 5.9 μS; *n*=14) when compared to αβγENaC, and was now unaffected by 10 μM TBB (64.1 ± 6.1 μS). Interestingly, mutating the Grk2 site also reduced ENaC conductance, however, eliminating both CK2 and Grk2 sites in βENaC produced a channel with similar activity than wtENaC (Fig. 5B). This suggests that the closely located phosphorylation sites of CK2 and Grk2 (S631, S633) influence each other.

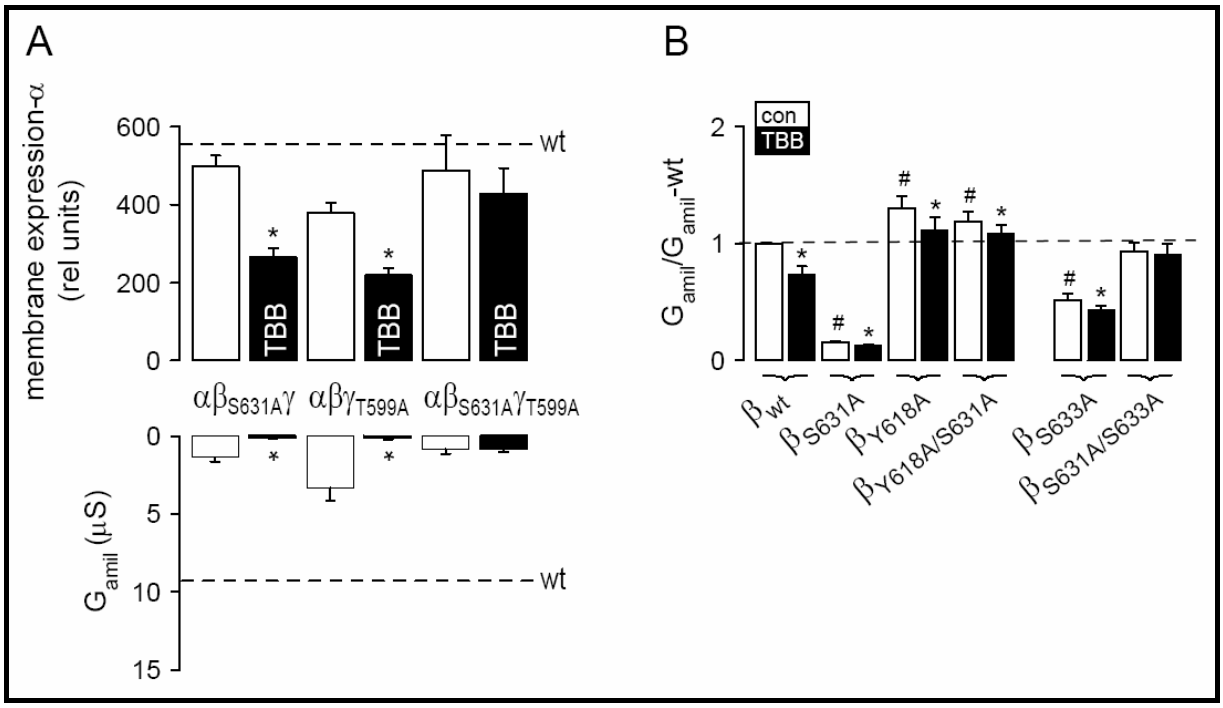

Fig. 5: CK2 is essential for ENaC activity and antagonizes inhibitory effect of Nedd4-2 on ENaC. A) Summary of αENaC membrane expression and G_{amil} after 40 h. TBB inhibited membrane expression of single mutants ($\alpha\beta_{S631A}\gamma$, $\alpha\beta\gamma_{T599A}$) but not that of the double mutant ($\alpha\beta_{S631A}\gamma_{T599A}$). G_{amil} was largely reduced for all mutants and G_{amil} produced by the double mutant was no longer inhibited by TBB. *Dashed lines* indicate membrane expression and G_{amil} of wtENaC. B) Whole cell conductances relative to wtENaC. A mutation in the PY motif (Y618A) increased Na^+ conductance and S631A no longer inhibited ENaC conductance. The Grk2 mutant S633A inhibited ENaC, but not as a double mutant S631A/S633A. *Indicates significant effects of TBB (paired *t*-tests). 9–24 experiments for each series.

CK2 controls expression of βENaC and γENaC

The activity of epithelial Na^+ channels largely depends on co-expression of both β- and γ subunits. Membrane expression of βENaC and γENaC was monitored by injecting $\alpha\beta_{Flag}\gamma$ENaC or $\alpha\beta\gamma_{Flag}$ENaC, respectively, and Na^+ conductances were measured in parallel. Na^+ conductances generated by either $\alpha\beta_{Flag}\gamma$ENaC or $\alpha\beta\gamma_{Flag}$ENaC, respectively, were almost completely abolished when oocytes were exposed to 10 μM TBB, while membrane expression of β_{Flag} and γ_{Flag} were reduced by only around 50% (Fig. 6A). This indicates regulation of membrane expression of βENaC and γENaC, of similar magnitude to that of αENaC. We further examined whether β_{Flag} and γ_{Flag} behave in a similar fashion in the absence of αENaC. Dimeric channels formed by $\beta_{Flag}\gamma$ENaC or $\beta\gamma_{Flag}$ENaC produced small

but detectable amiloride-sensitive whole cell conductances (0.74 ± 0.2 μS; *n*=8 and 0.2 ± 0.1 μS; *n*=7, respectively). Notably, expression of β_{Flag}ENaC and γ_{Flag}ENaC was not significantly reduced in the absence of αENaC and was not inhibited by TBB although both CK2 sites were present (data not shown). The results again suggest that CK2 sites control ENaC activity to a much greater degree than membrane expression.

In order to further assess the impact of CK2 phosphorylation on membrane expression of βENaC and γENaC in trimeric ($\alpha\beta_{Flag}\gamma$ENaC and $\alpha\beta\gamma_{Flag}$ENaC) channels, we expressed single mutants ($\alpha\beta_{S631A\text{-}Flag}\gamma$ENaC or $\alpha\beta\gamma_{T599A\text{-}Flag}$ENaC) or double mutants ($\alpha\beta_{S631A\text{-}Flag}\gamma_{T599A}$ENaC or $\alpha\beta_{S631A}\gamma_{T599A\text{-}Flag}$ENaC) in the absence or presence of 10 μM TBB. For all mutant combinations, Na^+ conductances were largely reduced and residual conductances generated by the double mutants were insensitive to TBB (Fig. 6B and C). In contrast membrane expression of βENaC and γENaC was not affected by any of the mutations and expression of the double mutants ($\alpha\beta_{S631A\text{-}Flag}\gamma_{T599A}$ENaC; $\alpha\beta_{S631A}\gamma_{T599A\text{-}Flag}$ENaC) was no longer inhibited by TBB (Fig. 6B and C). These data suggest that if CK2 sites are present in βENaC and γENaC, they need to be phosphorylated to allow proper membrane expression of all three subunits. However, while CK2 phosphorylation is essential for channel activity, it does not seem to be crucial for membrane expression of either α-, β- or γENaC.

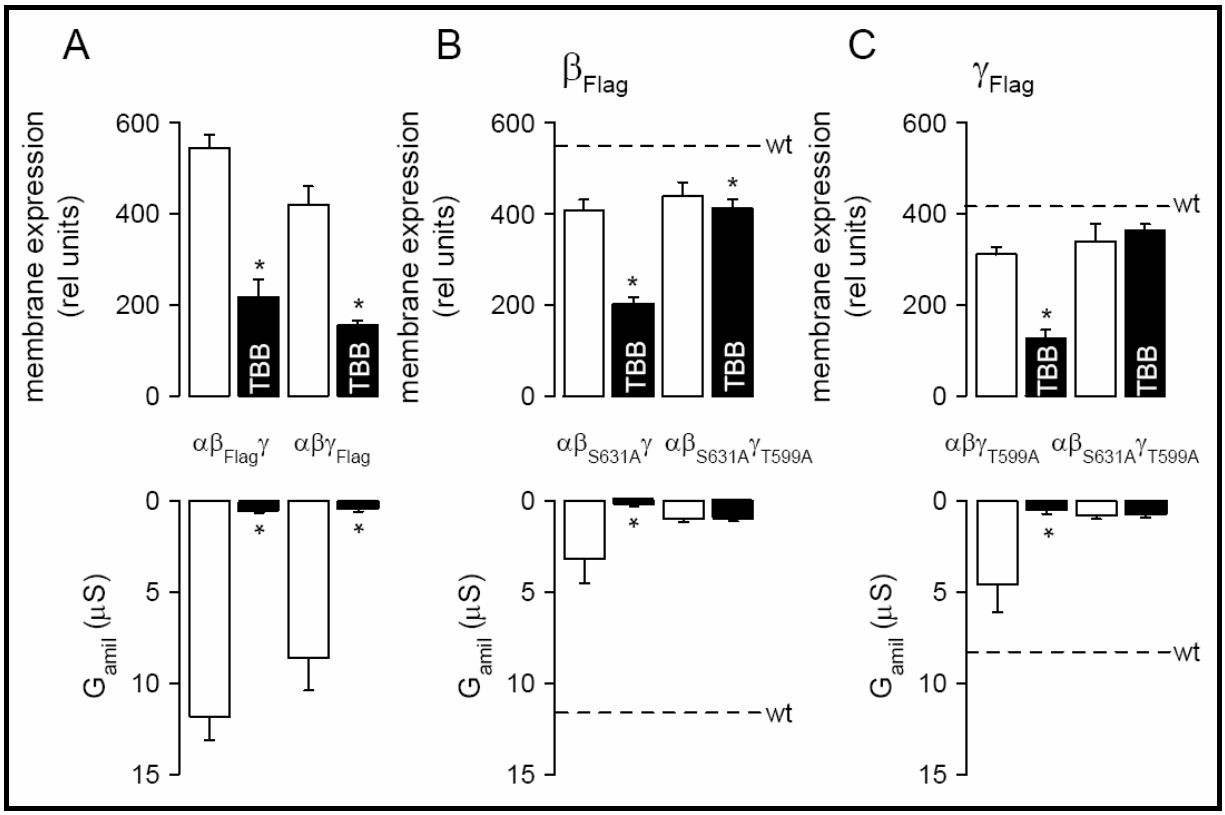

Fig. 6: CK2 is not essential for membrane expression of βENaC and γENaC. Summary of βENaC and γENaC expression and G_{amil} after 40 h. A) Inhibition of membrane expression of βENaC and γENaC and G_{amil} by 10 µM TBB. B and C) TBB inhibited membrane expression of β_{Flag}ENaC and γ_{Flag}ENaC in single mutants ($\alpha\beta_{S631A}\gamma$, $\alpha\beta\gamma_{T599A}$), but not in double mutants ($\alpha\beta_{S631A}\gamma_{T599A}$). G_{amil} was largely reduced for all mutants, and G_{amil} produced by the double mutants was no longer inhibited by TBB. *Dashed lines* indicate membrane expression and G_{amil} of wtENaC. *Indicates significant effects of TBB (paired *t*-tests). 6–12 experiments for each series.

ENaC translocates CK2 to the cell membrane

It has been reported that CK2 binds specifically to ENaC (198). This suggests that CK2 may be translocated by ENaC to the cell membrane as found CFTR (216). Oocytes expressing ENaC and non-injected control oocytes were immunolabeled, after embedding and cutting into 20 µm sections. Using an anti-Flag antibody, αENaC could be visualized in membranes of *Xenopus* oocytes expressing $\alpha_{Flag}\beta\gamma$ENaC (Fig. 7A). Moreover, upon expression of $\alpha\beta_{Flag}\gamma$ENaC or $\alpha\beta\gamma_{Flag}$ENaC, β- and γ subunits could be immunolabeled in the oocyte membrane (Fig. 7B, left panel). Expression of the three subunits was similar in $\alpha\beta_{S631A}\gamma_{T599A}$ENaC injected oocytes (Fig. 7B, right panel). However, while CK2 was detected

in membranes of oocytes expressing wtENaC, no membrane staining of CK2 was detectable in $\alpha\beta_{S631A}\gamma_{T599A}$ENaC injected oocytes (Fig. 7B, lower panel). These results suggest that CK2 may be translocated to oocyte membranes by binding to ENaC β- and γ subunits.

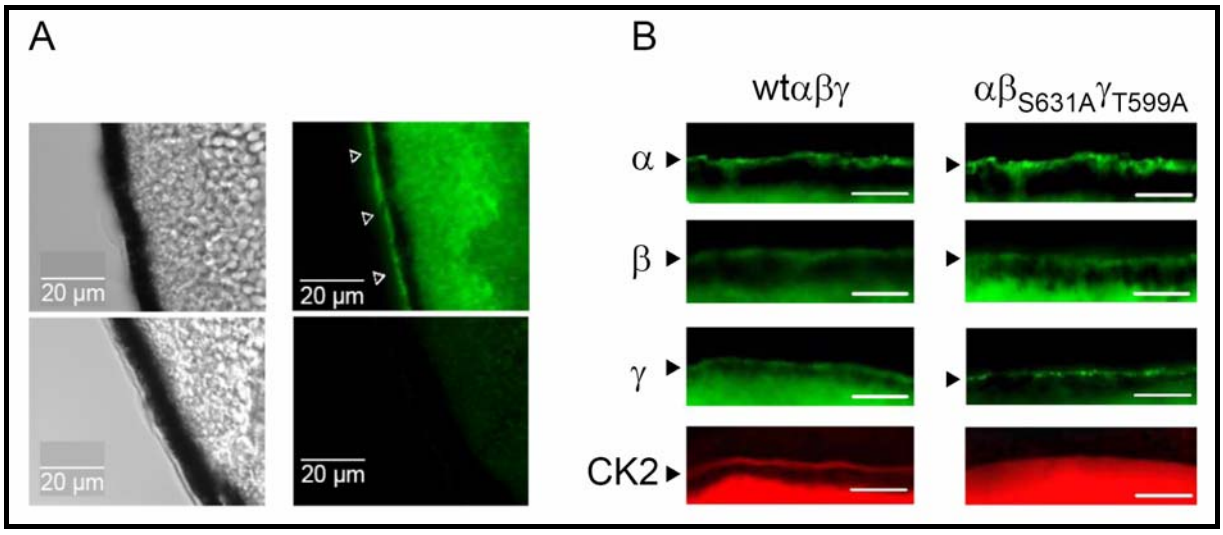

Fig. 7: wtENaC translocates CK2 to the cell membrane. A) DIC image of the oocyte membrane (left panels) and immunostaining of α_{Flag}ENaC in an ENaC expressing (right upper panel) and a non-injected (right lower panel) oocyte. B) Immunostaining of the three ENaC subunits (green) and CK2 (red) in wtENaC (left panel) and $\alpha\beta_{S631A}\gamma_{T599A}$ENaC (right panel) expressing oocytes. *Bars* indicate 10 µm. Experiments were performed at least in triplicates.

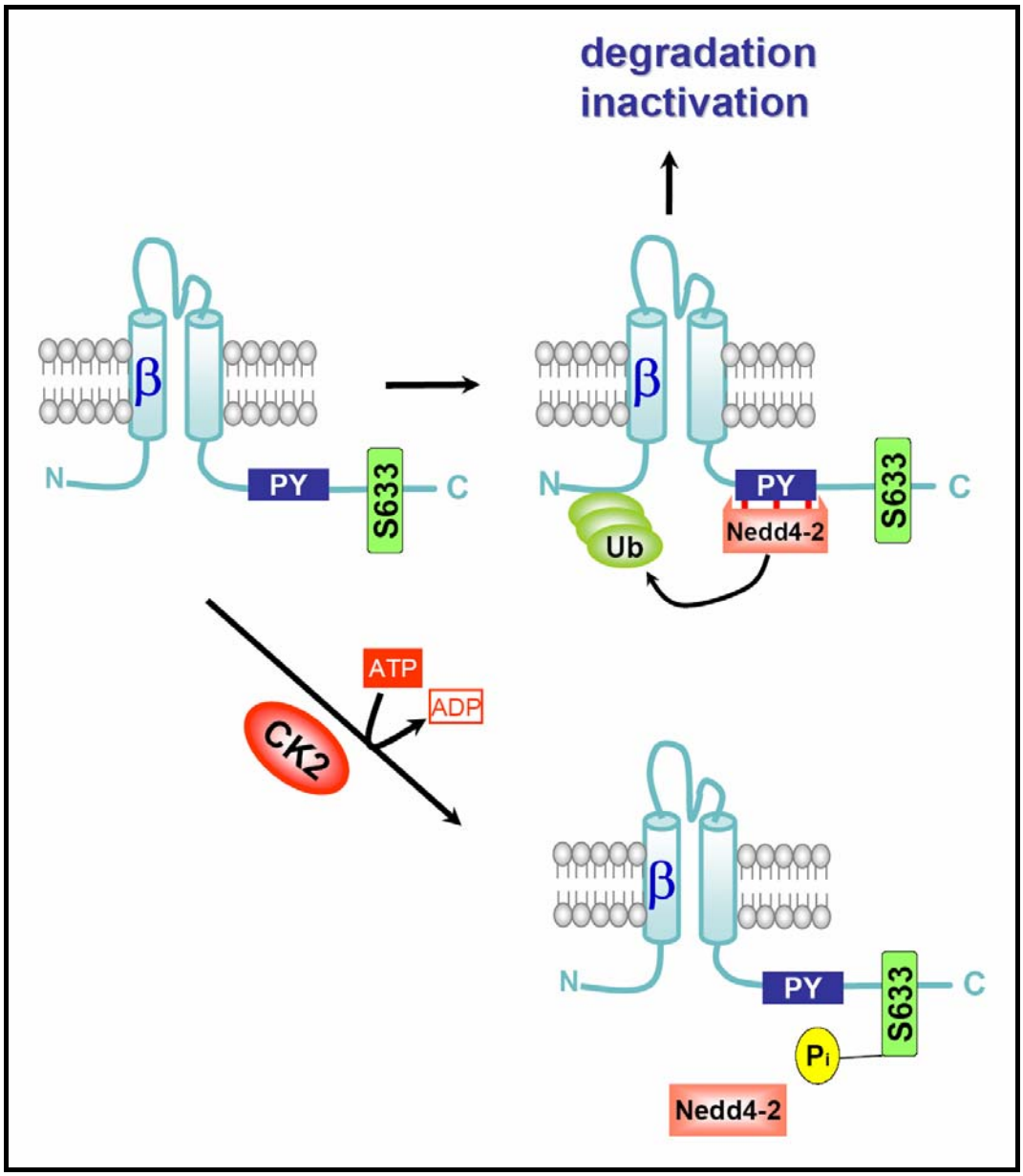

Fig. 8: Model for CK2 action on ENaC. Binding of the ubiquitin ligase Nedd4-2 leads to ubiquitination of ENaC and subsequent degradation of the channel and/or channel inactivation. Phosphorylation of ENaC at ser 633 reduces affinity of ENaC for Nedd4-2, thereby maintaining membrane localization and activity of ENaC.

Discussion

CK2 regulates ion channels

CK2 is an essential, constitutively regulated multifunctional protein kinase, whose functions are not fully understood (204). CK2 is thought to insert into protein complexes bringing its constitutive activity to many signalling complexes (p53, ion channels, actin capping at

membranes, lipid flippases etc). In this respect, it might also be relevant that CK2 controls trafficking and sorting of trans-Golgi proteins (albeit via a specific isoform). The constitutive activity of CK2 also affects a number of membrane channels and pumps. These include polycystin-2 (PC-2), a divalent cation-selective channel where CK2 maintains the Ca^{2+} sensitivity (36). Ca^{2+} sensitivity of PC-2 was significantly reduced by CK2 site mutation (S812A), whereas PC-2 expression was unaffected and we find that ENaC behaves in a related manner. However, our observed differential effect between channel function and expressions is not universal. For example, CK2-mediated phosphorylation of three critical serine residues within nephrocystin is essential for co-localization of nephrocystin with the sorting proteins PACS-1 at the base of cilia, and phosphorylation of CK2 sites within PC-2 were reported to be important for proper ciliary localization of the TRPP channels (88;189). Inhibition of CK2 was shown to eliminate interaction of PACS-1 and nephrocystin and to induce defective nephrocystin targeting. Thus, CK2 phosphorylation may be relevant to the common autosomal form of polycystic kidney disease.

Other ion channels are also described to be regulated by CK2. Thus CK2 regulates the current amplitude of voltage-dependent Ca^{2+} channels (106), as well as Ca^{2+}-dependent gating of small conductance Ca^{2+}-activated K^+ channels (22). SK channels are organized in multiprotein complexes together with CK2 and the protein phosphatase 2A, located in the postsynaptic pole of cochlear outer hair cells. Furthermore, CK2 has recently been found to regulate CFTR, the chloride channel that is defective in cystic fibrosis. As in this study, CK2 becomes membrane associated with CFTR. Once again both CK2 and PP2A co-localize with different domains of CFTR (149;216). Importantly, CK2 binding is disease relevant. It was shown that mutation of the CK2 target at S511 in the first nucleotide binding domain disrupts both CFTR channel gating and binding of CK2. TBB inhibited CFTR activity in mammalian cells and *Xenopus* oocytes. Notably, the interaction of CK2 with NBD1 of CFTR was abolished by the most common CFTR mutation, F508del. Loss of CK2 binding rendered F508del-CFTR insensitive to TBB and CK2 was no longer expressed in the cell membrane (216). Once again, CFTR expression determines the cellular localization of CK2, which could have effects on other membrane conductances as well such as amiloride-sensitive Na^+ absorption. It is interesting to note that CK2 is not stimulatory for the function of all proteins studied to date. CK2 is inhibitory towards another ABC family member ABCA1 thus constitutively suppressing the lipid ‘flippase’ activity of this CFTR related protein.

C terminus of βENaC - a target for kinase regulation of ENaC

Phosphorylation-dependent regulation of ENaC is demonstrated in the present study by heparin, a non-specific inhibitor of CK2 directed against acidic motifs, the peptide inhibitor of

CK2, poly E:Y and the specific CK2 inhibitors TBB and DMAT. Inhibition of protein phosphatases with okadaic acid further increased Na^+ conductance, indicating the importance of basal CK2-dependent phosphorylation for ENaC regulation (15) and elimination of CK2 phosphorylation sites abrogated Na^+ conductance in *Xenopus* oocytes. Thus ENaC is compellingly regulated by CK2 in *Xenopus* oocytes and epithelial tissues examined here. Yet in a previous report such a regulation could not be detected in salivary duct cells (52). Instead, activation of ENaC by the G protein-coupled receptor kinase 2 (Grk2) was found. Due to phosphorylation of S633 by Grk2 in the C terminus of βENaC, the affinity of Nedd4-2 binding to ENaC is apparently reduced, thus enhancing ENaC currents. According to the present data (Fig. 5B), a similar scenario may hold true for CK2-dependent regulation of ENaC. We note that both phosphorylation sites for Grk2 and CK2 are located in close proximity to one other. We speculate that since CK2 classically engages in hierarchical phosphorylation with other kinases, depending on the cell type and expression levels of the kinases involved, phosphorylation through either Grk2 or CK2 could control ENaC activity and membrane expression. Moreover, phosphorylation by CK2 is likely to affect regulation by Grk2 and vice versa (Fig. 5B). Further experiments will be needed to unravel this complex regulatory network and should focus on inhibitory phosphorylation by ERK and its counteraction by activation through PKA, Grk2 and CK2, with Nedd4-2 as the central control switch (7;52;197;232).

Summary

The epithelial Na^+ channel (ENaC) is located in the apical membrane of salt (re-) absorbing epithelia in kidney, colon, airways and glandular excretory ducts. A variety of mechanisms for the regulation of ENaC have been described, which may indicate the necessity for a tight control of ENaC and Na^+ absorption in the human body.
Essential tasks of ENaC comprise:
i) control of volume and electrolyte composition of extracellular fluids
ii) regulation of blood pressure
iii) control of Na^+ reabsorption

In the present thesis particular attention is given to the regulation of ENaC by
i) purinergic receptors
ii) CFTR and changes in the intracellular Cl^- concentration
iii) protein kinase CK2

Using electrophysiological and molecular biological methods it is demonstrated that both stimulation of purinergic receptors and activation of CFTR and other Cl^- channels lead to inhibition of epithelial Na^+ channels, resulting in reduced Na^+ absorption. Additional experiments showed that both mechanisms are additive. Activation of purinergic receptors is the starting point for a signalling cascade, leading to inhibition of ENaC via hydrolysis of the phospholipid PIP_2. The Na^+ channel is also inhibited by stimulation of CFTR- or other Cl^- channels, which change the intracellular Cl^- concentration upon activation in co-expression experiments. A correlation was found between the degree of ENaC inhibition and the increase in intracellular Cl^- concentration. A similar correlation was found for the inhibition of ENaC by stimulation of purinergic receptors. While binding of ENaC to PIP_2 keeps the channel in an active state, interference of ENaC with intracellular Cl^- seems inhibitory on ENaC function.

To carry out CFTR studies under conditions like in native tissue, two new cell lines were created from MDCK type II cells (polarized canine kidney epithelial cells), which stably express wt-CFTR or its mutant counterpart F508del-CFTR. The cell lines have been proven to grow as tight monolayers and are therefore suitable for Ussing chamber experiments. Subsequent co-expression of ENaC will allow to study the interaction between CFTR and ENaC in a polarized epithelium.

CK2 is a constitutively active protein kinase that influences the activity of the channel through its binding and phosphorylation of both β- and γ subunits of ENaC. Lack of these phosphorylation sites or dephosphorylation of one of these sites results in a significant attenuation of the activity of the epithelial Na^+ channel. These and other experiments suggest that phosphorylation of both β- and γENaC by CK2 prevents binding of the ubiquitin ligase Nedd4-2 to ENaC. Lack of binding of Nedd4-2 to ENaC may result in both reduced endocytosis and accumulation of ENaC in the cell membrane as well as increase in ENaC activity.

A better understanding of the mechanisms that are involved in the regulation of the epithelial Na^+ channel may contribute to the identification of new therapeutic targets. In this way, diseases that are connected with a dysfunction of ENaC could be treated more effective, which may improve quality of life and prognosis of patients.

Zusammenfassung

Der epitheliale Na^+-Kanal, kurz ENaC, wird in der apikalen Membran von Kochsalz-(re-) absorbierenden Epithelien in Niere, Kolon, Luftwegen und exkretorischen Drüsen exprimiert. Für die Regulation von ENaC sind eine Vielzahl von Mechanismen beschrieben, was die Notwendigkeit einer strengen Kontrolle des ENaC und der Na^+-Absorption im menschlichen Körper erkennen lassen dürfte.
Die wesentlichen Aufgaben von ENaC bestehen u.a. aus:
i) Kontrolle des Volumens und der Elektrolyt-Zusammensetzung des Extrazellulärraums
ii) Regulation des Blutdrucks
iii) Kontrolle der Na^+-Resorption

In der vorliegenden Arbeit richtet sich das besondere Augenmerk auf die Regulation von ENaC durch
i) purinerge Rezeptoren
ii) CFTR und Veränderungen in der intrazellulären Cl^--Konzentration
iii) Protein-Kinase CK2

Durch den Einsatz elektrophysiologischer und molekularbiologischer Methoden wird gezeigt, dass sowohl die Stimulation purinerger Rezeptoren als auch die Aktivierung von CFTR und anderer Cl^--Kanäle die Hemmung epithelialer Na^+-Kanäle bewirkt. Dies führt zu einer Verminderung der Na^+-Absorption. Weitere Experimente bewiesen, dass es sich hierbei um additive Mechanismen handelt. Die Aktivierung purinerger Rezeptoren markiert den Anfangspunkt einer Signalkaskade, die über Hydrolyse des Phospholipids PIP_2 zur Inhibition von ENaC führt. In Coexpressionsexperimenten hat die Stimulation von CFTR-Cl^--Kanälen oder anderer Cl^--Kanäle, die nach ihrer Aktivierung die intrazelluläre Cl^--Konzentration verändern, ebenfalls die Hemmung des epithelialen Na^+-Kanals zur Folge. Es ließ sich ein Zusammenhang herstellen zwischen dem Ausmaß der ENaC-Hemmung und dem Anstieg der intrazellulären Cl^--Konzentration. Eine ähnliche Korrelation wurde bezüglich der Inhibition von ENaC durch Stimulierung purinerger Rezeptoren gefunden. Während die Bindung von ENaC an PIP_2 den Kanal in einem aktiven Zustand hält, scheint sich das Interferieren von ENaC mit intrazellulärem Cl^- hemmend auf seine Funktion auszuwirken.

Um CFTR-Studien unter Bedingungen durchführen zu können, die denen im nativen Gewebe entsprechen, wurden aus MDCK Typ II-Zellen (polarisierte Hunde-Nierenepithelzellen) zwei neue Zelllinien geschaffen, die wt-CFTR oder dessen mutiertes Gegenstück F508del-CFTR stabil exprimieren. Die Zelllinien wachsen erwiesenermaßen als

dichte Ein-Zell-Schichten und eignen sich daher für Ussing Kammer-Experimente. Die spätere Coexpression von ENaC wird es erlauben, die Interaktion zwischen CFTR und ENaC in einem polarisierten Epithel zu untersuchen.

CK2 ist eine konstitutiv aktive Protein-Kinase, die Einfluss auf die Aktivität des Kanals nimmt, indem sie an die β- und γ Untereinheit von ENaC bindet und diese phosphoryliert. Das Fehlen dieser Phosphorylierungsstellen oder die Dephosphorylierung einer dieser Stellen führt zu einer deutliche Abnahme der Aktivität des epithelialen Na^+-Kanals. Diese und andere Experimente deuten darauf hin, dass die Phosphorylierung von β- und γENaC durch CK2 die Bindung der Ubiquitin-Ligase Nedd4-2 an ENaC verhindert. Die fehlende Bindung von Nedd4-2 an ENaC dürfte sowohl zu einer verringerten Endozytose und zur Anhäufung von ENaC in der Zellmembran als auch zu einer Zunahme der Aktivität von ENaC führen.

Ein besseres Verständnis der Mechanismen, die an der Regulation des epithelialen Na^+-Kanals beteiligt sind, könnte zur Identifizierung neuer therapeutischer Wege beitragen. Auf diese Weise könnten Erkrankungen, die mit einer Fehlfunktion von ENaC in Zusammenhang stehen, effektiver behandelt werden, wodurch sich Lebensqualität und Prognose der Patienten verbessern könnten.

References

1. Adam, G., Ousingsawat, J., Schreiber, R., and Kunzelmann, K. (2005) Increase in intracellular Cl^- concentration by cAMP and Ca^{2+}-dependent stimulation of M1 collecting duct cells. *Pflugers Arch.* **449,** 470-478

2. Aharonovitz, O., Zaun, H. C., Balla, T., York, J. D., Orlowski, J., and Grinstein, S. (2000) Intracellular pH regulation by Na(+)/H(+) exchange requires phosphatidylinositol 4,5-bisphosphate. *J. Cell Biol.* **150,** 213-224

3. Alvarez, d. l. R., Canessa, C. M., Fyfe, G. K., and Zhang, P. (2000) Structure and regulation of amiloride-sensitive sodium channels. *Annu. Rev. Physiol.* **62,** 573-594

4. Amaral, M. D. (2005) Traversing the cellular maze-How much CFTR needs to go through to avoid cystic fibrosis? *Pediatr. Pulmonol.* **39,** 479-491

5. Aoyagi, K., Sugaya, T., Umeda, M., Yamamoto, S., Terakawa, S., and Takahashi, M. (2005) The activation of exocytotic sites by the formation of phosphatidylinositol 4,5-bisphosphate microdomains at syntaxin clusters. *J. Biol. Chem.* **280,** 17346-17352

6. Arriza, J. L., Weinberger, C., Cerelli, G., Glaser, T. M., Handelin, B. L., Housman, D. E., and Evans, R. M. (1987) Cloning of human mineralocorticoid receptor complementary DNA: structural and functional kinship with the glucocorticoid receptor. *Science* **237,** 268-275

7. Awayda, M. S., Ismailov, I. I., Berdiev, B. K., Fuller, C. M., and Benos, D. J. (1996) Protein kinase regulation of a cloned epithelial Na^+ channel. *J. Gen. Physiol.* **108,** 49-65

8. Bachhuber, T., Almaca, J., Mehta, A., Schreiber, R., and Kunzelmann, K. (2007) Regulation of the epithelial Na^+ channel by protein kinase CK2. *J. Biol. Chem. (submitted)*

9. Bachhuber, T., König, J., Voelcker, T., Mürle, B., Schreiber, R., and Kunzelmann, K. (2005) Cl^- interference with the epithelial Na^+ channel ENaC. *J. Biol. Chem.* **280,** 31587-31594

10. Bae, Y. S., Lee, T. G., Park, J. C., Hur, J. H., Kim, Y., Heo, K., Kwak, J. Y., Suh, P. G., and Ryu, S. H. (2003) Identification of a compound that directly stimulates phospholipase C activity. *Mol. Pharmacol.* **63,** 1043-1050

11. Bannykh, S. I., Bannykh, G. I., Fish, K. N., Moyer, B. D., Riordan, J. R., and Balch, W. E. (2000) Traffic pattern of cystic fibrosis transmembrane regulator through the early exocytic pathway. *Traffic* **1,** 852-870

12. Baukrowitz, T., Schulte, U., Oliver, D., Herlitze, S., Krauter, T., Tucker, S. J., Ruppersberg, J. P., and Fakler, B. (1998) PIP2 and PIP as determinants for ATP inhibition of K_{ATP} channels. *Science* **282,** 1141-1144

13. Bebok, Z., Hicks, J. K., Clancy, J. P., Cobb, B., Sorscher, E. J., Wakefield, J., Zheng, R., Kappes, J. C., and Wu, X. (1999) Lentiviral vectors for stable CFTR cell line development. *Pediatr. Pulmonol. Suppl.* **19,** 218 (Abstr. 191)

14. Bebok, Z., Tousson, A., Schwiebert, L. M., and Venglarik, C. J. (2001) Improved oxygenation promotes CFTR maturation and trafficking in MDCK monolayers. *Am. J. Physiol. Cell Physiol.* **280,** C135-C145

15. Becchetti, A., Malik, B., Yue, G., Duchatelle, P., Al Khalili, O., Kleyman, T. R., and Eaton, D. C. (2002) Phosphatase inhibitors increase the open probability of ENaC in A6 cells. *Am. J. Physiol. Renal Physiol.* **283,** F1030-F1045

16. Benharouga, M., Sharma, M., and Lukacs, G. L. (2002) CFTR Folding and Maturation in Cells. *Methods Mol. Med.* **70,** 229-243

17. Benos, D. J., and Stanton, B. A. (1999) Functional domains within the degenerin/epithelial sodium channel (Deg/ENaC) superfamily of ion channels. *J. Physiol. (Lond.)* **520,** 631-644

18. Berdiev, B. K., Shlyonsky, V. G., Karlson, K. H., Stanton, B. A., and Ismailov, I. I. (2000) Gating of amiloride-sensitive Na^+ channels: subunit-subunit interactions and inhibition by the cystic fibrosis transmembrane conductance regulator. *Biophys. J.* **78,** 1881-1894

19. Bhalla, V., Daidie, D., Li, H., Pao, A. C., Lagrange, L. P., Wang, J., Vandewalle, A., Stockand, J. D., Staub, O., and Pearce, D. (2005) SGK1 regulates ubiquitin ligase Nedd4-2 by inducing interaction with 14-3-3. *Mol. Endocrinol.* **19,** 3073-3084

20. Bhalla, V., Soundararajan, R., Pao, A. C., Li, H., and Pearce, D. (2006) Disinhibitory pathways for control of sodium transport: regulation of ENaC by SGK1 and GILZ. *Am. J. Physiol. Renal Physiol.* **291,** F714-F721

21. Bijman, J., Veeze, H., Kansen, M., Tilly, B., Scholte, B., Hoogeveen, A., Halley, D., Sinaasappel, M., and De Jonge, H. (1991) Chloride transport in the cystic fibrosis enterocyte. *Adv. Exp. Med. Biol.* **290,** 287-294

22. Bildl, W., Strassmaier, T., Thurm, H., Andersen, J., Eble, S., Oliver, D., Knipper, M., Mann, M., Schulte, U., Adelman, J. P., and Fakler, B. (2004) Protein kinase CK2 is coassembled with small conductance Ca(2+)-activated K^+ channels and regulates channel gating. *Neuron.* **43,** 847-858

23. Blanquet, P. R. (2000) Casein kinase 2 as a potentially important enzyme in the nervous system. *Prog. Neurobiol.* **60,** 211-246

24. Blazer-Yost, B. L., Esterman, M. A., and Vlahos, C. J. (2003) Insulin-stimulated trafficking of ENaC in renal cells requires PI 3-kinase activity. *Am. J. Physiol. Cell Physiol.* **284,** C1645-C1653

25. Blazer-Yost, B. L., Vahle, J. C., Byars, J. M., and Bacallao, R. L. (2004) Real-time three-dimensional imaging of lipid signal transduction: apical membrane insertion of epithelial Na(+) channels. *Am. J. Physiol. Cell Physiol.* **287,** C1569-C1576

26. Boat, T. F., Welsh, M. J., and Beaudet, A. L. (1989) Cystic fibrosis. In: The metabolic basis of inherited disease, edited by C.R. Scriver, A.L. Beaudet, W.S. Sly, D. Valle, J.B. Stansbury, J.B. Wyngaarden and D.S. Frederickson. *New York: McGraw-Hill* **1,** 2649-2680

27. Bobadilla, J. L., Macek, M., Jr., Fine, J. P., and Farrell, P. M. (2002) Cystic fibrosis: a worldwide analysis of CFTR mutations-correlation with incidence data and application to screening. *Hum. Mutat.* **19,** 575-606

28. Bonny, O., and Hummler, E. (2000) Dysfunction of epithelial sodium transport: from human to mouse. *Kidney Int.* **57,** 1313-1318

29. Bonvalet, J. P. (1998) Regulation of sodium transport by steroid hormones. *Kidney Int.* **53,** S49-S56

30. Boucher, R. C. (1999) Molecular insights into the physiology of the 'thin film' of airway surface liquid. *J. Physiol.* **516,** 631-638

31. Boucher, R. C., Cotton, C. U., Gatzy, J. T., Knowles, M. R., and Yankaskas, J. R. (1988) Evidence for reduced Cl^- and increased Na^+ permeability in cystic fibrosis human primary cell cultures. *J. Physiol. (Lond.)* **405,** 77-103

32. Boucher, R. C., Stutts, M. J., Knowles, M. R., Cantley, L., and Gatzy, J. T. (1986) Na^+ transport in cystic fibrosis respiratory epithelia: Abnormal basal rate and response to adenylate cyclase. *J. Clin. Invest.* **78,** 1245-1252

33. Boucherot, A., Schreiber, R., and Kunzelmann, K. (2001) Role of CFTR's PDZ-binding domain, NBF1 and Cl^- conductance in inhibition of epithelial Na^+ channels in *Xenopus* oocytes. *BBA* **1515,** 64-71

34. Briel, M., Greger, R., and Kunzelmann, K. (1998) Cl^- transport by CFTR contributes to the inhibition of epithelial Na^+ channels in *Xenopus* ooyctes coexpressing CFTR and ENaC. *J. Physiol. (Lond.)* **508.3,** 825-836

35. Bruns, J. B., Carattino, M. D., Sheng, S., Maarouf, A. B., Weisz, O. A., Pilewski, J. M., Hughey, R. P., and Kleyman, T. R. (2007) Epithelial Na^+ channels are fully activated by furin- and prostasin-dependent release of an inhibitory peptide from the gamma-subunit. *J. Biol. Chem.* **282,** 6153-6160

36. Cai, Y., Anyatonwu, G., Okuhara, D., Lee, K. B., Yu, Z., Onoe, T., Mei, C. L., Qian, Q., Geng, L., Wiztgall, R., Ehrlich, B. E., and Somlo, S. (2004) Calcium-dependence of polycystin-2 channel activity is modulated by phosphorylation at Ser 812. *J. Biol. Chem.* **279,** 19987-19995

37. Canessa, C. M., Horisberger, J. D., and Rossier, B. C. (1993) Epithelial sodium channel related to proteins involved in neurodegeneration. *Nature* **361,** 467-470

38. Canessa, C. M., Schild, L., Buell, G., Thorens, B., Gautschl, I., Horisberger, J. D., and Rossier, B. C. (1994) Amiloride-sensitive epithelial Na^+ channel is made of three homologous subunits. *Nature* **367,** 463-467

39. Cantley, L. C. (2002) The phosphoinositide 3-kinase pathway. *Science* **296,** 1655-1657

40. Carattino, M. D., Edinger, R. S., Grieser, H. J., Wise, R., Neumann, D., Schlattner, U., Johnson, J. P., Kleyman, T. R., and Hallows, K. R. (2005) Epithelial sodium channel inhibition by AMP-activated protein kinase in oocytes and polarized renal epithelial cells. *J. Biol. Chem.* **280,** 17608-17616

41. Carattino, M. D., Sheng, S., Bruns, J. B., Pilewski, J. M., Hughey, R. P., and Kleyman, T. R. (2006) The epithelial Na^+ channel is inhibited by a peptide derived from proteolytic processing of its alpha subunit. *J. Biol. Chem.* **281,** 18901-18907

42. Chabot, H., Vives, M. F., Dagenais, A., Grygorczyk, C., Berthiaume, Y., and Grygorczyk, R. (1999) Downregulation of epithelial sodium channel (ENaC) by CFTR co-expressed in *Xenopus* oocytes is independent of Cl^- conductance. *J. Membr. Biol.* **169,** 175-188

43. Chalfant, M. L., Denton, J. S., Langloh, A. L., Karlson, K. H., Loffing, J., Benos, D. J., and Stanton, B. A. (1999) The NH(2) Terminus of the Epithelial Sodium Channel Contains an Endocytic Motif. *J. Biol. Chem.* **274,** 32889-32896

44. Chen, T. Y. (1998) Extracellular zinc ion inhibits ClC-0 chloride channels by facilitating slow gating. *J. Gen. Physiol.* **112,** 715-726

45. Cheng, S. H., Gregory, R. J., Marshall, J., Paul, S., Souza, D. W., White, G., O'Riordan, C. R., and Smith, A. E. (1990) Defective intracellular transport and processing of CFTR is the molecular basis of most cystic fibrosis. *Cell* **63,** 827-834

46. Crawford, I., Maloney, P. C., Zeitlin, P. L., Guggino, W. B., Hyde, S. C., Turley, H., Gatter, K. C., Harris, A., and Higgins, C. F. (1991) Immunocytochemical localization of the cystic fibrosis gene product CFTR. *Proc. Natl. Acad. Sci.* **88,** 9262-9266

47. Cuffe, J. E., Bielfeld-Ackermann, A., Thomas, J., Leipziger, J., and Korbmacher, C. (2000) ATP stimulates Cl^- secretion and reduces amiloride-sensitive Na^+ absorption in M1 mouse cortical collecting duct cells. *J. Physiol. (Lond.)* **524 Pt 1,** 77-90

48. Cukras, C. A., Jeliazkova, I., and Nichols, C. G. (2002) Structural and functional determinants of conserved lipid interaction domains of inward rectifying Kir6.2 channels. *J. Gen. Physiol.* **119,** 581-591

49. de Chaffoy de Courcelles DC, Roevens, P., and Van Belle, H. (1985) R 59022, a diacylglycerol kinase inhibitor. Its effect on diacylglycerol and thrombin-induced C kinase activation in the intact platelet. *J. Biol. Chem.* **260,** 15762-15770

50. Debonneville, C., Flores, S. Y., Kamynina, E., Plant, P. J., Tauxe, C., Thomas, M. A., Munster, C., Chraibi, A., Pratt, J. H., Horisberger, J. D., Pearce, D., Loffing, J., and Staub, O. (2001) Phosphorylation of Nedd4-2 by Sgk1 regulates epithelial Na(+) channel cell surface expression. *EMBO J.* **20,** 7052-7059

51. Diakov, A., and Korbmacher, C. (2004) A novel pathway of ENaC activation involves an SGK1 consensus motif in the C-terminus of the channel's alpha-subunit. *J. Biol. Chem.* **279,** 38134-38142

52. Dinudom, A., Fotia, A. B., Lefkowitz, R. J., Young, J. A., Kumar, S., and Cook, D. I. (2004) The kinase Grk2 regulates Nedd4/Nedd4-2-dependent control of epithelial Na^+ channels. *Proc. Natl. Acad. Sci. USA* **101,** 11886-11890

53. Dinudom, A., Komwatana, P., Young, J. A., and Cook, D. I. (1995) Control of the amiloride-sensitive Na^+ current in mouse salivary ducts by intracellular anions is mediated by a G protein. *J. Physiol. (Lond.)* **487,** 549-555

54. Dinudom, A., Young, J. A., and Cook, D. I. (1993) Na^+ and Cl^- conductances are controlled by cytosolic Cl^- concentration in the intralobular duct cells of mouse mandibular glands. *J. Membr. Biol.* **135,** 289-295

55. Dormer, R. L., Derand, R., McNeilly, C. M., Mettey, Y., Bulteau-Pignoux, L., Metaye, T., Vierfond, J. M., Gray, M. A., Galietta, L. J., Morris, M. R., Pereira, M. M., Doull, I. J., Becq, F., and McPherson, M. A. (2001) Correction of delF508-CFTR activity with benzo(c)quinolizinium compounds through facilitation of its processing in cystic fibrosis airway cells. *J. Cell Sci.* **114,** 4073-4081

56. Doucet, L., Mendes, F., Montier, T., Delepine, P., Penque, D., Ferec, C., and Amaral, M. D. (2003) Applicability of different antibodies for the immunohistochemical localization of CFTR in respiratory and intestinal tissues of human and murine origin. *J. Histochem. Cytochem.* **51,** 1191-1199

57. Drain, P., Li, L., and Wang, J. (1998) K_{ATP} channel inhibition by ATP requires distinct functional domains of the cytoplasmic C terminus of the pore-forming subunit. *Proc. Natl. Acad. Sci. USA* **95,** 13953-13958

58. Eaton, D. C., Malik, B., Saxena, N. C., Al-Khalili, O. K., and Yue, G. (2001) Mechanisms of aldosterone's action on epithelial Na^+ transport. *J. Membr. Biol.* **184,** 313-319

59. Ecelbarger, C. A., Kim, G. H., Wade, J. B., and Knepper, M. (2001) Regulation of the abundance of renal sodium transporters and channels by vasopressin. *Exp. Neurol.* **171,** 227-234

60. Engelhardt, J. F., Yankaskas, J. R., Ernst, S. A., Yang, Y., Marino, C. R., Boucher, R. C., Cohn, J. A., and Wilson, J. M. (1992) Submucosal glands are the predominant site of CFTR expression in the human bronchus. *Nature genetics* **2,** 240-248

61. Enkvetchakul, D., Loussouarn, G., Makhina, E., Shyng, S. L., and Nichols, C. G. (2000) The kinetic and physical basis of K(ATP) channel gating: toward an unified molecular understanding. *Biophys. J.* **78,** 2334-2348

62. Fan, Z., and Makielski, J. C. (1999) Phosphoinositides decrease ATP-sensitivity of the cardiac ATP-sensitive K(+) channel. A molecular probe for the mechanism of ATP-sensitive inhibition. *J. Gen. Physiol.* **114,** 251-269

63. Farinha, C., Penque, D., Roxo Rosa, M., Lukacs, G. L., Dormer, R., McPherson, M., Pereira, M., Bot, A. G. M., Jorna, H., Willemsen, R., DeJonge, R., Heda, G. D., Marino, C. R., Fanen, P., Hinzpeter, A., Lipecka, J., Fritsch, J., Gentzsch, M., Jensen, T., Aleksandrov, A., Aleksandrov, L., Riordan, J. R., Mengos, A., Rhim, A. D., Stoykova, L. I., Trindade, A. J., Glick, M. C., Scanlin, T., Ollero, M., Edelman, A., and Amaral, M. D. (2004) Biochemical methods to assess CFTR expression and membrane localization. *J. Cys. Fibros.* **S2,** 73-77

64. Farinha, C. M., Nogueira, P., Mendes, F., Penque, D., and Amaral, M. D. (2002) The human DnaJ homologue (Hdj)-1/heat-shock protein (Hsp) 40 co-chaperone is required for the *in vivo* stabilization of the cystic fibrosis transmembrane conductance regulator by Hsp70. *Biochem. J.* **366,** 797-806

65. Feldman, R. D. (2002) Deactivation of vasodilator responses by GRK2 overexpression: a mechanism or the mechanism for hypertension? *Mol. Pharmacol.* **61,** 707-709

66. Firsov, D., Gautschi, I., Merillat, A. M., Rossier, B. C., and Schild, L. (1998) The heterotetrameric architecture of the epithelial sodium channel (ENaC). *EMBO. J.* **17,** 344-352

67. Firsov, D., Schild, L., Gautschi, I., Merillat, A. M., Schneeberger, E., and Rossier, B. C. (1996) Cell surface expression of the epithelial Na^+ channel and a mutant causing Liddle syndrome: a quantitative approach. *Proc. Natl. Acad. Sci. USA* **93,** 15370-15375

68. Ford, C. P., Stemkowski, P. L., Light, P. E., and Smith, P. A. (2003) Experiments to test the role of phosphatidylinositol 4,5-bisphosphate in neurotransmitter-induced M-channel closure in bullfrog sympathetic neurons. *J. Neurosci.* **23,** 4931-4941

69. Fu, L., and Sztul, E. (2003) Traffic-independent function of the Sar1p/COPII machinery in proteasomal sorting of the cystic fibrosis transmembrane conductance regulator. *J. Cell Biol.* **160,** 157-163

70. Fuller, C. M., and Benos, D. J. (1992) CFTR! *Am. J. Physiol.* **263,** C267-C286

71. Fyfe, G. K., and Canessa, C. M. (1998) Subunit composition determines the single channel kinetics of the epithelial sodium channel. *J. Gen. Physiol.* **112,** 423-432

72. Gabev, E., Kasianowicz, J., Abbott, T., and McLaughlin, S. (1989) Binding of neomycin to phosphatidylinositol 4,5-bisphosphate (PIP2). *Biochim. Biophys. Acta* **979,** 105-112

73. Garty, H., and Benos, D. J. (1988) Characteristics and regulatory mechanisms of the amiloride-blockable Na^+ channel. *Physiol. Rev.* **68,** 309-373

74. Garty, H., and Palmer, L. G. (1997) Epithelial sodium channels: Function, structure and regulation. *Physiol. Rev.* **77,** 359-396

75. Gekle, M., Freudinger, R., Mildenberger, S., and Silbernagl, S. (2001) Aldosterone interaction with epidermal growth factor receptor signaling in MDCK cells. *Am. J. Physiol. Renal Physiol.* **282,** F669-F679

76. Gibson, G. A., Hill, W. G., and Weisz, O. A. (2000) Evidence against the acidification hypothesis in cystic fibrosis. *Am. J. Physiol. Cell Physiol.* **279,** C1088-C1099

77. Grossmann, C., Freudinger, R., Mildenberger, S., Krug, A. W., and Gekle, M. (2004) Evidence for epidermal growth factor receptor as negative-feedback control in aldosterone-induced Na^+ reabsorption. *Am. J. Physiol. Renal Physiol.* **286,** F1226-F1231

78. Grubb, B. R., and Boucher, R. C. (1999) Pathophysiology of gene-targeted mouse models for cystic fibrosis. *Physiol. Rev.* **79,** S193-S214

79. Grubb, B. R., Vick, R. N., and Boucher, R. C. (1994) Hyperabsorption of Na^+ and raised Ca^{2+} mediated Cl^- secretion in nasal epithelia of CF mice. *Am. J. Physiol.* **266,** C1478-C1483

80. Gruenert, D., Willems, M., Cassiman, J. J., and Frizzell, R. A. (2004) Established cell lines used in cystic fibrosis research. *J. Cystic. Fibros.* **3 S2,** 191-196

81. Hamilton, K. L., and Eaton, D. C. (1985) Single-channel recordings from amiloride-sensitive epithelial sodium channel. *Am. J. Physiol.* **249,** C200-C207

82. Hendron, E., and Stockand J.D. (2002) Activation of mitogen-activated protein kinase (mitogen-activated protein kinase/extracellular signal-regulated kinase) cascade by aldosterone. *Mol. Biol. Cell* **13,** 3042-3054

83. Hilgemann, D. W., Feng, S., and Nasuhoglu, C. (2001) The complex and intriguing lives of PIP2 with ion channels and transporters. *Sci. STKE.* **111,** RE19

84. Hill, W. G., An, B., and Johnson, J. P. (2002) Endogenously expressed epithelial sodium channel is present in lipid rafts in A6 cells. *J. Biol. Chem.* **277,** 33541-33544

85. Himmel, B., and Nagel, G. (2004) Protein kinase-independent activation of CFTR by phosphatidylinositol phosphates. *EMBO Rep.* **5,** 85-90

86. Hopf, A., Schreiber, R., Greger, R., and Kunzelmann, K. (1999) CFTR inhibits the activity of epithelial Na^+ channels carrying Liddle's syndrome mutations. *J. Biol. Chem.* **274,** 13894-13899

87. Howard, M., Jiang, X., Stolz, D. B., Hill, W. G., Johnson, J. A., Watkins, S. C., Frizzell, R. A., Bruton, C. M., Robbins, P. D., and Weisz, O. A. (2000) Forskolin-induced apical membrane insertion of virally expressed, epitope-tagged CFTR in polarized MDCK cells. *Am. J. Physiol. Cell Physiol.* **279,** C375-C382

88. Hu, J., Bae, Y. K., Knobel, K. M., and Barr, M. M. (2006) Casein kinase II and calcineurin modulate TRPP function and ciliary localization. *Mol. Biol. Cell* **17,** 2200-2211

89. Huang, C. L., Feng, S., and Hilgemann, D. W. (1998) Direct activation of inward rectifier potassium channels by PIP2 and its stabilization by Gbetagamma. *Nature* **391,** 803-806

90. Huang, P., Lazarowski, E. R., Tarran, R., Milgram, S. L., Boucher, R. C., and Stutts, M. J. (2001) From the Cover: Compartmentalized autocrine signaling to cystic fibrosis transmembrane conductance regulator at the apical membrane of airway epithelial cells. *Proc. Natl. Acad. Sci. USA* **98,** 14120-14125

91. Hübner, M., Schreiber, R., Boucherot, A., Sanchez-Perez, A., Poronnik, P., Cook, D. I., and Kunzelmann, K. (1999) Feedback inhibition of epithelial Na^+ channels in *Xenopus* oocytes does not require G_0- or G_{i2}-proteins. *FEBS Lett.* **459,** 443-447

92. Hughey, R. P., Bruns, J. B., Kinlough, C. L., Harkleroad, K. L., Tong, Q., Carattino, M. D., Johnson, J. P., Stockand, J. D., and Kleyman, T. R. (2004) Epithelial sodium channels are activated by furin-dependent proteolysis. *J. Biol. Chem.* **279,** 18111-18114

93. Ichimura, T., Yamamura, H., Sasamoto, K., Tominaga, Y., Taoka, M., Kakiuchi, K., Shinkawa, T., Takahashi, N., Shimada, S., and Isobe, T. (2005) 14-3-3 proteins modulate the expression of epithelial Na^+ channels by phosphorylation-dependent interaction with Nedd4-2 ubiquitin ligase. *J. Biol. Chem.* **280,** 13187-13194

94. Ishikawa, T., Jiang, C., Stutts, M. J., Marunaka, Y., and Rotin, D. (2003) Regulation of the epithelial Na^+ channel (ENaC) by cytosolic ATP. *J. Biol. Chem.* **278,** 38276-38286

95. Ismailov, I. I., Awayda, M. S., Jovov, B., Berdiev, B. K., Fuller, C. M., Dedman, J. R., Kaetzel, M. A., and Benos, D. J. (1996) Regulation of epithelial sodium channels by the cystic fibrosis transmembrane conductance regulator. *J. Biol. Chem.* **271,** 4725-4732

96. Jensen, T. J., Loo, M. A., Pind, S., Williams, D. B., Goldberg, A. L., and Riordan, J. R. (1995) Multiple proteolytic systems, including the proteasome, contribute to CFTR processing. *Cell* **83,** 13-20

97. Ji, H. L., Chalfant, M. L., Jovov, B., Lockhart, J. P., Parker, S. B., Fuller, C. M., Stanton, B. A., and Benos, D. J. (2000) The cytosolic termini of the beta- and gamma ENaC subunits are involved in the functional interactions between CFTR and ENaC. *J. Biol. Chem.* **275,** 27947-27951

98. Jiang, Q., Li, J., Dubroff, R., Ahn, Y. J., Foskett, J. K., Engelhardt, J., and Kleyman, T. R. (2000) Epithelial Sodium Channels Regulate Cystic Fibrosis Transmembrane Conductance Regulator Chloride Channels in *Xenopus* Oocytes. *J. Biol. Chem.* **275,** 13266-13274

99. Kalin, N., Claass, A., Sommer, M., Puchelle, E., and Tummler, B. (1999) DeltaF508 CFTR protein expression in tissues from patients with cystic fibrosis. *J. Clin. Invest.* **103,** 1379-1389

100. Kanzaki, M., Furukawa, M., Raab, W., and Pessin, J. E. (2004) Phosphatidylinositol 4,5-bisphosphate regulates adipocyte actin dynamics and GLUT4 vesicle recycling. *J. Biol. Chem.* **279,** 30622-30633

101. Kappes, J. C., Wu, X., and Wakefield, J. (2002) Production of trans-lentiviral vector with predictable safety. *Methods Mol. Med.* **76,** 449-465

102. Kartner, N., Augustinas, T., Jensen, T. J., Naismith, A. L., and Riordan, J. R. (1992) Mislocalization of deltaF508-CFTR in cystic fibrosis sweat gland. *Nature genetics* **1,** 321-327

103. Kellenberger, S., and Schild, L. (2002) Epithelial sodium channel/degenerin family of ion channels: a variety of functions for a shared structure. *Physiol. Rev.* **82,** 735-767

104. Khan, T. Z., Wagener, J. S., Bost, T., Martinez, J., Accurso, F. J., and Riches, D. W. (1995) Early pulmonary inflammation in infants with cystic fibrosis. *Am. J. Respir. Crit. Care Med.* **151,** 1075-1082

105. Kieferle, S., Fong, P., Bens, M., Vandewalle, A., and Jentsch, T. J. (1994) Two highly homologous members of the ClC chloride channel family in both rat and human kidney. *Proc. Natl. Acad. Sci. USA* **91,** 6943-6947

106. Kimura, T., Kubo, T. (2003) Cloning and functional characterization of squid voltage-dependent Ca^{2+} channel beta subunits: involvement of N-terminal sequences in differential modulation of the current. *Neurosci. Res.* **46,** 105-117

107. Komwatana, P., Dinudom, A., Young, J. A., and Cook, D. I. (1998) Activators of epithelial Na^+ channels inhibit cytosolic feedback control. Evidence for the existence of a G protein-coupled receptor for cytosolic Na^+. *J. Membr. Biol.* **162,** 225-232

108. König, J., Schreiber, R., Mall, M., and Kunzelmann, K. (2002) No evidence for inhibition of ENaC through CFTR mediated release of ATP. *Biochim. Biophys. Acta* **1565,** 17-28

109. König, J., Schreiber, R., Voelcker, T., Mall, M., and Kunzelmann, K. (2001) CFTR inhibits ENaC through an increase in the intracellular Cl^- concentration. *EMBO Rep.* **2,** 1-5

110. Konstas, A. A., Koch, J. P., and Korbmacher, C. (2003) cAMP-dependent activation of CFTR inhibits the epithelial sodium channel (ENaC) without affecting its surface expression. *Pflugers Arch.* **445,** 513-521

111. Konstas, A. A., Koch, J. P., Tucker, S. J., and Korbmacher, C. (2002) Cystic fibrosis transmembrane conductance regulator-dependent up-regulation of Kir1.1 (ROMK) renal K^+ channels by the epithelial sodium channel. *J. Biol. Chem.* **277,** 25377-25384

112. Kowalski, M. P., and Pier, G. B. (2004) Localization of cystic fibrosis transmembrane conductance regulator to lipid rafts of epithelial cells is required for *Pseudomonas aeruginosa*-induced cellular activation. *J. Immunol.* **172,** 418-425

113. Kreda, S. M., Mall, M., Mengos, A., Rochelle, L. G., Yankaskas, J., Riordan, J. R., and Boucher, R. C. (2005) CFTR in human airways. *Mol. Biol. Cell* **16,** 2154-2167

114. Krug, A. W., Grossmann, C., Schuster, C., Freudinger, R., Mildenberger, S., Govindan, M. V., and Gekle, M. (2003) Aldosterone stimulates epidermal growth factor receptor (EGFR) expression. *J. Biol. Chem.* **278,** 43060-43066

115. Krug, A. W., Schuster, C., Gassner, B., Freudinger, R., Mildenberger, S., Troppmair, J., and Gekle, M. (2002) Human EGF receptor 1 (HER1) expression renders CHO cells sensitive to alternative aldosterone signaling. *J. Biol. Chem.* **277,** 45892-45897

116. Kunzelmann, K. (1997) Regulation and amiloride binding site of epithelial Na^+ channels. *Kidney and Blood Press. Res.* **20,** 151-153

117. Kunzelmann, K. (1999) The Cystic Fibrosis Transmembrane Conductance Regulator and its function in epithelial transport. *Rev. Physiol. Biochem. Pharmacol.* **137,** 1-70

118. Kunzelmann, K. (2003) ENaC is inhibited by an increase in the intracellular Cl^- concentration mediated through activation of Cl^- channels. *Pflugers Arch.* **445,** 505-512

119. Kunzelmann, K., Bachhuber, T., Regeer, R., Markovich, D., Sun, J., and Schreiber, R. (2004) Purinergic inhibition of the epithelial Na^+ transport via hydrolysis of PIP_2. *FASEB J.* **18,** 142-163

120. Kunzelmann, K., Kathöfer, S., and Greger, R. (1995) Na^+ and Cl^- conductances in airway epithelial cells: Increased Na^+ conductance in cystic fibrosis. *Pflugers Arch.* **431,** 1-9

121. Kunzelmann, K., Kiser, G., Schreiber, R., and Riordan, J. R. (1997) Inhibition of epithelial sodium currents by intracellular domains of the cystic fibrosis transmembrane conductance regulator. *FEBS Lett.* **400,** 341-344

122. Kunzelmann, K., and Mall, M. (2001) Pharmacotherapy of the ion transport defect in cystic fibrosis. *Clin. Exp. Pharmacol. Physiol.* **28,** 857-867

123. Kunzelmann, K., Schreiber, R., and Boucherot, A. (2001) Mechanism of the inhibition of epithelial Na^+ channels by CFTR and purinergic stimulation. *Kidney Int.* **60,** 455-461

124. Kunzelmann, K., Schreiber, R., and Cook, D. I. (2002) Mechanisms for inhibition of amiloride-sensitive Na^+ absorption by extracellular nucleotides in mouse trachea. *Pflugers Arch.* **444,** 220-226

125. Kunzelmann, K., Schreiber, R., Nitschke, R., and Mall, M. (2000) Control of epithelial Na^+ conductance by the Cystic Fibrosis Transmembrane Conductance Regulator. *Pflugers Arch.* **440,** 193-201

126. Lam, K., Carpenter, C. L., Ruderman, N. B., Friel, J. C., and Kelly, K. L. (1994) The phosphatidylinositol 3-kinase serine kinase phosphorylates IRS-1. Stimulation by insulin and inhibition by Wortmannin. *J. Biol. Chem.* **269,** 20648-20652

127. Leipziger, J. (2003) Control of epithelial transport via luminal P2 receptors. *Am. J. Physiol. Renal Physiol.* **284,** F419-F432

128. Lemmon, M. A., Ferguson, K. M., O'Brien, R., Sigler, P. B., and Schlessinger, J. (1995) Specific and high-affinity binding of inositol phosphates to an isolated pleckstrin homology domain. *Proc. Natl. Acad. Sci. USA* **92,** 10472-10476

129. Letz, B., and Korbmacher, C. (1997) cAMP stimulates CFTR-like Cl^- channels and inhibits amiloride-sensitive Na^+ channels in mouse CCD cells. *Am. J. Physiol.* **272,** C657-C666

130. Lingueglia, E., Voilley, N., Waldmann, R., Lazdunski, M., and Barbry, P. (1993) Expression cloning of an epithelial amiloride-sensitive Na^+ channel. *FEBS Lett.* **318,** 95-99

131. Litchfield, D. W. (2003) Protein kinase CK2: structure, regulation and role in cellular decisions of life and death. *Biochem. J.* **369,** 1-15

132. Liu, D., and Liman, E. R. (2003) Intracellular Ca^{2+} and the phospholipid PIP2 regulate the taste transduction ion channel TRPM5. *Proc. Natl. Acad. Sci. USA* **100,** 15160-15165

133. Loffing-Cueni, D., Loffing, J., Shaw, C., Taplin, A. M., Govindan, M., Stanton, C. R., and Stanton, B. A. (2001) Trafficking of GFP-tagged DeltaF508-CFTR to the plasma

membrane in a polarized epithelial cell line. *Am. J. Physiol. Cell Physiol.* **281,** C1889-C1897

134. Loussouarn, G., Park, K. H., Bellocq, C., Baro, I., Charpentier, F., and Escande, D. (2003) Phosphatidylinositol 4,5-bisphosphate, PIP2, controls KCNQ1/KCNE1 voltage-gated potassium channels: a functional homology between voltage-gated and inward rectifier K^+ channels. *EMBO J.* **22,** 5412-5421

135. Lukacs, G. L., Abdalla, M., Kartner, N., Riordan, J. R., and Grinstein, S. (1994) Conformational maturation of CFTR but not its mutant counterpart (deltaF508) occurs in the endoplasmic reticulum and requires ATP. *EMBO J.* **13,** 6076-6086

136. Ma, H. P., Li, L., Zhou, Z. H., Eaton, D. C., and Warnock, D. G. (2002) ATP masks stretch activation of epithelial sodium channels in A6 distal nephron cells. *Am. J. Physiol.* **282,** F501-F505

137. Ma, H. P., Saxena, S., and Warnock, D. G. (2002) Anionic phospholipids regulate native and expressed ENaC. *J. Biol. Chem.* **277,** 7641-7644

138. Mall, M., Bleich, M., Greger, R., Schreiber, R., and Kunzelmann, K. (1998) The amiloride inhibitable Na^+ conductance is reduced by CFTR in normal but not in CF airways. *J. Clin. Invest.* **102,** 15-21

139. Mall, M., Bleich, M., Kühr, J., Brandis, M., Greger, R., and Kunzelmann, K. (1999) CFTR-mediated inhibition of amiloride-sensitive sodium conductance by CFTR in human colon is defective in cystic fibrosis. *Am. J. Physiol.* **277,** G709-G716

140. Mall, M., Grubb, B. R., Harkema, J. R., O'Neal, W. K., and Boucher, R. C. (2004) Increased airway epithelial Na(+) absorption produces cystic fibrosis-like lung disease in mice. *Nat. Med.* **10,** 452-454

141. Mall, M., Hipper, A., Greger, R., and Kunzelmann, K. (1996) Wild-type but not deltaF508 CFTR inhibits Na^+ conductance when coexpressed in *Xenopus* oocytes. *Pflugers Arch.* **431S,** O-57

142. Mall, M., Hipper, A., Greger, R., and Kunzelmann, K. (1996) Wild-type but not deltaF508 CFTR inhibits Na^+ conductance when coexpressed in *Xenopus* oocytes. *FEBS Lett.* **381,** 47-52

143. Mall, M., Wissner, A., Kühr, J., Gonska, T., Brandis, M., and Kunzelmann, K. (2000) Inhibition of amiloride-sensitive epithelial Na^+ absorption by extracellular nucleotides in human normal and CF airways. *Am. J. Respir. Cell Mol. Biol.* **23,** 755-761

144. Mall, M., Wissner, A., Seydewitz, H. H., Kühr, J., Brandis, M., Greger, R., and Kunzelmann, K. (2000) Defective cholinergic Cl^- secretion and detection of K^+ secretion in rectal biopsies from cystic fibrosis patients. *Am. J. Physiol.* **278,** G617-G624

145. Markadieu, N., Blero, D., Boom, A., Erneux, C., and Beauwens, R. (2004) Phosphatidylinositol 3,4,5-trisphosphate: an early mediator of the insulin-stimulated sodium transport in A6 cells. *Am. J. Physiol. Renal Physiol.* **287,** F319-F328

146. Mastroberardino, L., Spindler, B., Forster, I., Loffing, J., Assandri, R., May, A., and Verrey, F. (1998) Ras pathway activates epithelial Na^+ channel and decreases its surface expression in *Xenopus* oocytes. *Mol. Biol. Cell* **9,** 3417-3427

147. Matsui, H., Davis, C. W., Tarran, R., and Boucher, R. C. (2000) Osmotic water permeabilities of cultured, well-differentiated normal and cystic fibrosis airway epithelia. *J. Clin. Invest.* **105,** 1419-1427

148. McNicholas, C. M., and Canessa, C. M. (1997) Diversity of channels generated by different combinations of epithelial sodium channel subunits. *J. Gen. Physiol.* **109,** 681-692

149. Meggio, F., Boldyreff, B., Issinger, O. G., and Pinna, L. A. (1994) Casein kinase 2 down-regulation and activation by polybasic peptides are mediated by acidic residues in the 55-64 region of the beta-subunit. A study with calmodulin as phosphorylatable substrate. *Biochem. J.* **33,** 4336-4342

150. Meggio, F., Marin, O., and Pinna, L. A. (1994) Substrate specificity of protein kinase CK2. *Cell. Mol. Biol. Res.* **40,** 401-409

151. Meggio, F., and Pinna, L. A. (2003) One-thousand-and-one substrates of protein kinase CK2? *FASEB J.* **17,** 349-368

152. Mehta, A. (2005) CFTR: More than just a chloride channel. *Pediatr. Pulmonol.* **39,** 292-298

153. Mellman, I., Yamamoto, E., Whitney, J. A., Kim, M., Hunziker, W., and Matter, K. (1993) Molecular sorting in polarized and non-polarized cells: common problems, common solutions. *J. Cell Sci. Suppl.* **17,** 1-7

154. Mendes, F., Farinha, C., Roxo Rosa, M., Fanen, P., Edelman, A., Dormer, R., McPherson, M., Davidson, H., Puchelle, E., De Jonge, H. R., Heda, G. D., Gentzsch, M., Lukacs, G. L., Penque, D., and Amaral, M. D. (2004) Antibodies for CFTR Studies. *J. Cys. Fibros.* **3 S2,** 69-72

155. Mendes, F., Wakefield, J., Bachhuber, T., Barroso, M., Bebok, Z., Penque, D., Kunzelmann, K., and Amaral, M. (2005) Establishment and characterization of a novel polarized MDCK epithelial cellular model for CFTR studies. *Cell. Physiol. Biochem.* **16,** 281-290

156. Michlig, S., Harris, M., Loffing, J., Rossier, B. C., and Firsov, D. (2005) Progesterone down-regulates the open probability of the amiloride-sensitive epithelial sodium channel via a Nedd4-2-dependent mechanism. *J. Biol. Chem.* **280,** 38264-38270

157. Mickle, J. E., Macek, M., Jr., Fulmer-Smentek, S. B., Egan, M. M., Schwiebert, E., Guggino, W., Moss, R., and Cutting, G. R. (1998) A mutation in the cystic fibrosis transmembrane conductance regulator gene associated with elevated sweat chloride concentrations in the absence of cystic fibrosis*. Hum. Mol. Genet.* **7,** 729-735

158. Misfeldt, D. S., Hamamoto, S. T., and Pitelka, D. R. (1976) Transepithelial transport in cell culture. *Proc. Natl. Acad. Sci. USA* **73,** 1212-1216

159. Mohamed, A., Ferguson, D., Seibert, F. S., Cai, H. M., Kartner, N., Grinstein, S., Riordan, J. R., and Lukacs, G. L. (1997) Functional expression and apical localization of the cystic fibrosis transmembrane conductance regulator in MDCK I cells*. Biochem. J.* **322,** 259-265

160. Monneret, C. (2005) Histone deacetylase inhibitors. *Eur. J. Med. Chem.* **40,** 1-13

161. Mostov, K. E., Verges, M., and Altschuler, Y. (2000) Membrane traffic in polarized epithelial cells*. Curr. Opin. Cell Biol.* **12,** 483-490

162. Moyer, B. D., Denton, J., Karlson, K. H., Reynolds, D., Wang, S., Mickle, J. E., Milewski, M., Cutting, G. R., Guggino, W. B., Li, M., and Stanton, B. A. (1999) A PDZ-interacting domain in CFTR is an apical membrane polarization signal. *J Clin. Invest.* **104,** 1353-1361

163. Moyer, B. D., Duhaime, M., Shaw, C., Denton, J., Reynolds, D., Karlson, K. H., Pfeiffer, J., Wang, S., Mickle, J. E., Milewski, M., Cutting, G. R., Guggino, W. B., Li, M., and Stanton, B. A. (2000) The PDZ-interacting domain of CFTR is required for functional expression in the apical plasma membrane. *J. Biol. Chem.* **275,** 27069-27074

164. Moyer, B. D., Loffing-Cueni, D., Loffing, J., Reynolds, D., and Stanton, B. A. (1999) Butyrate increases apical membrane CFTR but reduces chloride secretion in MDCK cells. *Am. J. Physiol.* **277,** F271-F276

165. Nagel, G., Barbry, P., Chabot, H., Brochiero, E., Hartung, K., and Grygorczyk, R. (2005) CFTR fails to inhibit the epithelial sodium channel ENaC, when expressed in *Xenopus laevis* oocytes. *J. Physiol.* **564,** 671-682

166. Nagel, G., Szellas, T., Riordan, J. R., Frierich, T., and Hartung, K. (2001) Non-specific activation of the epithelial sodium channel by the CFTR chloride channel. *EMBO Rep.* **2,** 249-254

167. Nakanishi, S., Catt, K. J., and Balla, T. (1995) A wortmannin-sensitive phosphatidylinositol 4-kinase that regulates hormone-sensitive pools of inositolphospholipids. *Proc. Natl. Acad. Sci. USA* **92,** 5317-5321

168. Nichols, G. E., Lovejoy, J. C., Borgman, C. A., Sanders, J. M., and Young, W. W., Jr. (1986) Isolation and characterization of two types of MDCK epithelial cell clones based on glycosphingolipid pattern. *Biochim. Biophys. Acta* **887,** 1-12

169. Niisato, N., Eaton, D. C., and Marunaka, Y. (2004) Involvement of cytosolic Cl^- in osmoregulation of {alpha}ENaC gene expression. *Am. J. Physiol. Renal Physiol.* **287,** F932-F939

170. Oceandy, D., McMorran, B. J., Smith, S. N., Schreiber, R., Kunzelmann, K., Alten, E. W. F., Hume, D. A., and Wainwright, B. J. (2002) Gene complementation of airway epithelium in the cystic fibrosis mouse is necessary and sufficient to correct the pathogen clearance and inflammatory abnormalities. *Hum. Mol. Genet.* **11,** 1059-1067

171. Oude Weernink, P. A., Schulte, P., Guo, Y., Wetzel, J., Amano, M., Kaibuchi, K., Haverland, S., Voss, M., Schmidt, M., Mayr, G. W., and Jakobs, K. H. (2000) Stimulation of phosphatidylinositol 4-phosphate 5-kinase by Rho-kinase. *J. Biol. Chem.* **275,** 10168-10174

172. Palmer, L. G. (1992) Epithelial Na^+ channels: function and diversity. *Annu. Rev. Physiol.* **54,** 51-66

173. Park, J., Leong, M. L., Buse, P., Maiyar, A. C., Firestone, G. L., and Hemmings B.A. (1999) Serum and glucocorticoid-inducible kinase (SGK) is a target of the PI 3-kinase-stimulated signaling pathway. *EMBO J.* **18,** 3024-3033

174. Penque, D., Mendes, F., Beck, S., Farinha, C., Pacheco, P., Nogueira, P., Lavinha, J., Malhó, R., and Amaral, M. D. (2000) Cystic Fibrosis F508del Patients Have Apically Localized CFTR in a Reduced Number of Airway Cells. *Lab. Invest.* **80,** 857-868

175. Pochynyuk, O., Medina, J., Gamper, N., Genth, H., Stockand, J. D., and Staruschenko A. (2006) Rapid translocation and insertion of the epithelial Na^+ channel in response to RhoA signaling. *J. Biol. Chem.* **281,** 26520-26527

176. Pochynyuk, O., Staruschenko, A., Bugaj, V., LaGrange, L., and Stockand, J. D. (2007) Quantifying RhoA facilitated trafficking of the epithelial Na^+ channel toward the plasma membrane with total internal reflection fluorescence - fluorescence recovery after photobleaching. *J. Biol. Chem.* **282,** 14576-14585

177. Pochynyuk, O., Staruschenko, A., Tong, Q., Medina, J., and Stockand, J. D. (2005) Identification of a functional phosphatidylinositol 3,4,5-trisphosphate binding site in the epithelial Na^+ channel. *J. Biol. Chem.* **280,** 37565-37571

178. Powis, G., Seewald, M. J., Gratas, C., Melder, D., Riebow, J., and Modest, E. J. (1992) Selective inhibition of phosphatidylinositol phospholipase C by cytotoxic ether lipid analogues. *Cancer Res.* **52,** 2835-2840

179. Qu, B. H., and Thomas, P. J. (1996) Alteration of the cystic fibrosis transmembrane conductance regulator folding pathway. *J. Biol. Chem.* **271,** 7261-7264

180. Ramalho, A. S., Beck, S., Meyer, M., Penque, D., Cutting, G., and Amaral, M. D. (2002) 5% of normal CFTR mRNA ameliorates the severity of pulmonary disease in Cystic Fibrosis. *Am. J. Respir. Cell Mol. Biol.* **27,** 619-627

181. Ratjen, F., and Doring, G. (2003) Cystic fibrosis. *Lancet* **361,** 681-689

182. Record, R. D., Froelich, L. L., Vlahos, C. J., and Blazer-Yost, B. L. (1998) Phosphatidylinositol 3-kinase activation is required for insulin-stimulated sodium transport in A6 cells. *Am. J. Physiol.* **274,** E611-E617

183. Reddy, M. M., and Quinton, P. M. (1999) Activation of the epithelial Na^+ channel (ENaC) requires CFTR Cl^- channel function. *Nature* **402,** 301-304

184. Richardson, J. C., Scalera, V., and Simmons, N. L. (1981) Identification of two strains of MDCK cells which resemble separate nephron tubule segments. *Biochim. Biophys. Acta* **673,** 26-36

185. Ridley, A. J. (2001) Rho proteins: linking signaling with membrane trafficking. *Traffic* **2,** 303-310

186. Rochelle, L. G., Li, D. C., Ye, H., Lee, E., Talbot, C. R., and Boucher, R. C. (2000) Distribution of ion transport mRNAs throughout murine nose and lung. *Am. J. Physiol.* **279,** L14-L24

187. Rossier, B. C., Pradervand, S., Schild, L., and Hummler, E. (2002) Epithelial Na^+ channels and the control of sodium balance: Interaction between genetic and environmental factors. *Annu. Rev. Physiol.* **64,** 877-897

188. Sarkadi, B., Bauzon, D., Huckle, W. R., Earp, H. S., Berry, A., Suchindran, H., Price, E. M., Olson, J. C., Boucher, R. C., and Scarborough, G. A. (1992) Biochemical characterization of the cystic fibrosis transmembrane conductance regulator in normal and cystic fibrosis epithelial cells. *J. Biol. Chem.* **267,** 2087-2095

189. Schermer, B., Hopker, K., Omran, H., Ghenoiu, C., Fliegauf, M., Fekete, A., Horvath, J., Kottgen, M., Hackl, M., Zschiedrich, S., Huber, T. B., Kramer-Zucker, A., Zentgraf, H., Blaukat, A., Walz, G., and Benzing, T. (2005) Phosphorylation by casein kinase 2 induces PACS-1 binding of nephrocystin and targeting to cilia. *EMBO J.* **24,** 4415-4424

190. Schreiber, R., Boucherot, A., Mürle, B., Sun, J., and Kunzelmann, K. (2004) Control of epithelial ion transport by Cl^- and PDZ proteins. *J. Membr. Biol.* **199,** 89-98

191. Schreiber, R., Hopf, A., Mall, M., Greger, R., and Kunzelmann, K. (1999) The first nucleotide binding fold of the cystic fibrosis transmembrane conductance regulator is important for inhibition of the epithelial Na^+ channel. *Proc. Natl. Acad. Sci. USA* **96,** 5310-5315

192. Schreiber, R., König, J., Sun, J., Markovich, D., and Kunzelmann, K. (2003) Impact of Cl^- but not osmotic swelling on inhibition of Na^+ absorption by purinergic stimulation and activation of CFTR. *J. Membr. Biol.* **192,** 101-110

193. Schwiebert, E. M., Benos, D. J., Egan, M. E., Stutts, M. J., and Guggino, W. B. (1999) CFTR is a conductance regulator as well as a chloride channel. *Physiol. Rev.* **79,** S145-S166

194. Schwiebert, E. M., and Zsembery, A. (2003) Extracellular ATP as a signaling molecule for epithelial cells. *Biochim. Biophys. Acta* **1615,** 7-32

195. Sharma, M., Pampinella, F., Nemes, C., Benharouga, M., So, J., Du, K., Bache, K. G., Papsin, B., Zerangue, N., Stenmark, H., and Lukacs, G. L. (2004) Misfolding diverts CFTR from recycling to degradation: quality control at early endosomes. *J. Cell Biol.* **164,** 923-933

196. Shen, J. P., and Cotton, C. U. (2003) Epidermal growth factor inhibits amiloride-sensitive sodium absorption in renal collecting duct cells. *Am. J. Physiol. Renal Physiol.* **284,** F57-F64

197. Shi, H., Asher, C., Chigaev, A., Yung, Y., Reuveny, E., Seger, R., and Garty, H. (2002) Interactions of beta and gamma ENaC with Nedd4 can be facilitated by an ERK-mediated phosphorylation. *J. Biol. Chem.* **277,** 13539-13547

198. Shi, H., Asher, C., Yung, Y., Kligman, L., Reuveny, E., Seger, R., and Garty, H. (2002) Casein kinase 2 specifically binds to and phosphorylates the carboxy termini of ENaC subunits. *Eur. J. Biochem.* **269,** 4551-4558

199. Shyng, S. L., and Nichols, C. G. (1998) Membrane phospholipid control of nucleotide sensitivity of K_{ATP} channels. *Science* **282,** 1138-1141

200. Simmons, N. L. (1982) Cultured monolayers of MDCK cells: a novel model system for the study of epithelial development and function. *Gen. Pharmacol.* **13,** 287-291

201. Simonsen, A., Wurmser, A. E., Emr, S. D., and Stenmark, H. (2001) The role of phosphoinositides in membrane transport. *Curr. Opin. Cell Biol.* **13,** 485-492

202. Snyder, P. M., Cheng, C., Prince, L. S., Rogers, J. C., and Welsh, M. J. (1998) Electrophysiological and biochemical evidence that DEG/ENaC cation channels are composed of nine subunits. *J. Biol. Chem.* **273,** 681-684

203. Snyder, P. M., Olson, D. R., Kabra, R., Zhou, R., and Steines, J. C. (2004) cAMP and serum and glucocorticoid-inducible kinase (SGK) regulate the epithelial Na(+) channel through convergent phosphorylation of Nedd4-2. *J. Biol. Chem.* **279,** 45753-45758

204. Snyder, P. M., Olson, D. R., and Thomas, B. C. (2002) Serum and Glucocorticoid-regulated Kinase Modulates Nedd4-2-mediated Inhibition of the Epithelial Na^+ Channel. *J. Biol. Chem.* **277,** 5-8

205. Staruschenko, A., Nichols, A., Medina, J. L., Camacho, P., Zheleznova, N. N., and Stockand, J. D. (2004) Rho small GTPases activate the epithelial Na(+) channel. *J. Biol. Chem.* **279,** 49989-49994

206. Staruschenko, A., Patel, P., Tong, Q., Medina, J. L., and Stockand, J. D. (2004) Ras activates the epithelial Na(+) channel through phosphoinositide 3-OH kinase signaling. *J. Biol. Chem.* **279,** 37771-37778

207. Stockand J.D., Spier, B. J., Worrell R.T., Yue, G., Al-Baldawi, N., and Eaton, D. C. (1999) Regulation of Na^+ reabsorption by the aldosterone-induced, small G protein K-Ras2A. *J. Biol. Chem.* **274,** 35449-35454

208. Stockand, J. D. (2002) New ideas about aldosterone signaling in epithelia. *Am. J. Physiol. Renal Physiol.* **282,** F559-F576

209. Strayer, D. S. (2000) SV40-based gene therapy vectors: turning an adversary into a friend. *Curr. Opin. Mol. Ther.* **2,** 570-578

210. Stutts, M. J., Canessa, C. M., Olsen, J. C., Hamrick, M., Cohn, J. A., Rossier, B. C., and Boucher, R. C. (1995) CFTR as a cAMP-dependent regulator of sodium channels. *Science* **269,** 847-850

211. Suaud, L., Carattino, M., Kleyman, T. R., and Rubenstein, R. C. (2002) Genistein improves regulatory interactions between G551D-cystic fibrosis transmembrane conductance regulator and the epithelial sodium channel in *Xenopus* oocytes. *J. Biol. Chem.* **277,** 50341-50347

212. Suaud, L., Li, J., Jiang, Q., Rubenstein, R. C., and Kleyman, T. R. (2001) Genistein restores functional interactions between {delta}F508-CFTR and ENaC in *Xenopus* oocytes. *J. Biol. Chem.* **277,** 8928-8933

213. Swiatecka-Urban, A., Duhaime, M., Coutermarsh, B., Karlson, K. H., Collawn, J., Milewski, M., Cutting, G. R., Guggino, W. B., Langford, G., and Stanton, B. A. (2002) PDZ domain interaction controls the endocytic recycling of the cystic fibrosis transmembrane conductance regulator. *J. Biol. Chem.* **277,** 40099-40105

214. Symons, M., and Rusk, N. (2003) Control of vesicular trafficking by Rho GTPases. *Curr. Biol.* **13,** R409-R418

215. Tong, Q., Gamper, N., Medina, J. L., Shapiro, M. S., and Stockand, J. D. (2004) Direct activation of the epithelial Na^+ channel by phosphatidylinositol 3,4,5-trisphosphate and phosphatidylinositol 3,4-bisphosphate produced by phosphoinositide 3-OH kinase. *J. Biol. Chem.* **277,** 22654-22663

216. Treharne, K. J., Crawford, R. M., Best, O. G., Schulte, E. A., Chen, J.-H., Gruenert, D. C., Wilson, S. M., Kunzelmann, K., Sheppard, D. N., and Mehta, A. (2007) Protein kinase CK2, cystic fibrosis transmembrane conductance regulator, and the deltaF508 mutation - deltaF508 deletion disrupts a kinase-binding site. *J. Biol. Chem.* **282,** 10804-10813

217. Tucker, S. J., Gribble, F. M., Proks, P., Trapp, S., Ryder, T. J., Haug, T., Reimann, F., and Ashcroft, F. M. (1998) Molecular determinants of K_{ATP} channel inhibition by ATP. *EMBO J.* **17,** 3290-3296

218. Varga, K., Jurkuvenaite, A., Wakefield, J., Hong, J. S., Guimbellot, J. S., Venglarik, C. J., Niraj, A., Mazur, M., Sorscher, E. J., Collawn, J. F., and Bebok, Z. (2004) Efficient intracellular processing of the endogenous cystic fibrosis transmembrane conductance regulator in epithelial cell lines. *J. Biol. Chem.* **279,** 22578-22584

219. Varnai, P., and Balla, T. (1998) Visualization of phosphoinositides that bind pleckstrin homology domains: calcium- and agonist-induced dynamic changes and relationship to myo-[3H]inositol-labeled phosphoinositide pools. *J. Cell Biol.* **143,** 501-510

220. Veeze, H. J., Sinaasappel, M., Bijman, J., Bouquet, J., and De Jonge, H. R. (1991) Ion transport abnormalities in rectal suction biopsies from children with cystic fibrosis. *Gastroenterology* **101,** 398-403

221. Venta, P. J., Brouillette, J. A., Yuzbasiyan-Gurkan, V., and Brewer, G. J. (1996) Gene-specific universal mammalian sequence-tagged sites: application to the canine genome. *Biochem. Genet.* **34,** 321-341

222. Verrey, F. (1999) Early aldosterone action: toward filling the gap between transcription and transport. *Am. J. Physiol.* **277,** F319-F327

223. Verrey, F., Pearce, D., Pfeiffer, R., Spindler, B., Mastroberardino, L., Summa, V., and Zecevic, M. (2000) Pleiotropic action of aldosterone in epithelia mediated by transcription and post-transcription mechanisms. *Kidney Int.* **57,** 1277-1282

224. Volk, T., Konstas, A. A., Bassalay, P., Ehmke, H., and Korbmacher, C. (2004) Extracellular Na(+) removal attenuates rundown of the epithelial Na(+) channel (ENaC) by reducing the rate of channel retrieval. *Pflugers Arch.* **447,** 884-894

225. Wang, S., Raab, R. W., Schatz, P. J., Guggino, W. B., and Li, M. (1998) Peptide binding consensus of the NHE-RF-PDZ1 domain matches the C-terminal sequence of cystic fibrosis transmembrane conductance regulator (CFTR). *FEBS Lett.* **427,** 103-108

226. Ward, C. L., Omura, S., and Kopito, R. R. (1995) Degradation of CFTR by the ubiquitin-proteasome pathway. *Cell* **83,** 121-127

227. Waselle, L., Gerona, R. R., Vitale, N., Martin, T. F., Bader, M. F., and Regazzi, R. (2005) Role of phosphoinositide signaling in the control of insulin exocytosis. *Mol. Endocrinol.* **19,** 3097-3106

228. Weernink, P. A., Meletiadis, K., Hommeltenberg, S., Hinz, M., Ishihara, H., Schmidt, M., and Jakobs, K. H. (2004) Activation of type I phosphatidylinositol 4-phosphate 5-kinase isoforms by the Rho GTPases, RhoA, Rac1, and Cdc42. *J. Biol. Chem.* **279,** 7840-7849

229. Xie, Y., and Schafer, J. A. (2004) Inhibition of ENaC by Intracellular Cl^- in an MDCK Clone with High ENaC Expression. *Am. J. Physiol. Renal Physiol.* **287,** F722-F731

230. Xu, C., Watras, J., and Loew, L. M. (2003) Kinetic analysis of receptor-activated phosphoinositide turnover. *J. Cell Biol.* **161,** 779-791

231. Yan, W., Samaha, F. F., Ramkumar, M., Kleyman, T. R., and Rubenstein, R. C. (2004) CFTR differentially regulates human and mouse epithelial sodium channels in *Xenopus* oocytes. *J. Biol. Chem.* **279,** 23183-23192

232. Yang, L. M., Rinke, R., and Korbmacher, C. (2006) Stimulation of the epithelial sodium channel (ENaC) by cAMP involves putative ERK phosphorylation sites in the C-termini of the channel's beta- and gamma-subunit. *J. Biol. Chem.* **281,** 9859-9868

233. Yang, S. A., Carpenter, C. L., and Abrams, C. S. (2004) Rho and Rho-kinase mediate thrombin-induced phosphatidylinositol 4-phosphate 5-kinase trafficking in platelets. *J. Biol. Chem.* **279,** 42331-42336

234. Yoo, J. S., Moyer, B. D., Bannykh, S., Yoo, H. M., Riordan, J. R., and Balch, W. E. (2002) Non-conventional trafficking of the cystic fibrosis transmembrane conductance regulator through the early secretory pathway. *J. Biol. Chem.* **277,** 11401-11409

235. Yue, G., Malik, B., and Eaton, D. C. (2002) Phosphatidylinositol 4,5-bisphosphate (PIP2) stimulates epithelial sodium channel activity in A6 cells. *J. Biol. Chem.* **277,** 11965-11969

236. Zeitlin, P. L., Crawford, I., Lu, L., Woel, S., Cohen, M. E., Donowitz, M., Montrose, M. H., Hamosh, A., Cutting, G. R., and Gruenert D. (1992) CFTR protein expression in primary and cultured epithelia. *Proc. Natl. Acad. Sci. USA* **89,** 344-347

237. Zhang, F., Kartner, N., and Lukacs, G. L. (1998) Limited proteolysis as a probe for arrested conformational maturation of delta F508 CFTR. *Nat. Struct. Biol.* **5,** 180-183

238. Zhang, H., Craciun, L. C., Mirshahi, T., Rohacs, T., Lopes, C. M., Jin, T., and Logothetis, D. E. (2003) PIP(2) activates KCNQ channels, and its hydrolysis underlies receptor-mediated inhibition of M currents. *Neuron* **37,** 963-975

239. Zhang, L., Lee, J. K., John, S. A., Uozumi, N., and Kodama, I. (2003) Mechanosensitivity of GIRK channels is mediated by PKC-dependent channel-PIP2 interaction. *J. Biol. Chem.* **279,** 7037-7047

240. Zheng, J., Cahill, S. M., Lemmon, M. A., Fushman, D., Schlessinger, J., and Cowburn, D. (1996) Identification of the binding site for acidic phospholipids on the pH domain of dynamin: implications for stimulation of GTPase activity. *J. Mol. Biol.* **255,** 14-21

241. Zhou, R., and Snyder, P. M. (2005) Nedd4-2 phosphorylation induces serum and glucocorticoid-regulated kinase (SGK) ubiquitination and degradation. *J. Biol. Chem.* **280,** 4518-4523

Dank

Ich möchte mich bei Herrn Prof. Dr. Karl Kunzelmann herzlich für die Betreuung dieser Arbeit bedanken. Die mit ihm geführten Diskussionen und seine innovativen Ideen gewährten mir zudem oftmals einen neuen Zugang zu den Fragestellungen meiner Arbeit und halfen stets bei der Erkennung und Lösung von Problemen.

Mein Dank gilt auch in besonderem Maße Herrn PD Dr. Rainer Schreiber, der durch seine nützlichen Ratschläge zur rechten Zeit und durch seine wissenschaftliche Tätigkeit großen Anteil am Gelingen meiner Arbeit hatte.

Bei Herrn Dr. Vladimir Milenkovic möchte ich mich für die große Unterstützung bedanken, die er mir besonders während der Anfertigung dieser Arbeit zukommen ließ.

Ernestine Tartler und Agnes Paech gebührt mein vielfacher Dank sowohl für die Durchführung von Experimenten als auch für ihre große und stets vorhandene Hilfsbereitschaft, mit der mir beide das Arbeiten im Labor sehr erleichterten.

Melanie Spitzner stand mir stets mit Rat und Tat zur Seite. Unsere angeregten Gespräche erwiesen sich oft als äußerst hilfreich bei der Lösung von Problemen und trugen viel zu der angenehmen Arbeitsatmosphäre bei.

Joana Almaça und Roswitha Seitz danke ich für die Durchführung von Experimenten.

Mein ausdrücklicher Dank gilt all jenen Personen, die auf den in diese Dissertation eingefügten Veröffentlichungen als Autoren angeführt werden und bisher noch keine Erwähnung fanden.
Derer wären:
Margarida Barroso, Zsuzsa Bebok, Jens König, Daniel Markovich, Filipa Mendes, Bettina Mürle, Deborah Penque, Ralf Regeer, Jane Sun, Thilo Voelcker und John Wakefield. In diesem Rahmen möchte ich insbesondere Frau Prof. Dr. Margarida D. Amaral und Herrn Prof. Dr. Anil Mehta danken.

Diese Arbeit wurde durchgeführt mit der finanziellen Unterstützung von:
DFG SFB699 A6, DFG Ku756/7-1, Else Kröner-Fresenius Stiftung, Mukoviszidose e.V., ARC A00104609 und NHMRC 252823.

Allen Mitarbeitern der Arbeitsgruppe von Herrn Prof. Dr. Karl Kunzelmann möchte ich für die gute und angenehme Zusammenarbeit danken, die stets von Hilfsbereitschaft und freundschaftlichem Umgang miteinander geprägt war.

Beiträge zu Publikationen

Unter Verwendung der im Laufe dieser Promotion erzielten Ergebnisse entstanden:

In die Doktorarbeit eingefügte Publikationen:

1. Kunzelmann, K., Bachhuber, T., Regeer, R., Markovich, D., Sun, J., and Schreiber, R. (2004) Purinergic inhibition of the epithelial Na^+ transport via hydrolysis of PIP_2. *FASEB J.* **18,** 142-163
2. Bachhuber, T., König, J., Voelcker, T., Mürle, B., Schreiber, R., and Kunzelmann, K. (2005) Cl^- interference with the epithelial Na^+ channel ENaC. *J. Biol. Chem.* **280,** 31587-31594
3. Mendes, F., Wakefield, J., Bachhuber, T., Barroso, M., Bebok, Z., Penque, D., Kunzelmann, K., and Amaral, M. D. (2005) Establishment and characterization of a novel polarized MDCK epithelial cellular model for CFTR studies. *Cell. Physiol. Biochem.* **16,** 281-290
4. Bachhuber, T., Almaça J., Mehta, A., Schreiber, R., and Kunzelmann, K. (2007) Regulation of the epithelial Na^+ channel by protein kinase CK2. *J. Biol. Chem.* (submitted)

Weitere Veröffentlichungen und Vorträge:

- Kunzelmann, K., Bachhuber, T., Adam, G., Voelcker, T., Mürle, B., Mall, M., and Schreiber, R. (2005) Role of CFTR and other ion channels in cystic fibrosis. In: Defects of secretion in cystic fibrosis. Carsten Schultz (Ed.). *Adv. Exp. Med. Biol.* **558,** 23-41
- Bachhuber, T., Schreiber, R., and Kunzelmann, K. (2004) Increase in intracellular Cl^- concentration mediated by ClC-0 and activation of purinergic receptors inhibit the activity but not surface expression of ENaC (Abstract). *Pflugers Arch.* **447,** P11-1
- Bachhuber, T., Schreiber, R., and Kunzelmann, K. (2005) Purinergic inhibition of the epithelial Na^+ transport via hydrolysis of PIP_2 (Abstract). *Pflugers Arch.* **449,** P19-8
- Bachhuber, T., Almaça, J., Schreiber, R., and Kunzelmann, K. (2006) Cl^- interference with the epithelial Na^+ channel ENaC (Abstract und Vortrag). *Acta Physiologica* **186,** OW04-24

Erklärung

Hiermit versichere ich, dass ich die vorliegende Arbeit selbstständig verfasst und keine anderen als die angegebenen Hilfsmittel verwendet habe.

Regensburg, im Juli 2007 _____